DLR TAU Simulations for the Second AIAA Sonic Boom Prediction Workshop

Jochen Kirz and Ralf Rudnik

German Aerospace Center (DLR), Institute of Aerodynamics and Flow Technology

AIAA Aviation, June 05, 2017

Outline

- Motivation and Background
- SBPW2 Configurations and Grids
- Flow Solver and Computing Platform
- Simulation Results and Data Comparison
- Summary, Conclusions and Outlook

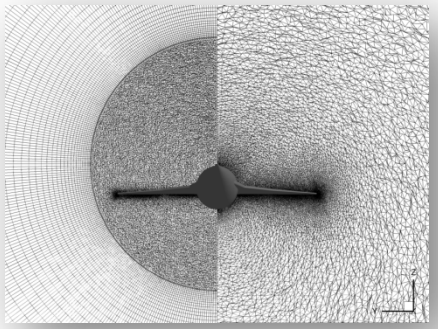

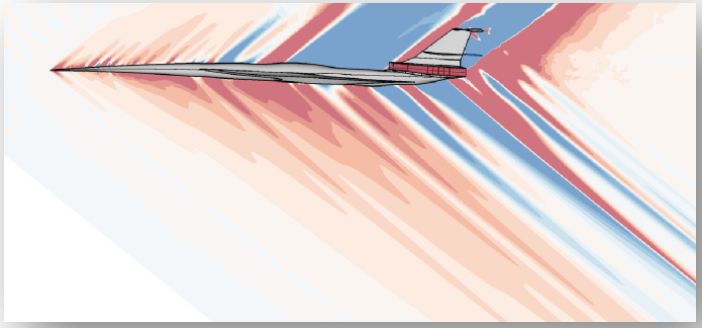

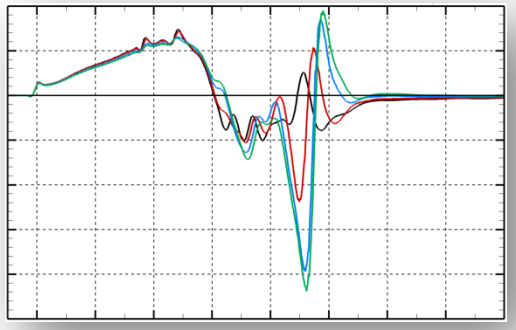

Motivation and Background

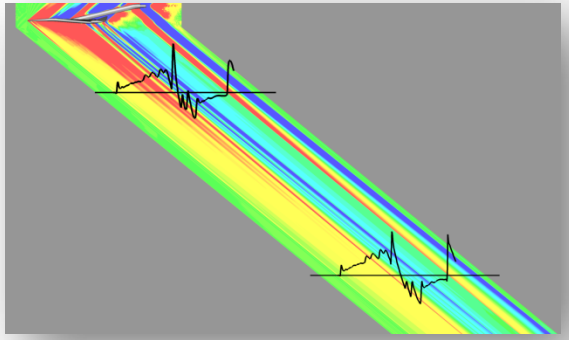

- Considerable market for supersonic aircraft
- Certification of a low boom aircraft to fly super-sonically over land would allow new routes
- AIAA Sonic Boom Prediction Workshop intends to assess the state of the art for predicting near-field pressure signatures, ground signatures and perceived loudness levels
- DLR did not upload data for the first SBPW (January 2014) but participated as an observer
- In early 2016 DLR started to use the available data from SBPW1 to build a best practice for near-field pressure signature prediction with the DLR TAU code
- DLR uploaded near-field pressure signatures for SBPW2 and participated in January 2017

SBPW2 Configurations

Overview

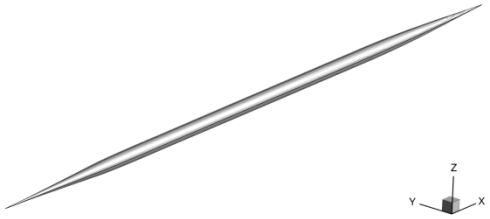

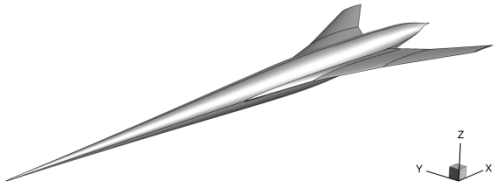

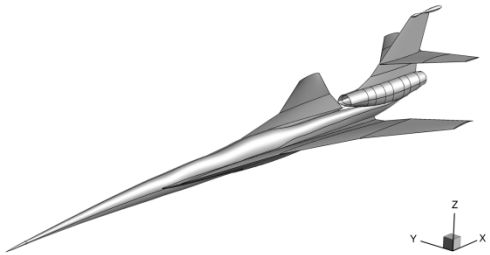

AXIE

Axisymmetric body

- Matching the pressure signature of C25F at 3 body lengths

JWB

JAXA delta wing body

- Same equivalent area as the C25D

NASA C25D

Full configuration with tail

- **C25F**: flow-through nacelle
- **C25P**: powered engine

Available Data

- Geometries and grids
- Pressure signatures from other participants

Simulation Conditions

- $M = 1.6$
- $H = 15760\ m$
- $T = 216.65\ K$
- $Re = 5.7 \cdot 10^6/m$

Cases Analyzed and Grids Used

AXIE-inv	JWB-inv	C25F-inv	C25F-visc	C25P-inv
WS-mixed, h=4.42		**WS-mixed, h=2.00**	**WS-mixed, h=2.00**	*WS-mixed, h=2.00*
WS-mixed, h=3.27		**WS-mixed, h=1.60**		*WS-mixed, h=1.60*
WS-mixed, h=2.23		**WS-mixed, h=1.28**	**WS-mixed, h=1.28**	
WS-mixed, h=1.52		**WS-mixed, h=1.00**	**WS-mixed, h=1.00**	*WS-mixed, h=1.00*
		WS-mixed, h=0.80	**WS-mixed, h=0.80**	*WS-mixed, h=0.80*
		WS-mixed, h=0.64		
WS-tet, h=4.42	**WS-tet, h=1.00**	**WS-tet, h=2.00**	**WS-tet h=2.00**	
WS-tet, h=3.27	**WS-tet, h=0.83**	**WS-tet, h=1.60**		
WS-tet, h=2.23	**WS-tet, h=0.70**	**WS-tet, h=1.28**	**WS-tet h=1.28**	
WS-tet, h=1.52		**WS-tet, h=1.00**	**WS-tet h=1.00**	
CENT-mixed	**CENT-mixed, h=1.68**	*CENT-mixed, h=1.00*		
	CENT-mixed, h=1.00			
	CENT-mixed, h=0.81			
	CENT-mixed, h=0.65			

Grids JWB

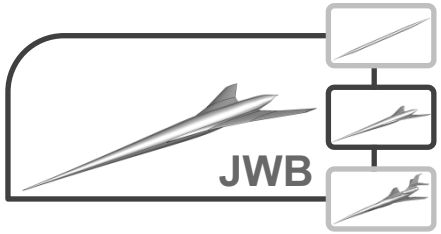

CENTAUR-generated

- Core grid
  - ➢ Tetrahedra
- Collar grid
  - ➢ Hexahedra

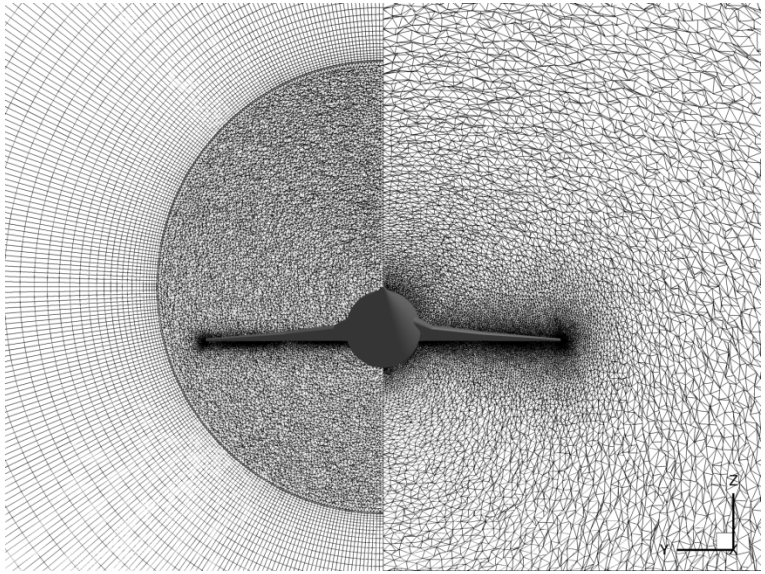

Workshop-provided

- Purely tetrahedral

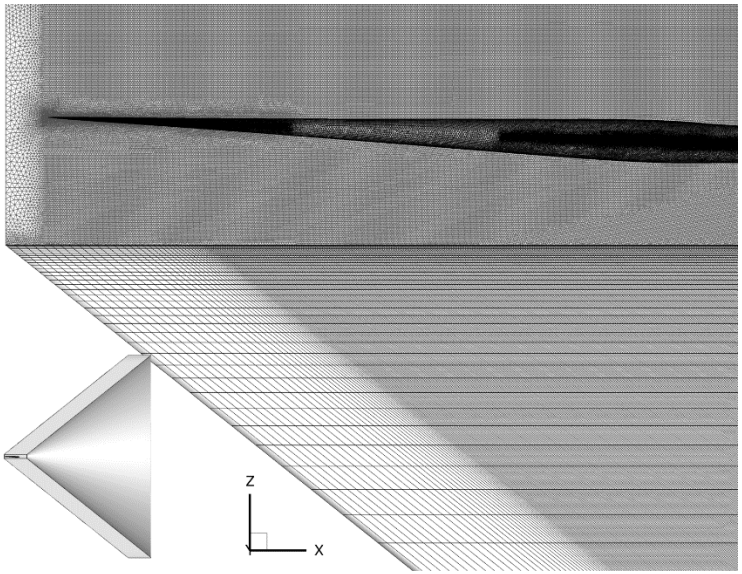

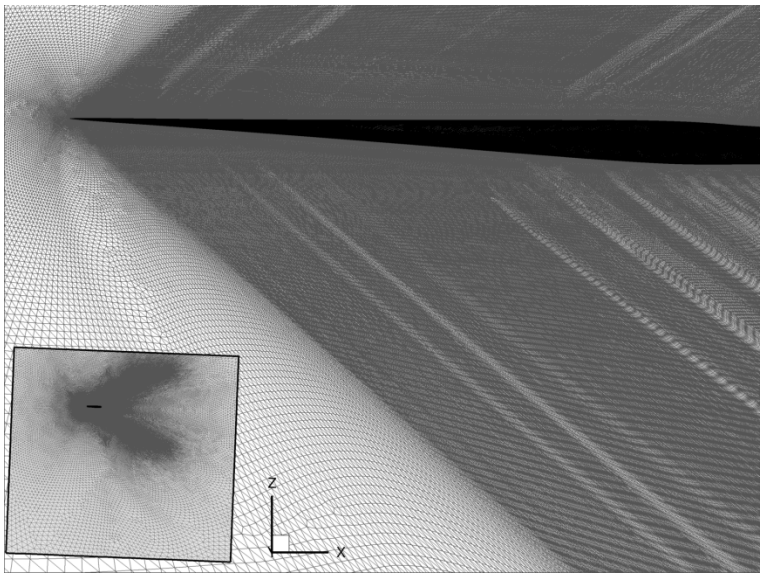

Grids C25F

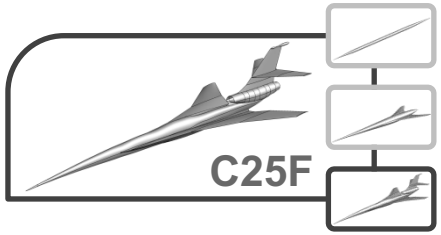

CENTAUR-generated

- Core grid
  - ➢ Tetrahedra
- Collar grid
  - ➢ Hexahedra

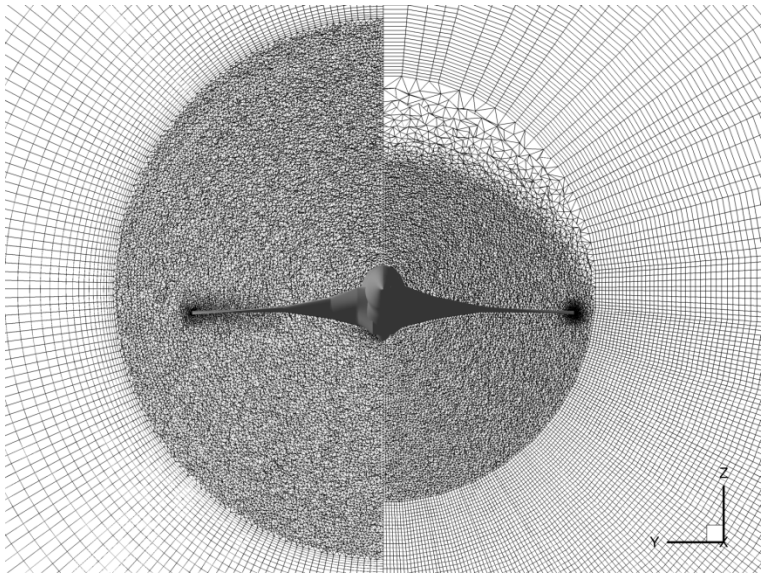

Workshop-provided

- Core grid
  - ➢ Tetrahedra
- Collar grid
  - ➢ Prisms/ Tetrahedra

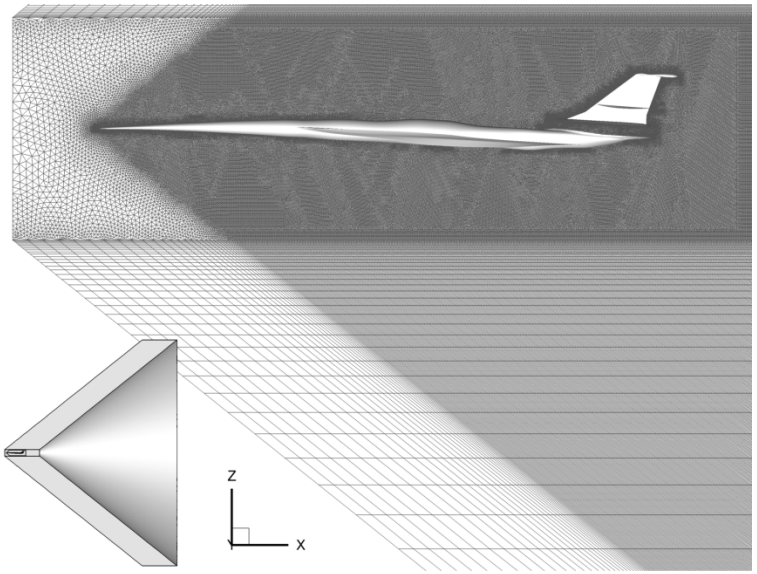

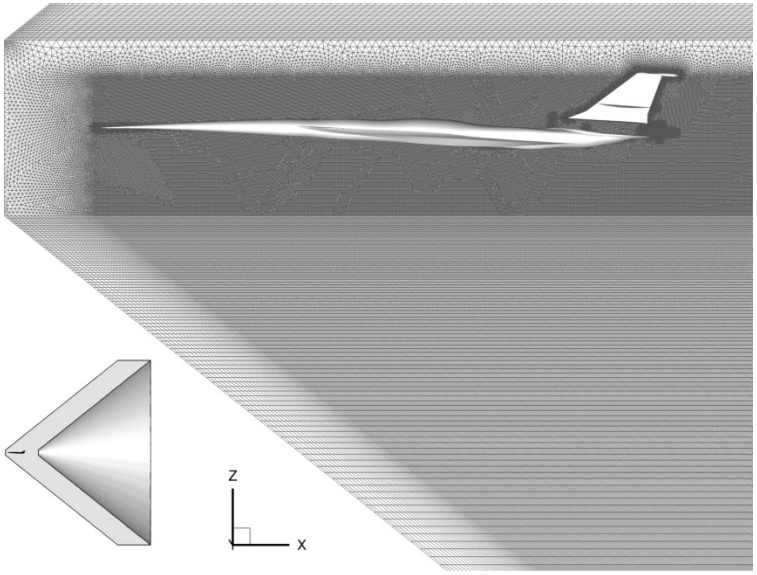

Flow Solver and Computing Platform

- DLR TAU Code
  - Unstructured finite-volume
  - Euler, RANS
  - Hybrid grids
  - Backward Euler and Runge-Kutta timestepping
  - Central and upwind schemes (Roe, Van Leer, AUSMDV, AUSMP(W+))
  - 2nd order upwind limiter functions (Barth Jesperson, Venkatakrishnan, SRR)

- C²A²S²E-2 Cluster
  - 1 computing node (24 cores) per 300.000 grid nodes

Convergence

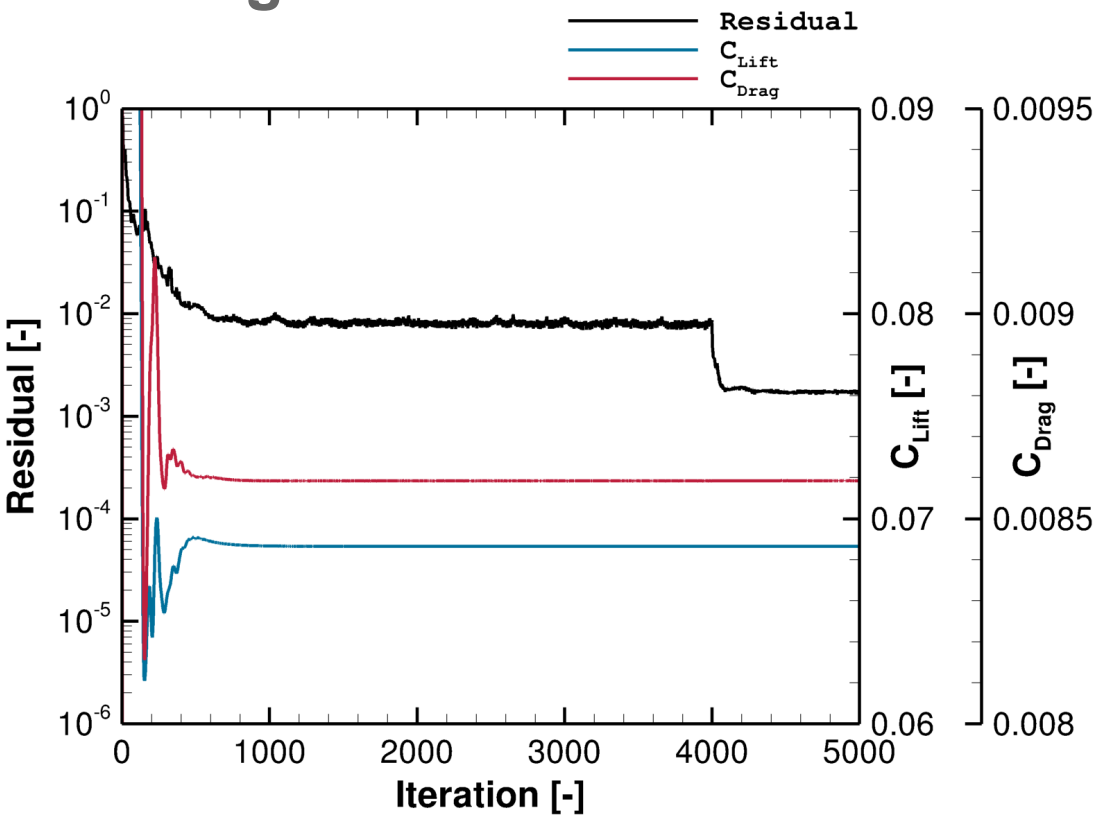

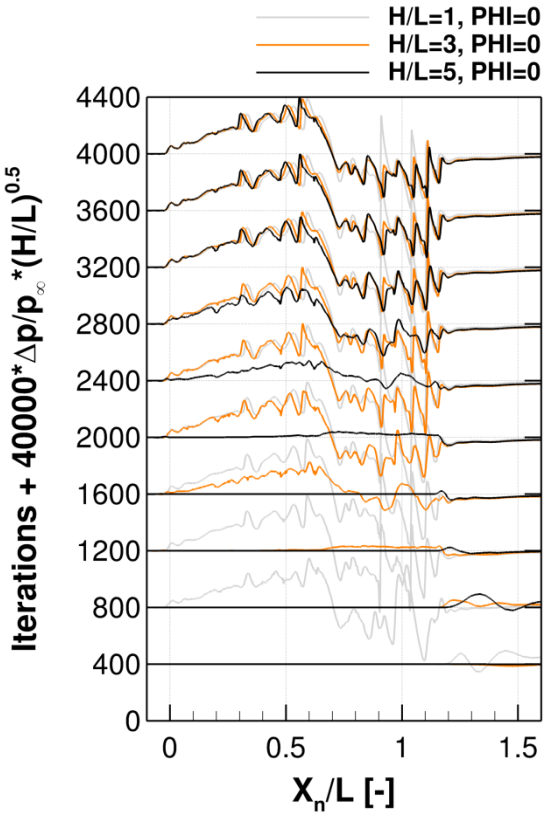

- CFL Ramping
- Aerodynamic coefficients converged at 1000 iterations
- Pressure signatures in the farfield converged significantly later
- Convergence criteria:

  5000 Iterations (inviscid simulations) / 15000 iterations (viscous simulations)

Results AXIE

Pressure Contours

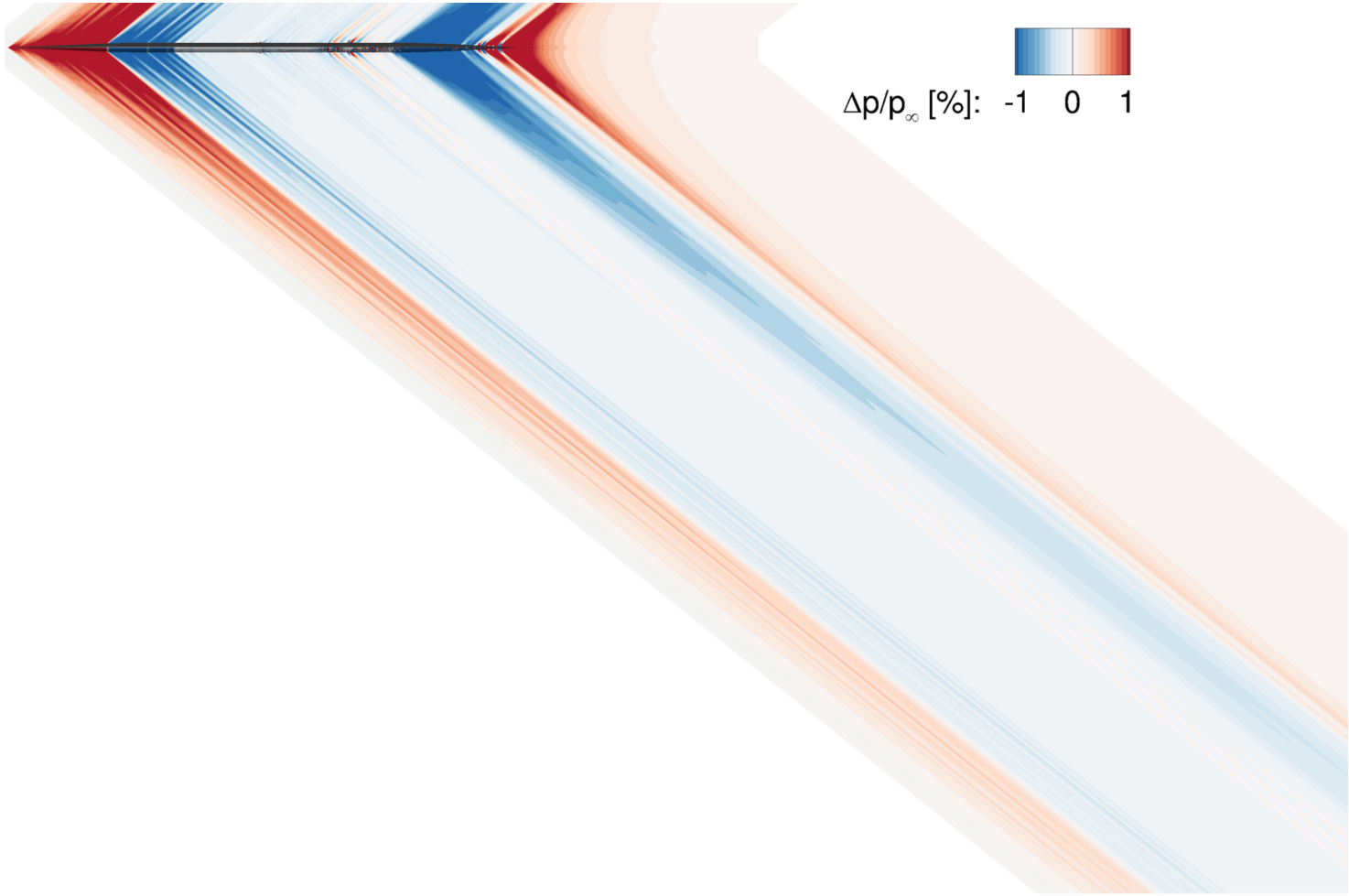

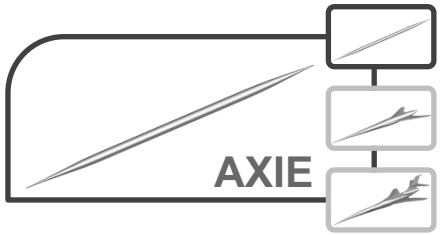

Results AXIE

Normalization and Pressure Signature Extraction

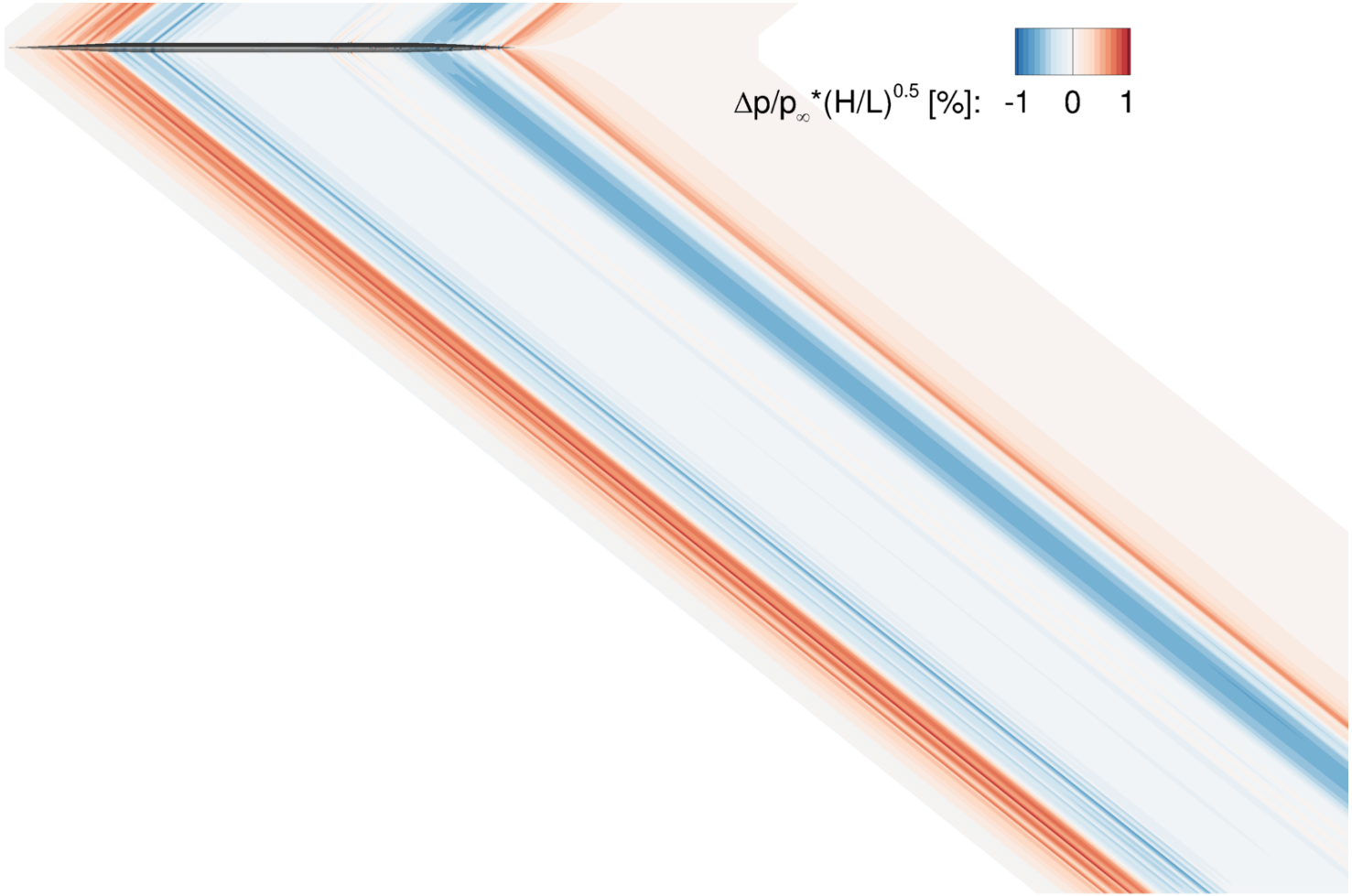

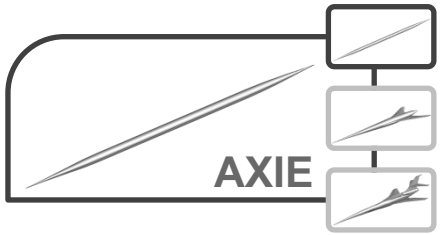

Results AXIE

Normalization and Pressure Signature Extraction

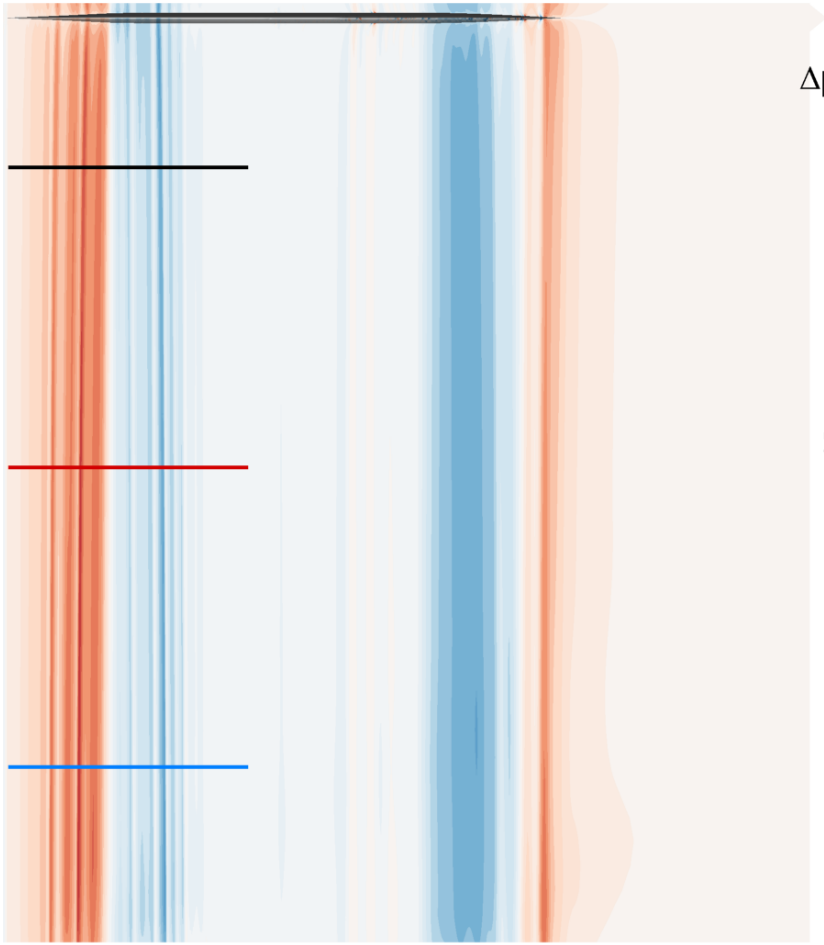

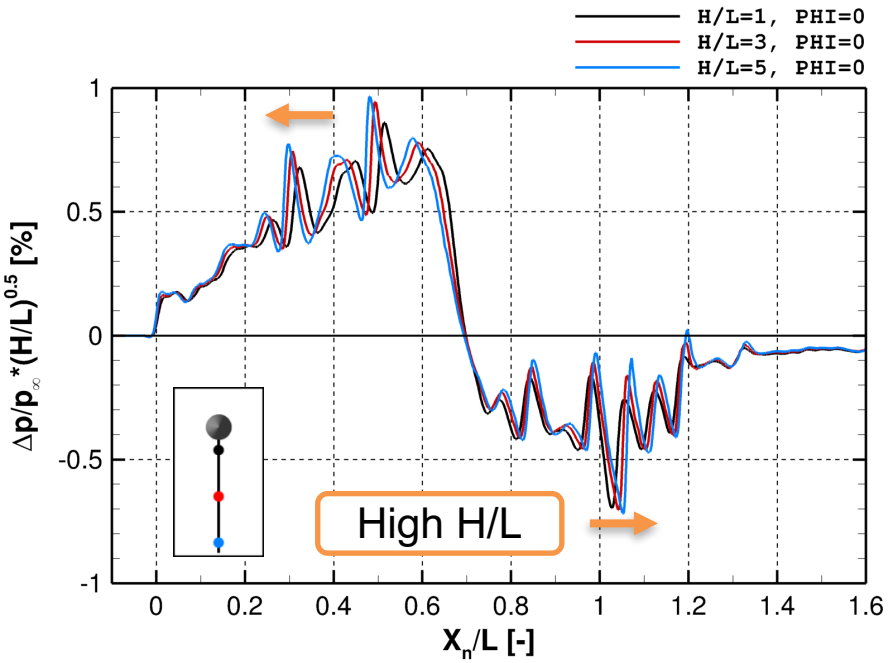

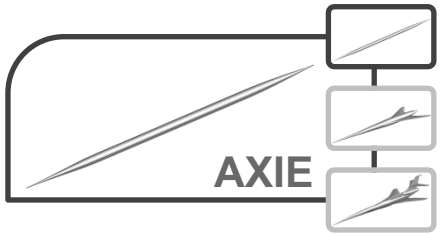

Results AXIE

Pressure Signature Convergence (H/L=5, PHI=0)

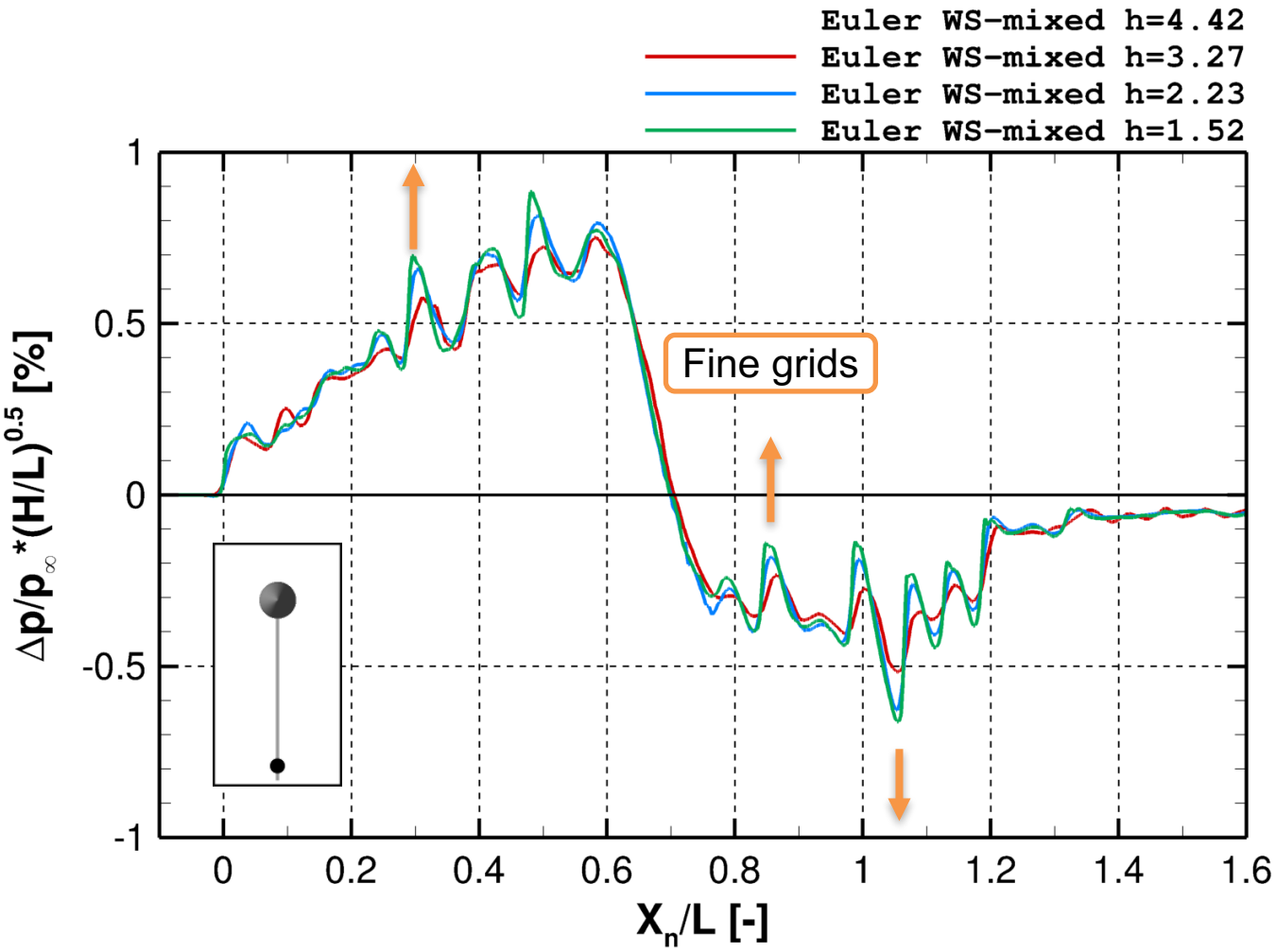

- Positions of shocks and expansions coincide for medium to fine grids
- Magnitudes are larger on fine grids (less dissipative)

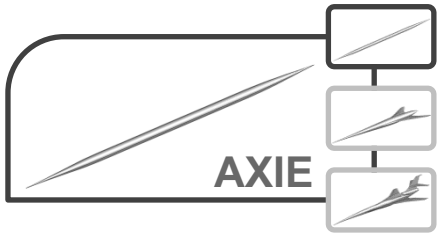

Results AXIE

Pressure Signature Convergence (H/L=5, PHI=0)

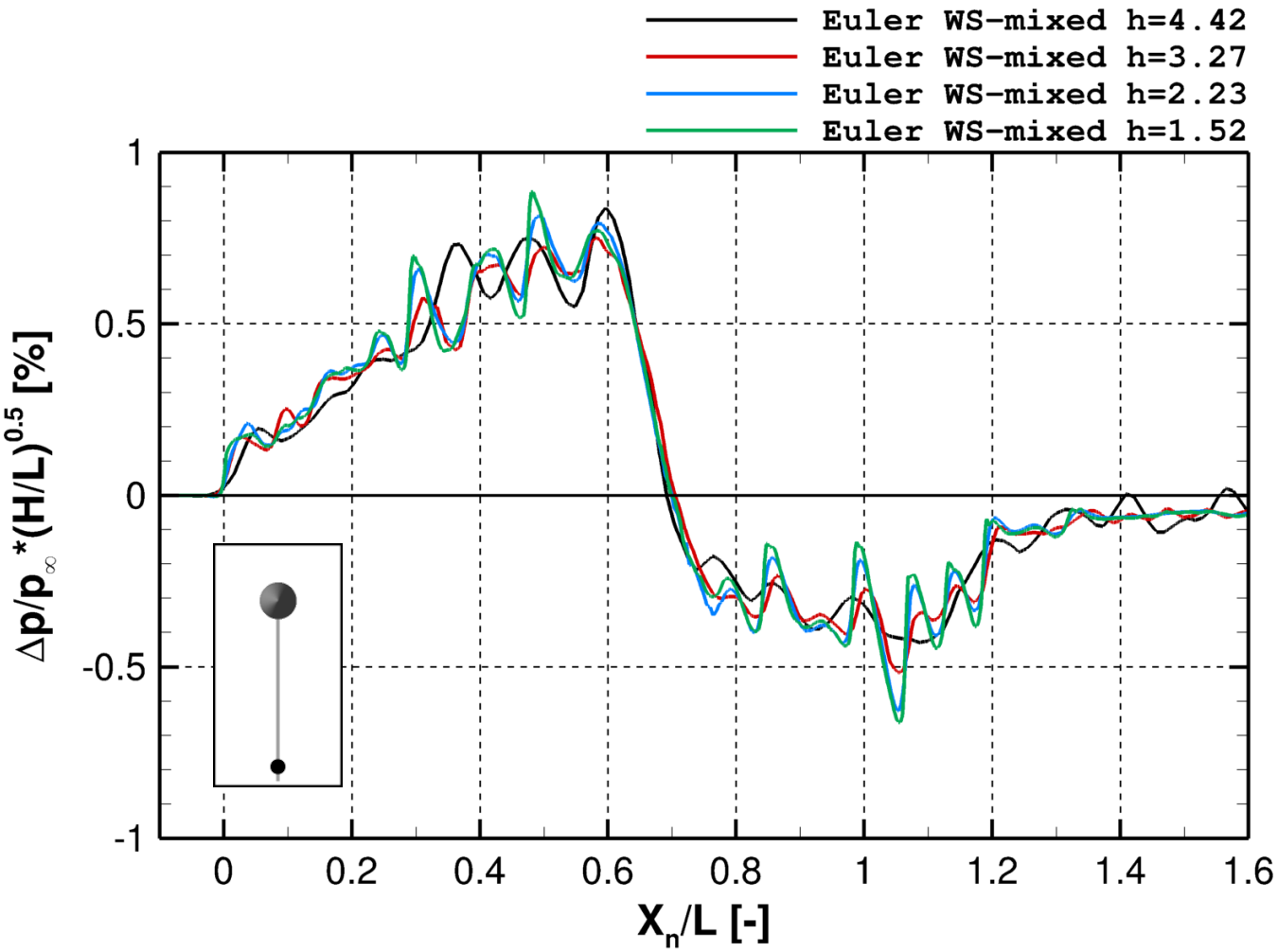

- Positions of shocks and expansions coincide for medium to fine grids
- Magnitudes are larger on fine grids (less dissipative)

- Positions of shocks and expansions differ for very coarse grids

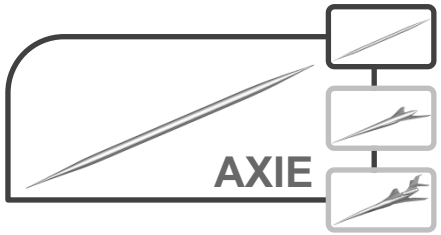

Results AXIE

Mesh-Induced Pressure Disturbances

AXIE Euler WS-mixed h=4.42 (very coarse)

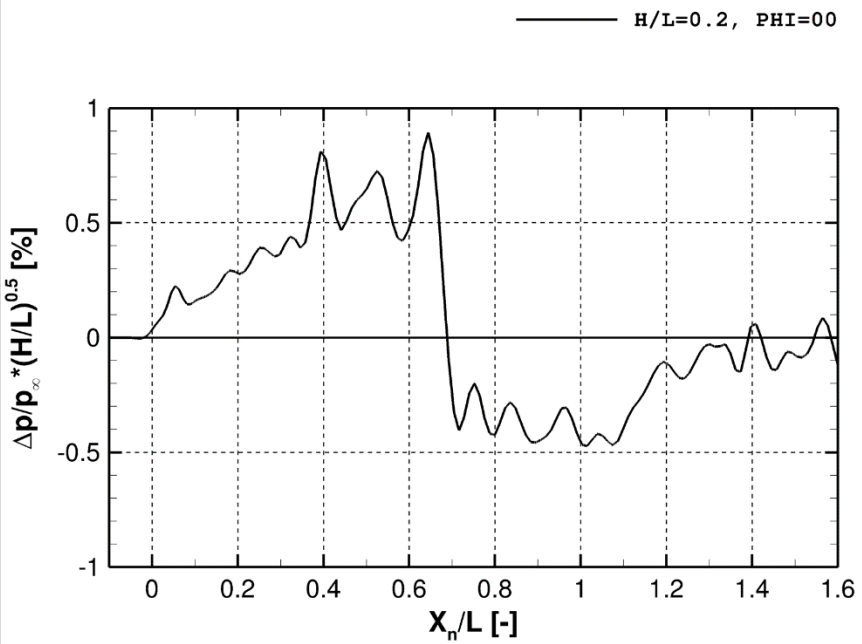

AXIE Euler WS-mixed h=1.52 (fine)

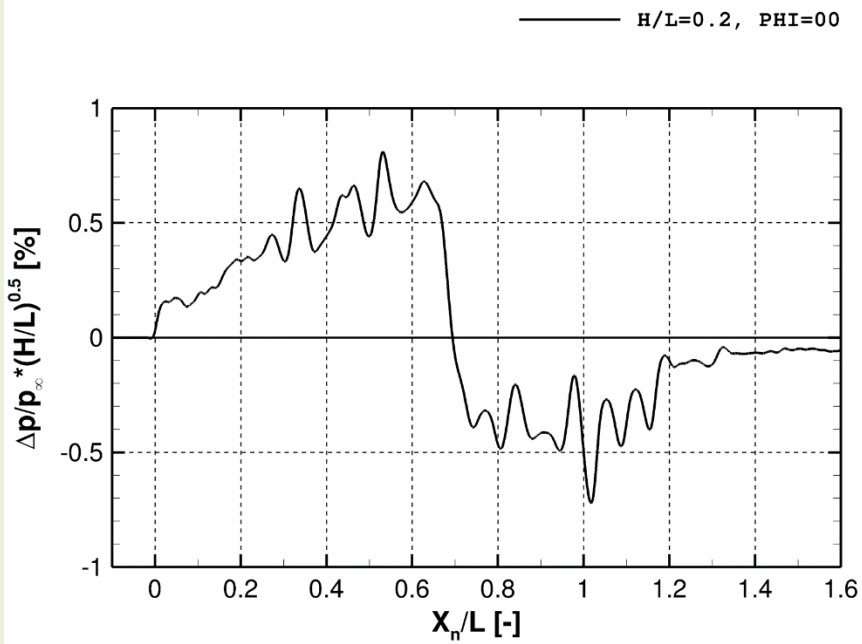

DLR

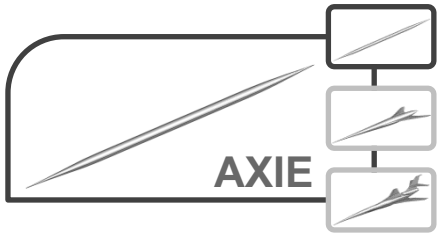

Results AXIE

Mesh-Induced Pressure Disturbances

AXIE Euler WS-mixed h=4.42 (very coarse)

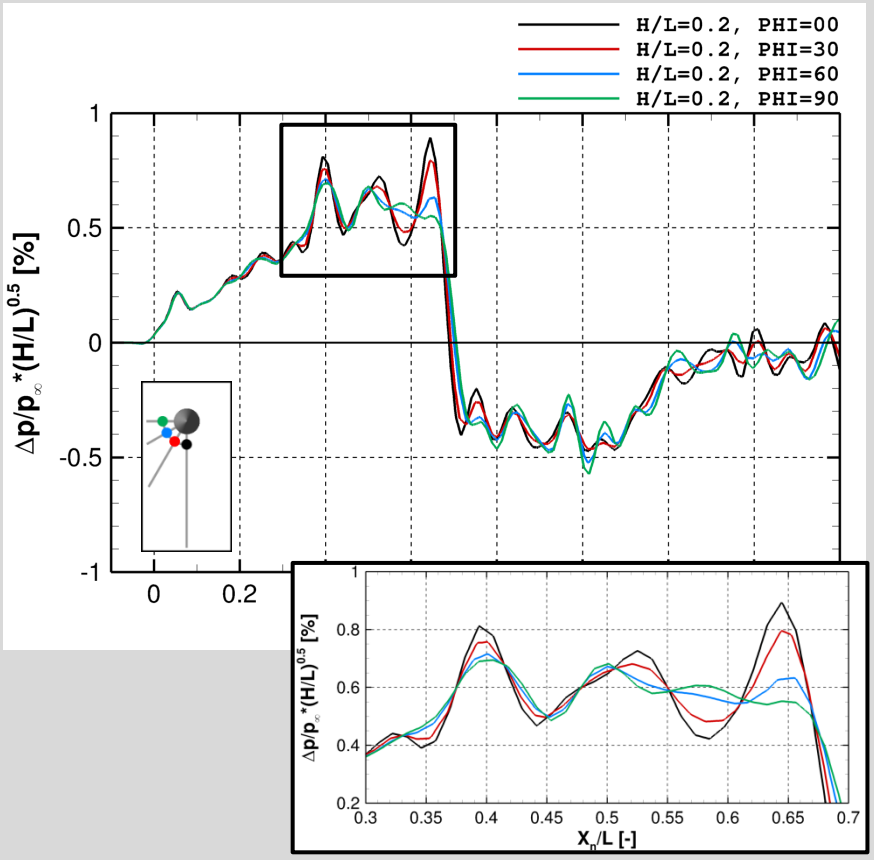

AXIE Euler WS-mixed h=1.52 (fine)

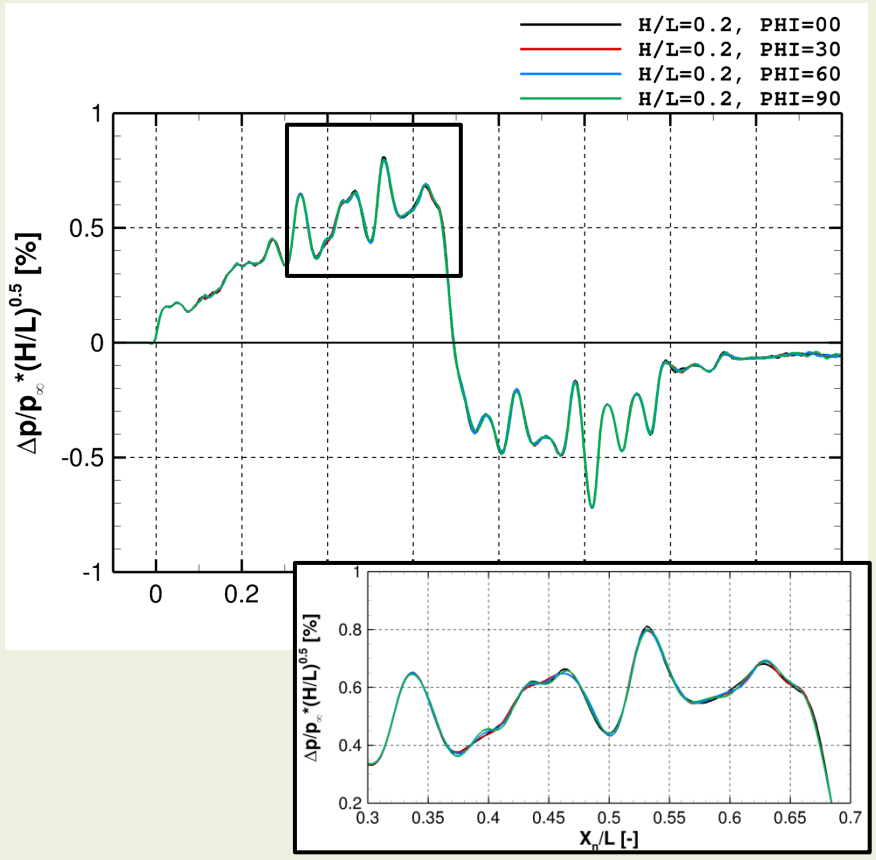

DLR

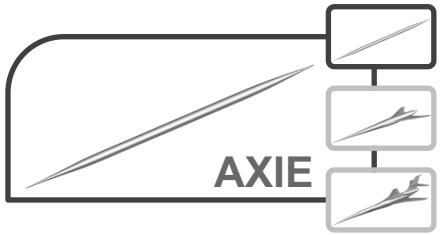

Results AXIE

Mesh-Induced Pressure Disturbances

AXIE Euler WS-mixed h=4.42 (very coarse)

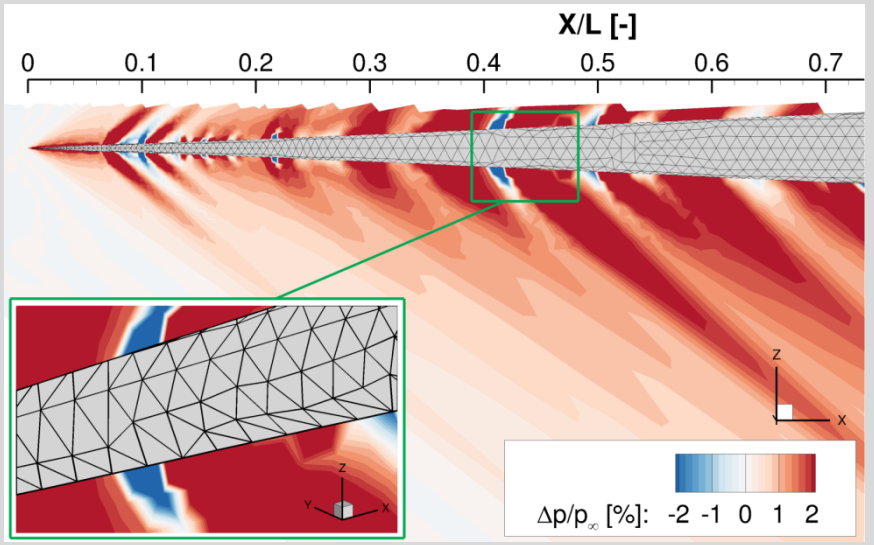

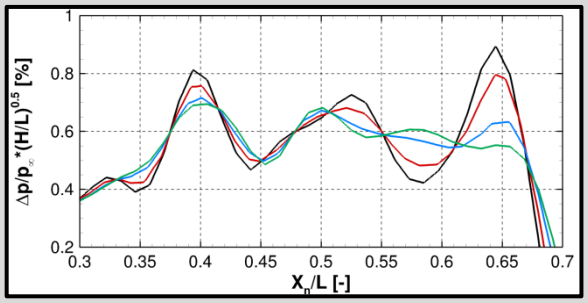

AXIE Euler WS-mixed h=1.52 (fine)

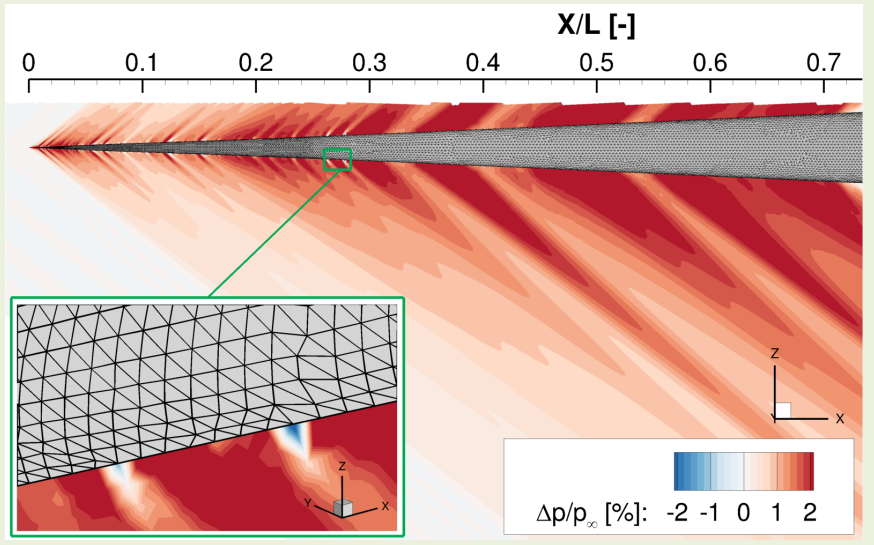

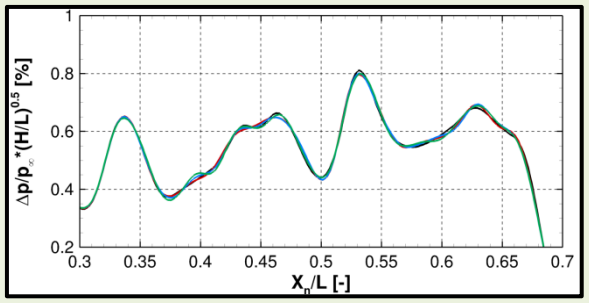

DLR

Results JWB

Results JWB

Pressure Contours and Near Field Signatures

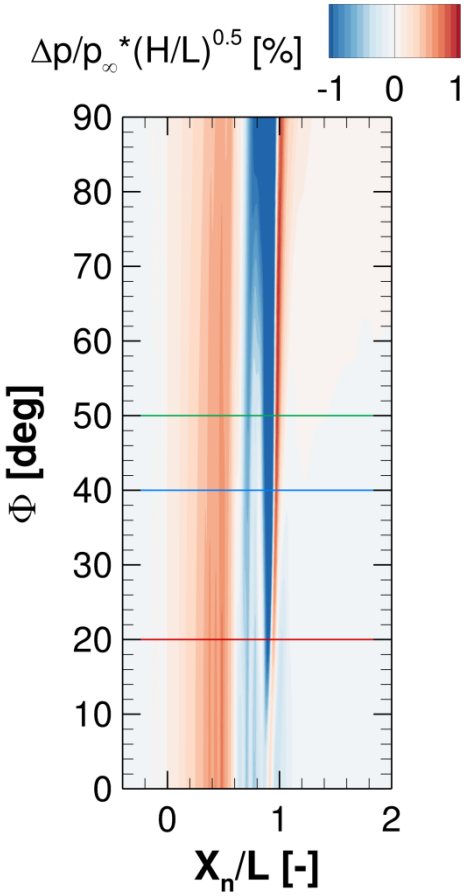

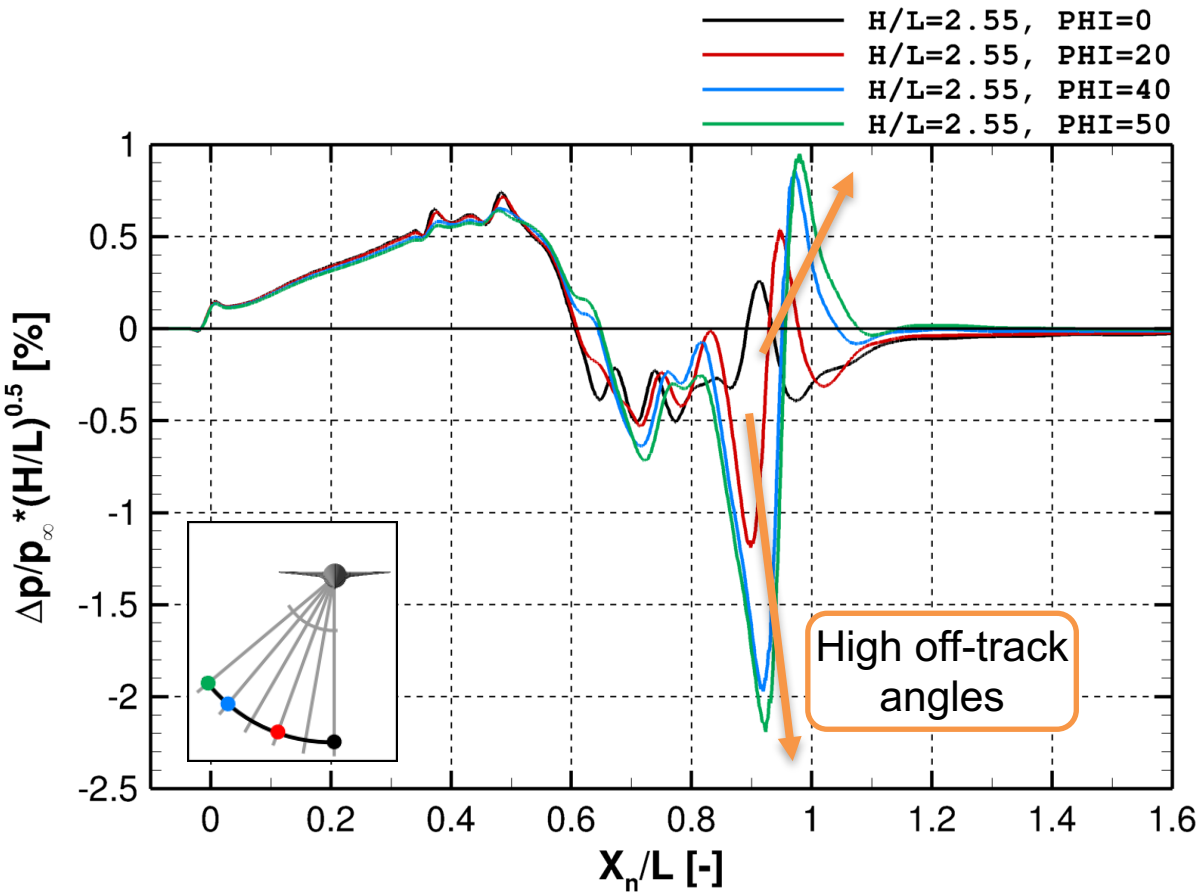

Results JWB

Pressure Signature Convergence (H/L=2.55, PHI=0)

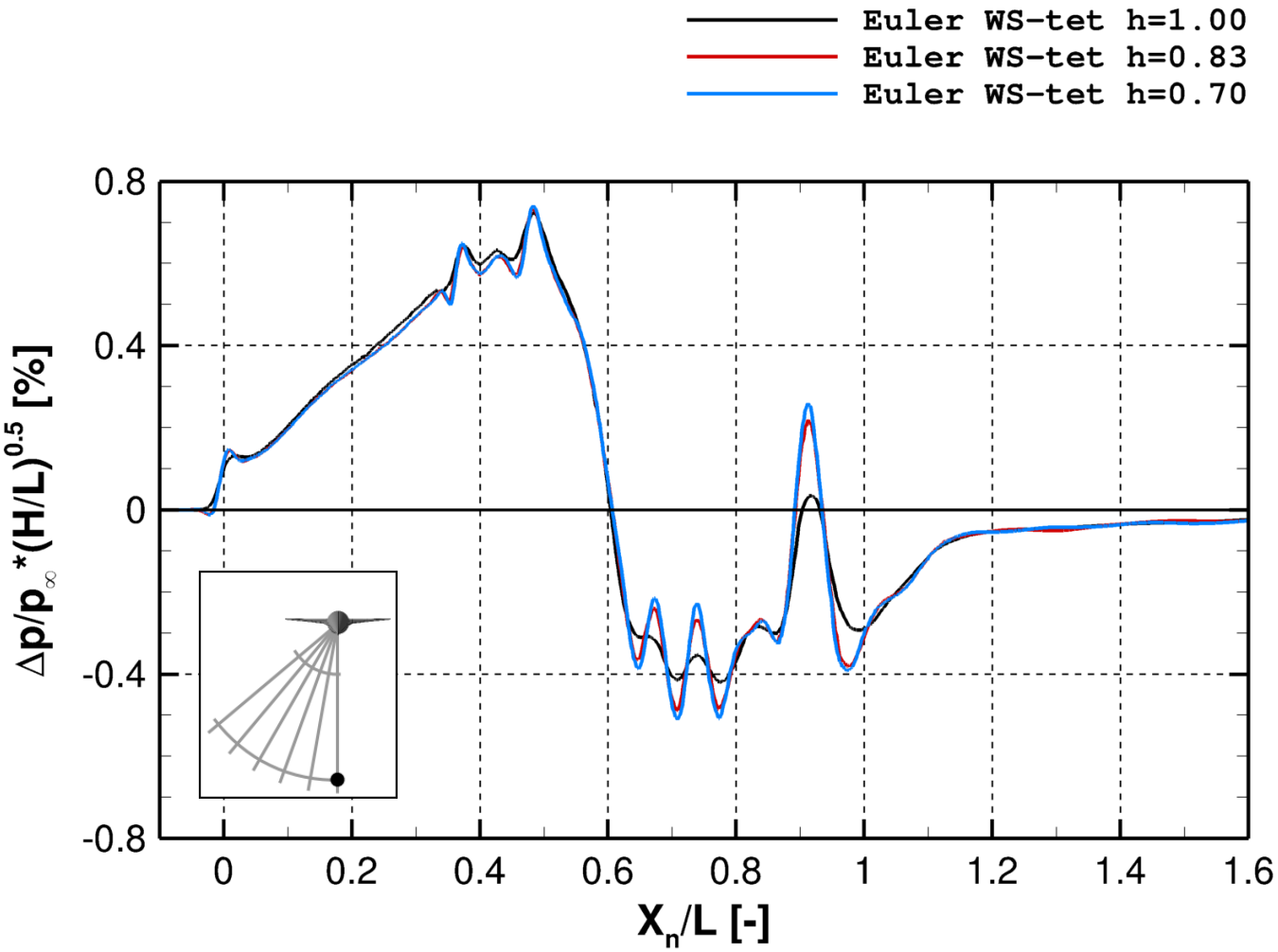

WS-provided grids

- Positions of shocks and expansions coincide
- Signature convergence with grid refinement

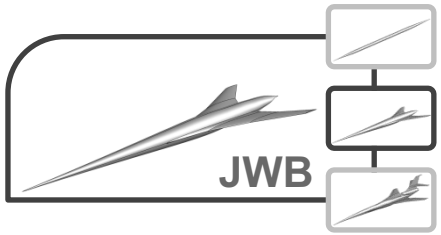

Results JWB

Pressure Signature Convergence (H/L=2.55, PHI=0)

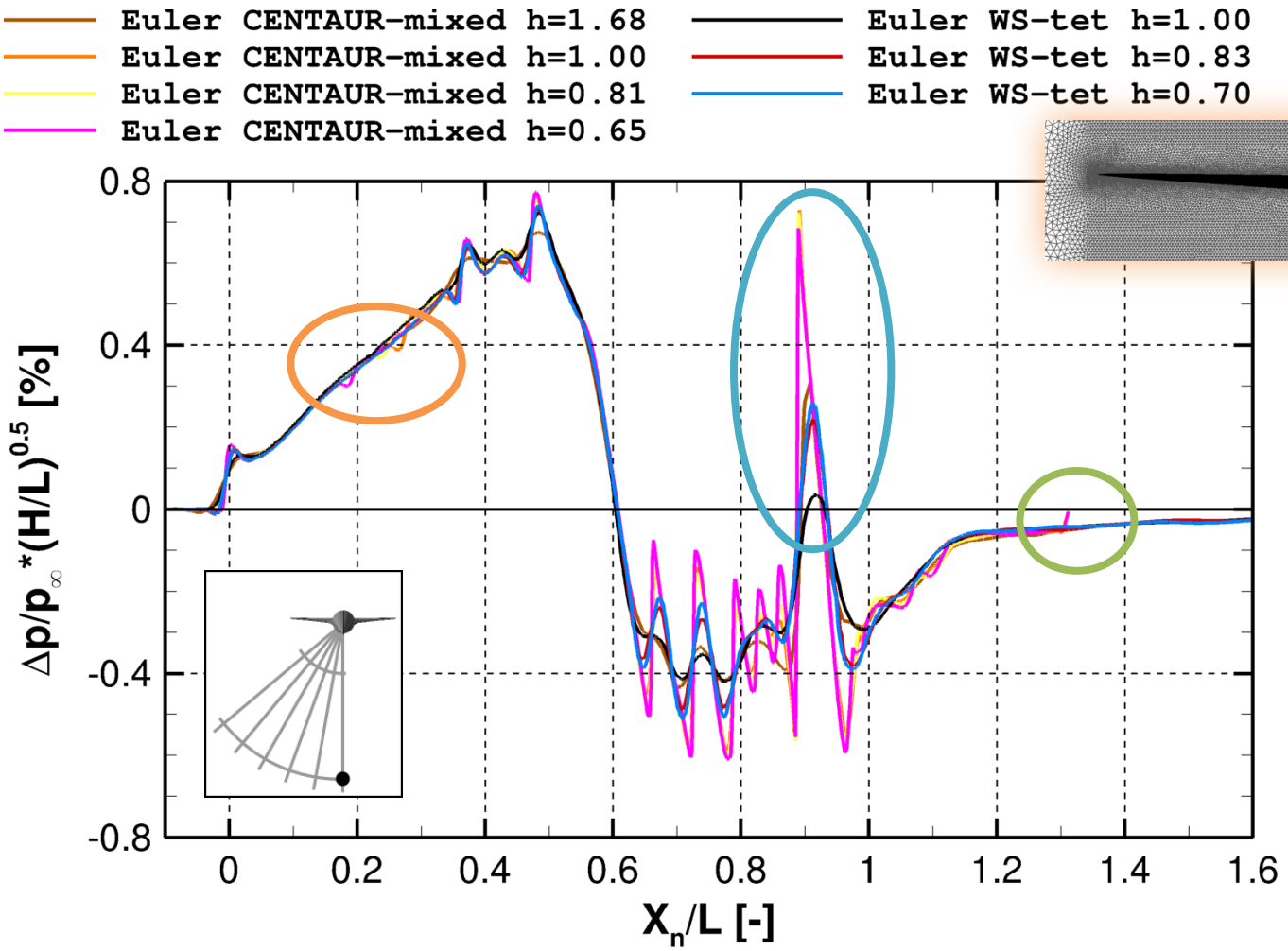

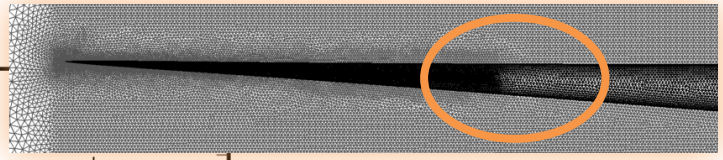

CENTAUR grids

- Mesh-induced pressure disturbances at the nose
- Lower streamwise extent
- Larger magnitudes at tail shock

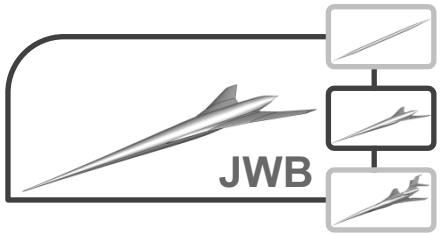

Results JWB

Pressure Signature Convergence (H/L=2.55, PHI=0)

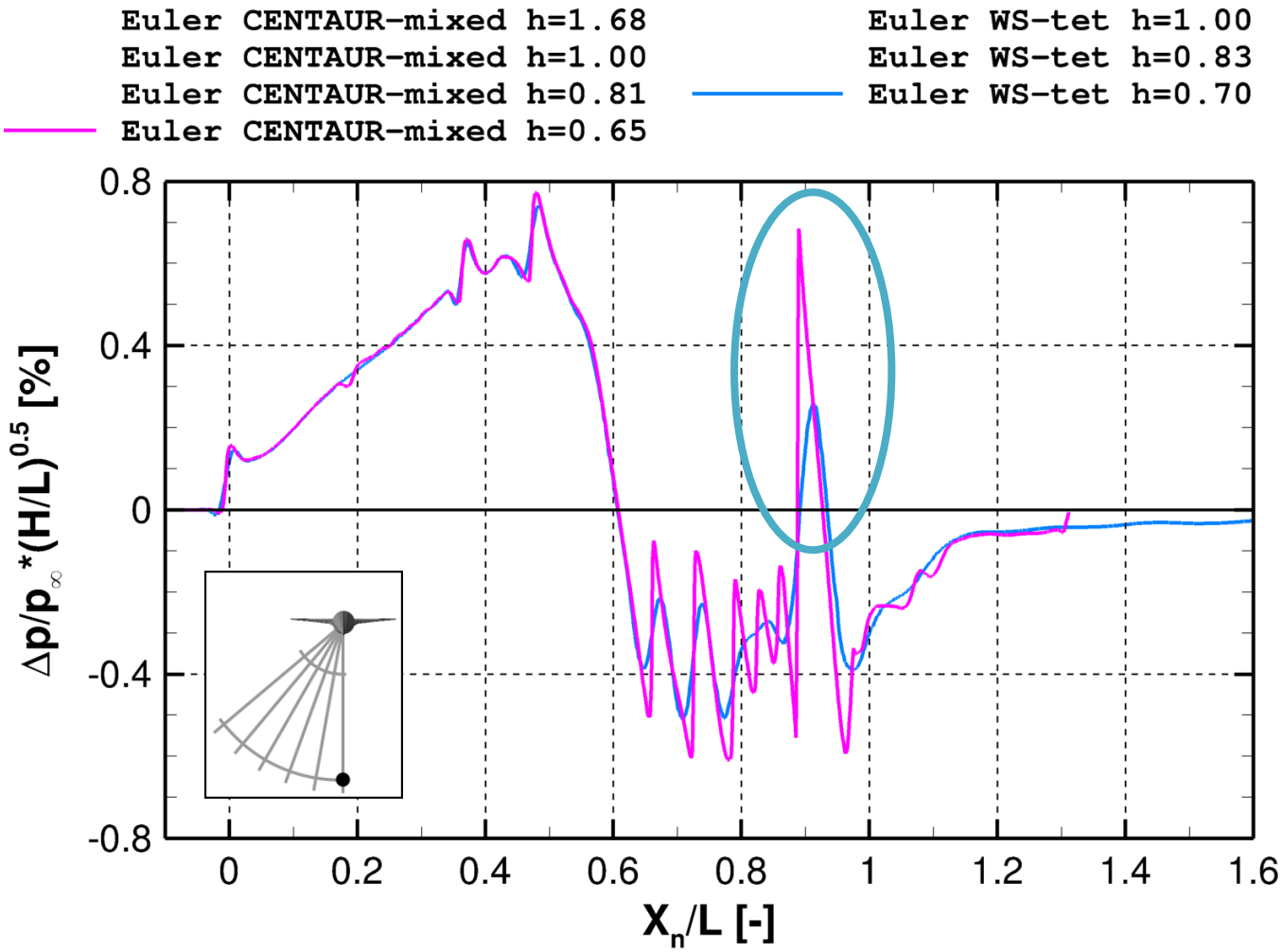

CENTAUR grids

- Mesh-induced pressure disturbances at the nose
- Lower streamwise extent
- Larger magnitudes at tail shock

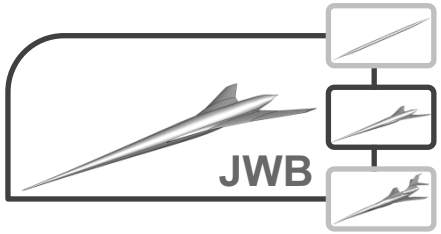

Results JWB

Smoothing of the Pressure Signature (Symmetry Plane)

JWB Euler CENTAUR-mixed h=0.65

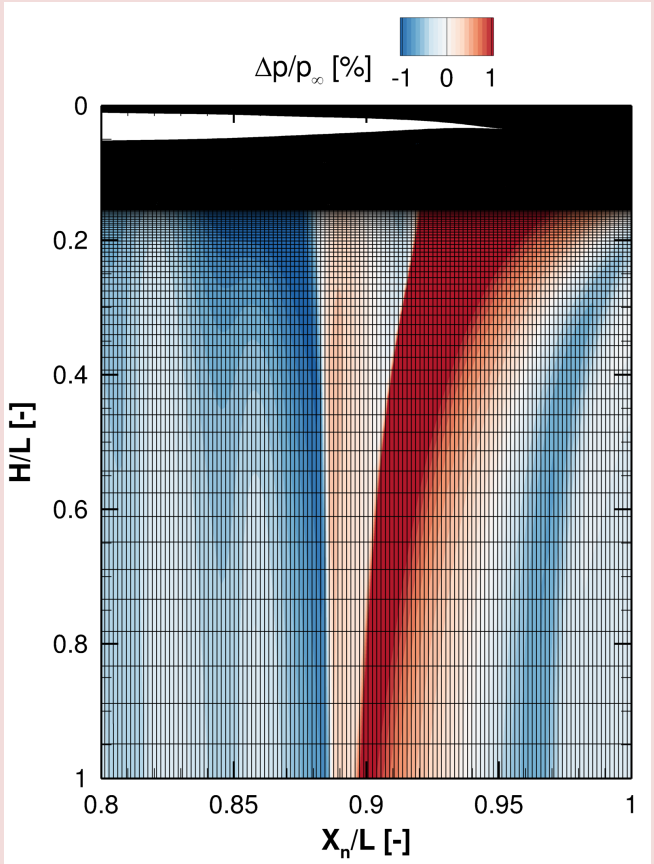

JWB Euler WS-tet h=0.7

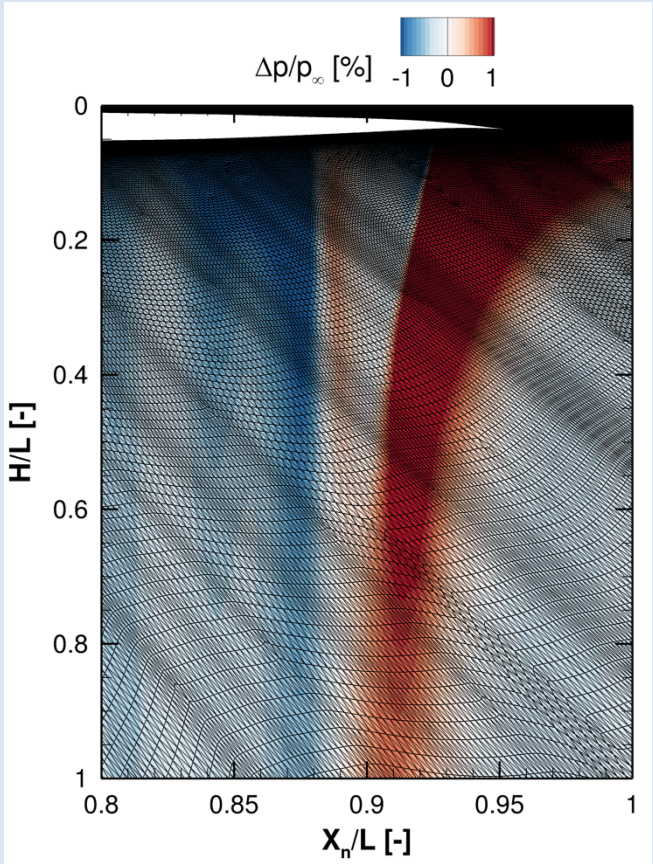

Results C25D flow-through

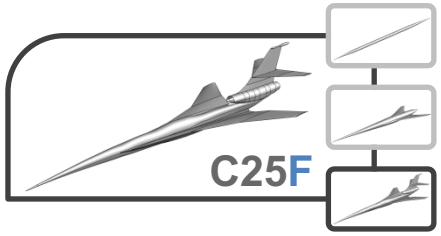

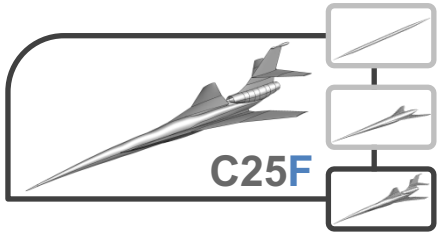

Results C25D flow-through

Pressure Signature Convergence (H/L=5, PHI=0)

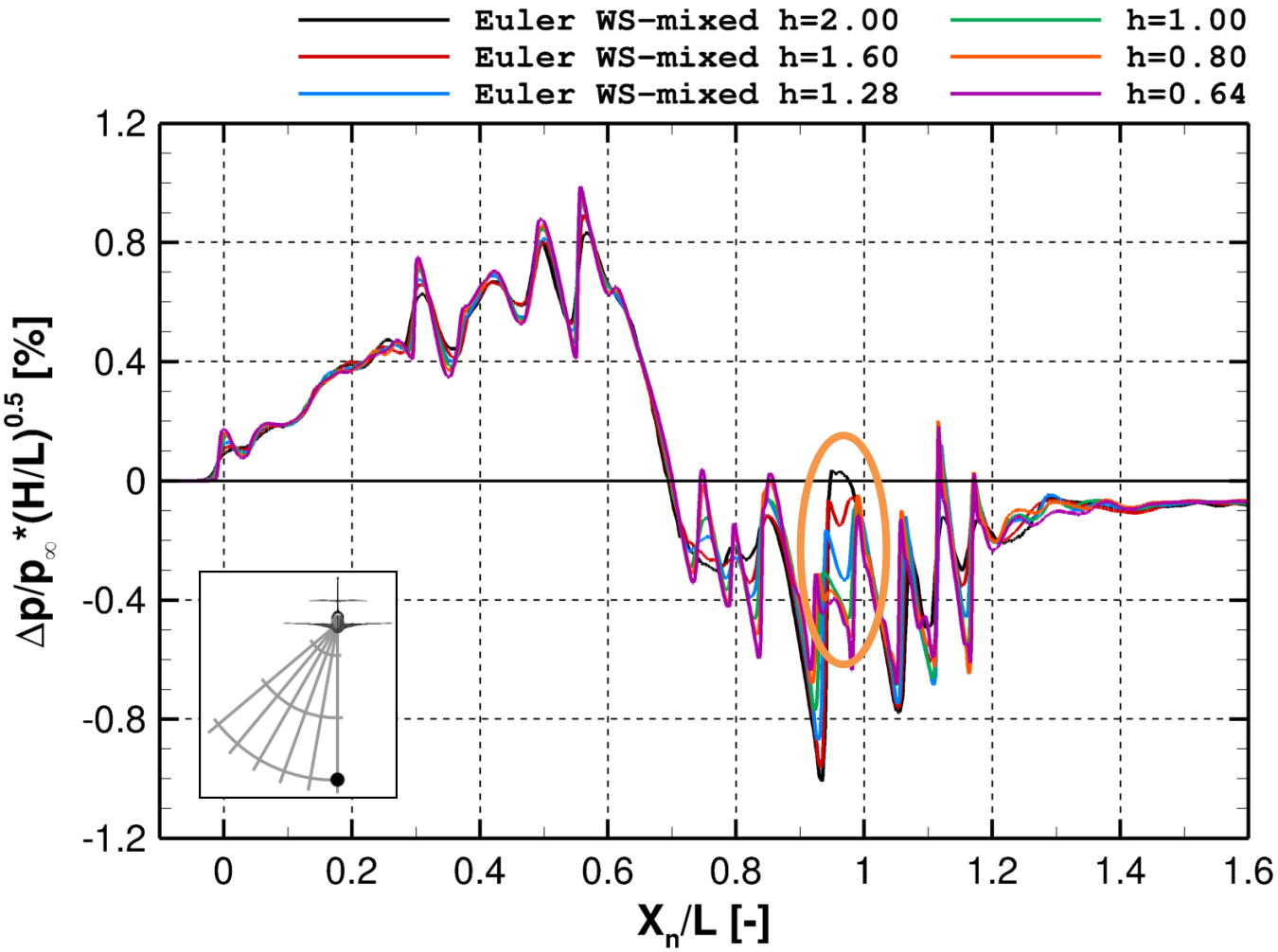

- Large differences at $0.9 < \frac{X_N}{L} < 1$
- Reflections of nacelle leading edge shock on the upper wing and lower HTP surfaces
- Grid convergence for h<1.00

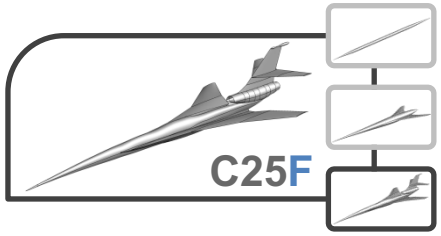

Results C25D flow-through

TAU Signatures and SBPW2 Statistics (H/L=5, PHI=0)

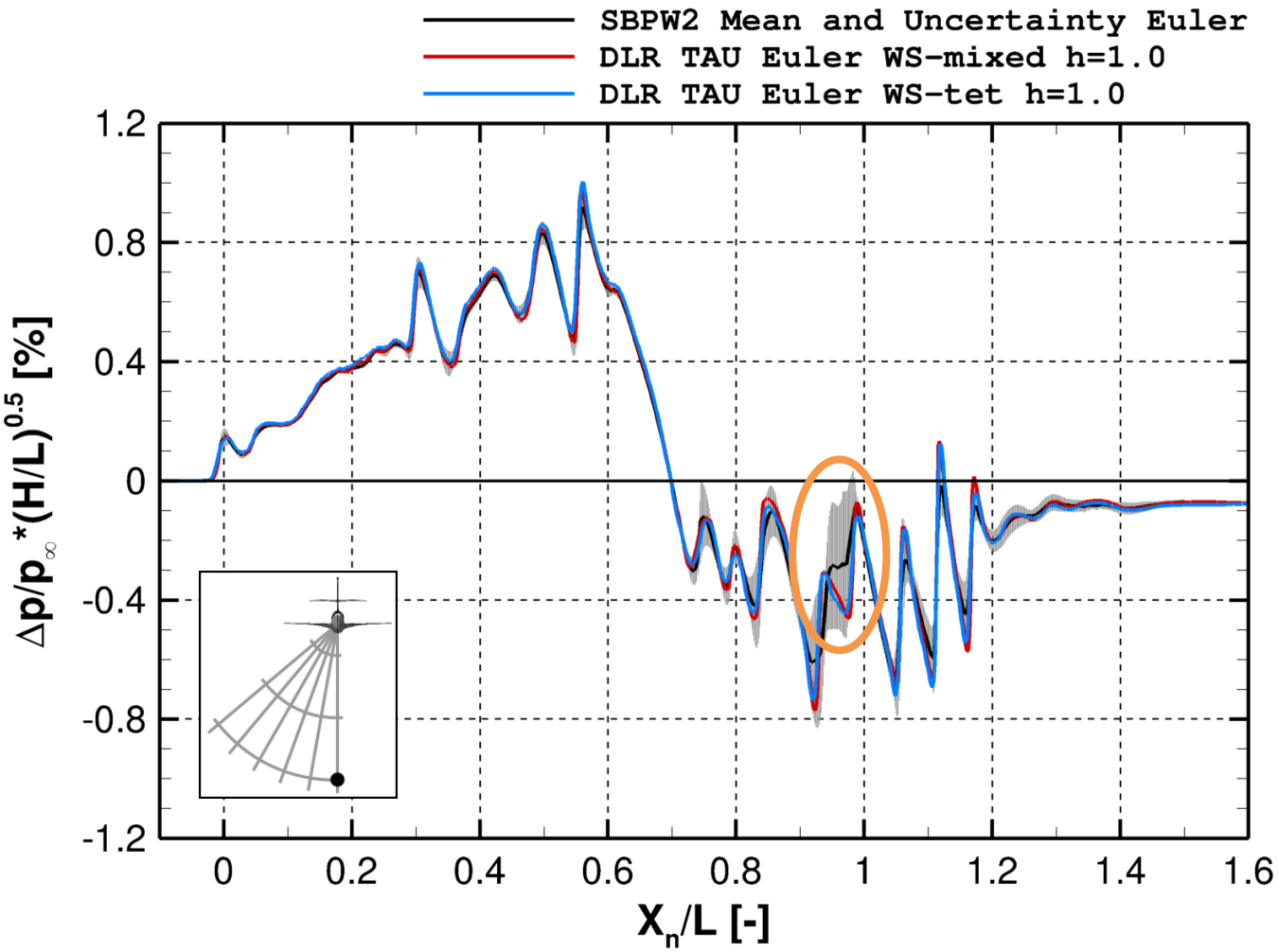

- Pressure signatures for fine mixed-element and fine purely tetrahedral grid very similar
- Both match the workshop mean well
- Differences at the reflections of the nacelle leading edge shock due to averaging

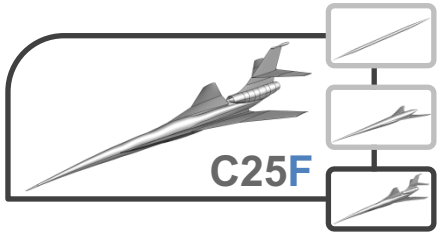

Results C25D flow-through

Same Grid Comparison (H/L=5, PHI=0)

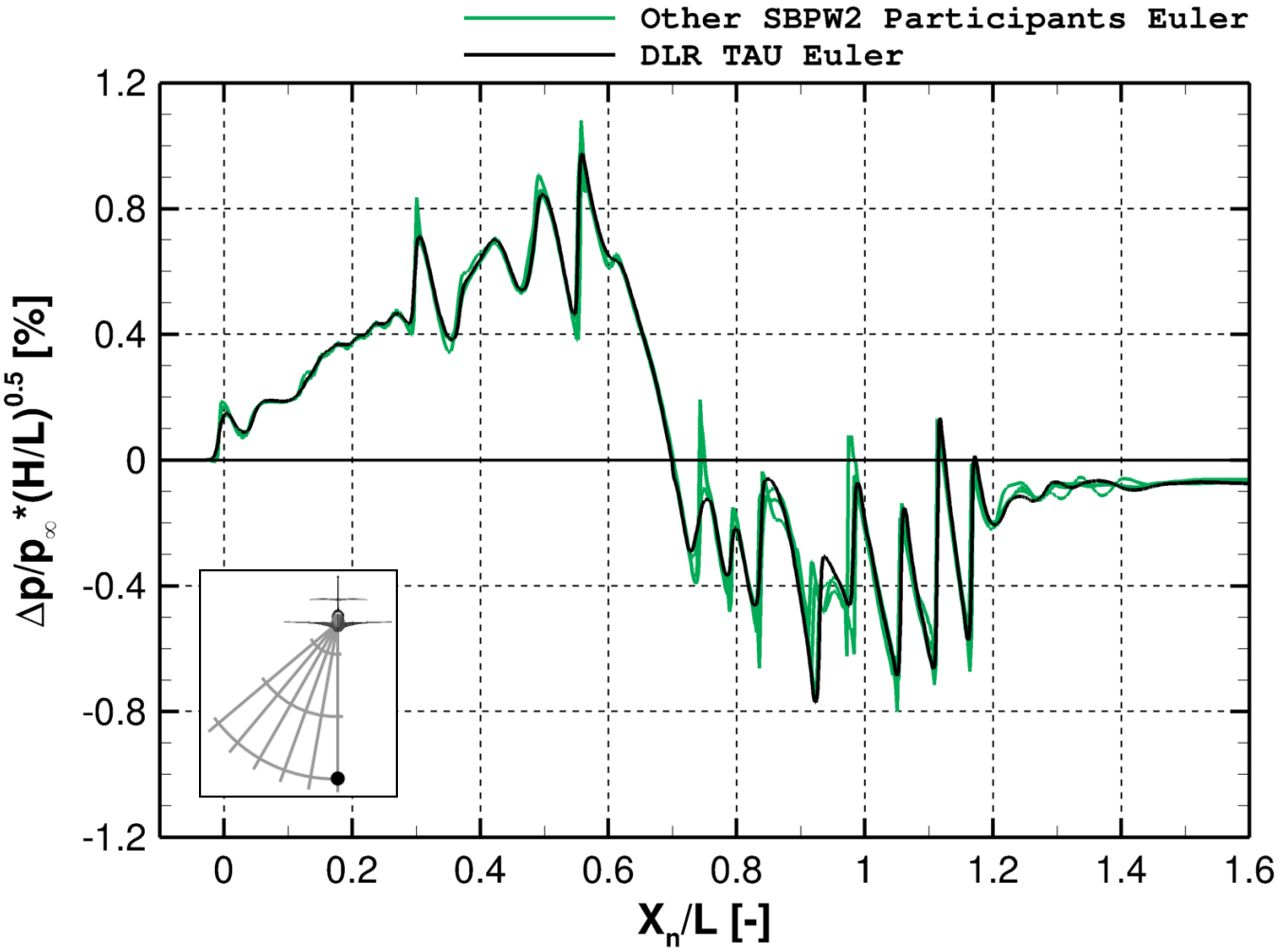

- Pressure magnitudes slightly lower for TAU code compared to other participants' pressure signatures on the same grid
- Positions of shocks and expansions in good agreement

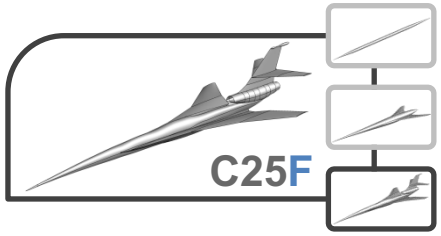

Results C25D flow-through

Euler and RANS Simulations (H/L=5, PHI=0)

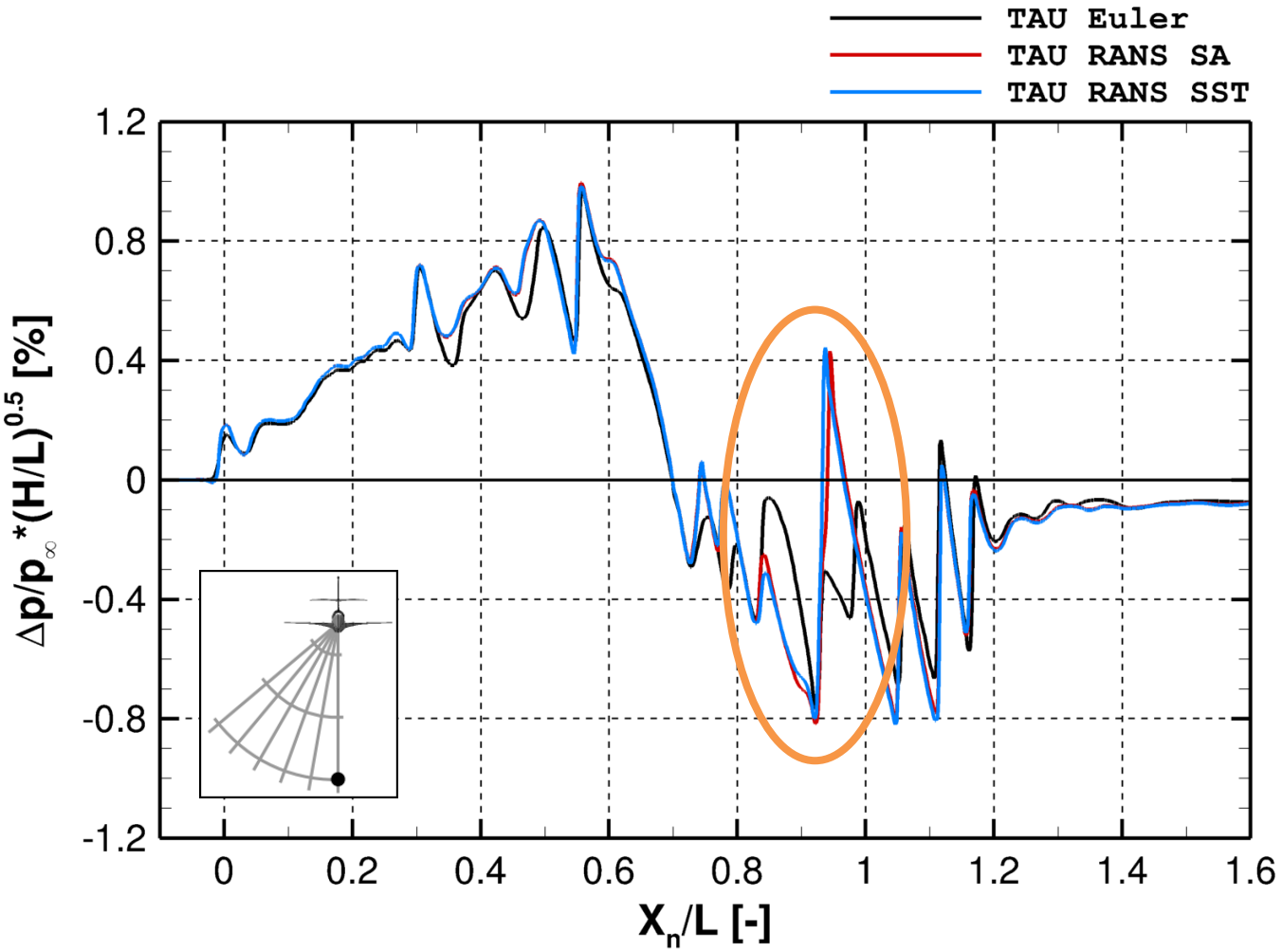

- Small influence of turbulence model
- Larger pressure magnitudes at initial compression for RANS simulations due to effective thickening of the body through the boundary layer
- Significant differences at nacelle inlet shock reflections

Results C25D powered

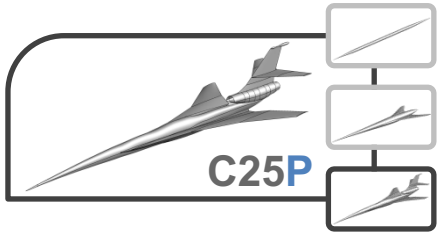

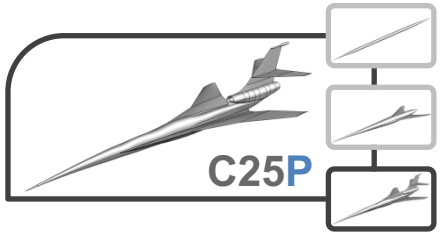

Results C25D powered

Pressure Signature Convergence (H/L=5, PHI=0)

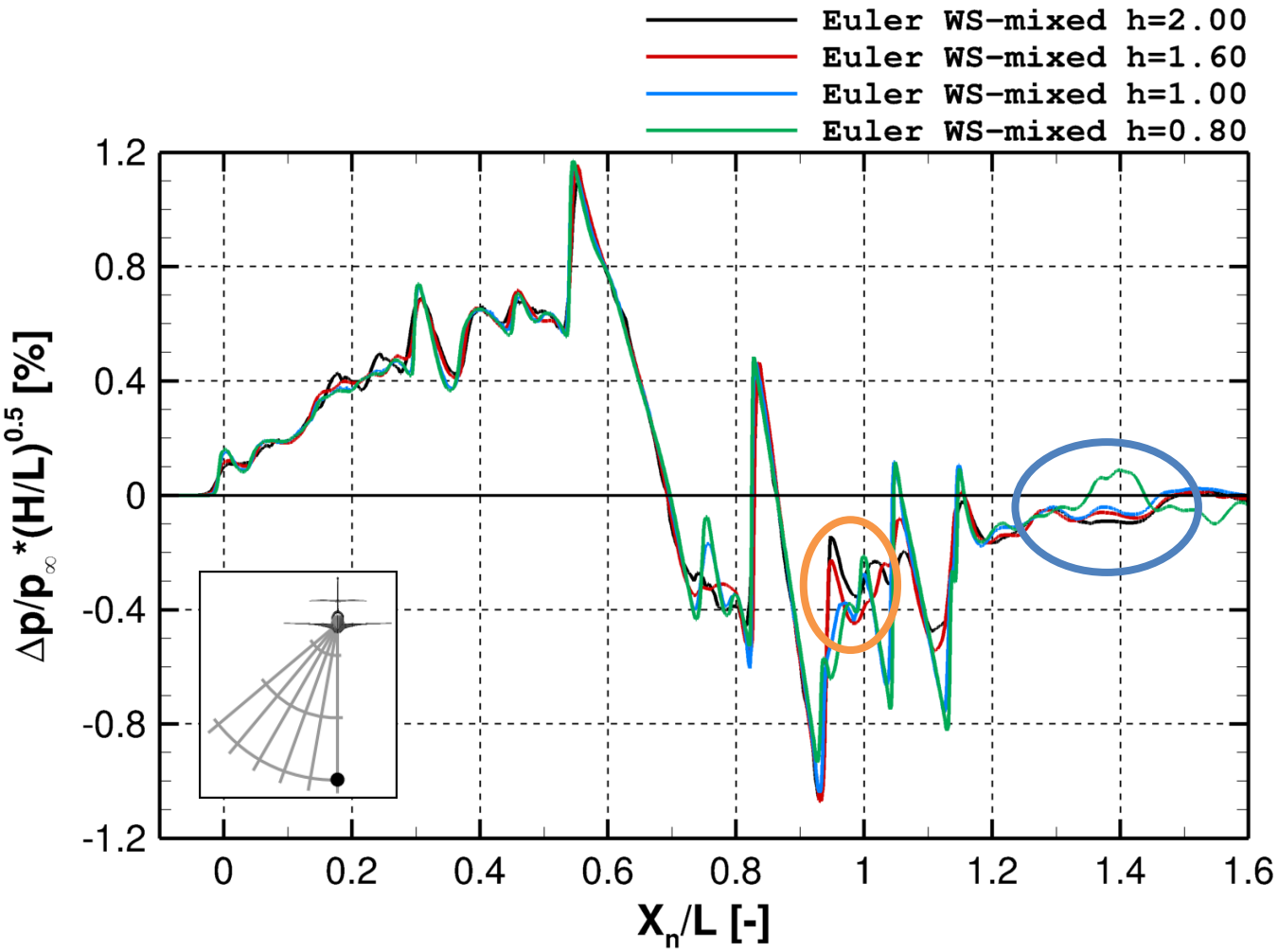

- Largest differences at nacelle inlet shock reflections
- Similar to the C25F
- Artificial compression due to grid coarsening in the plume

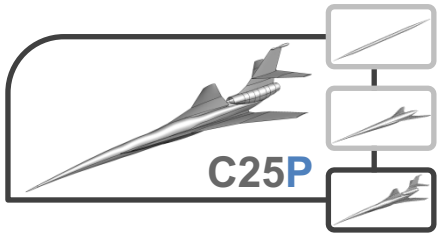

Results C25D powered

TAU Signatures and SBPW2 Statistics (H/L=5, PHI=0)

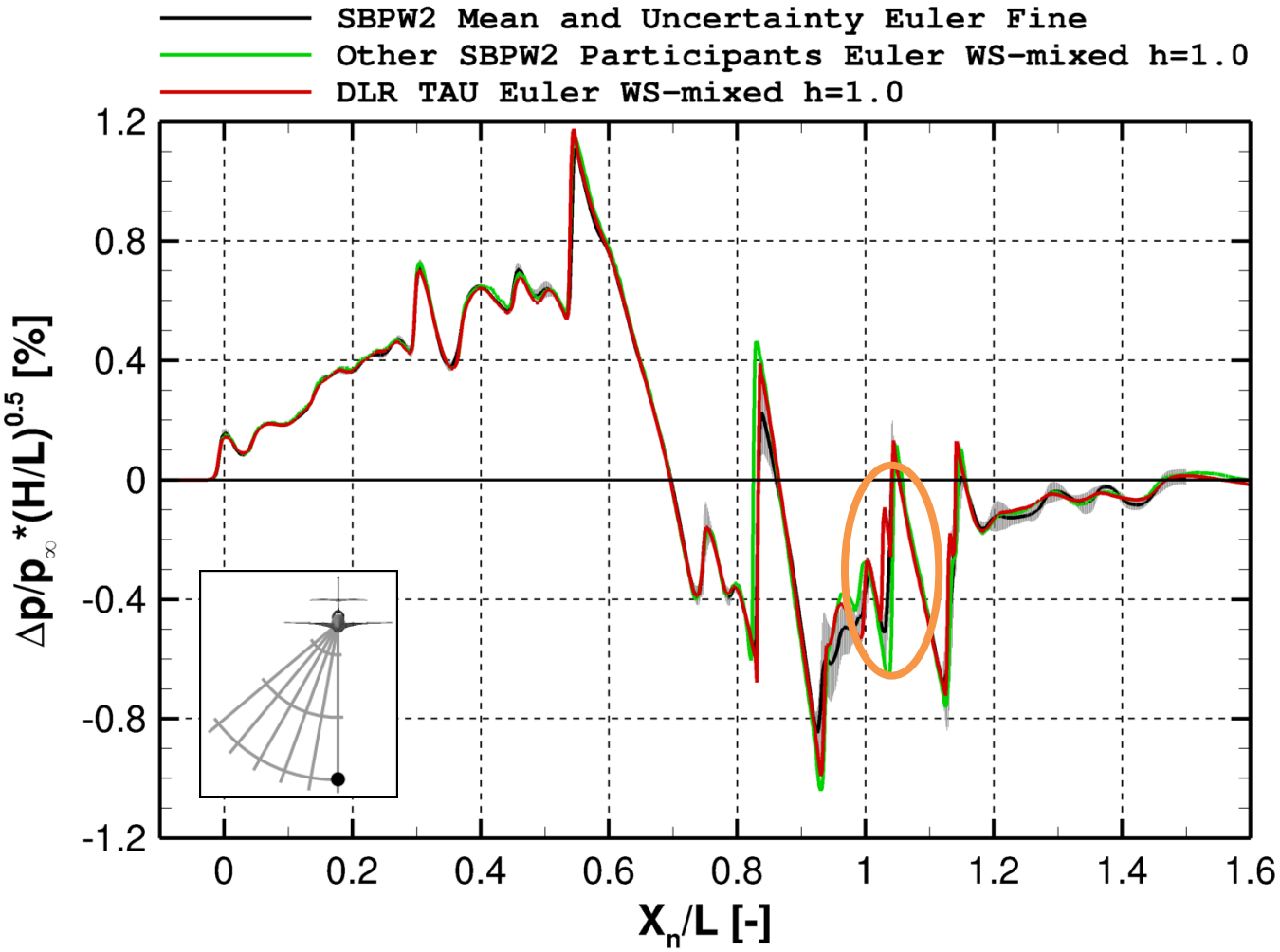

- TAU pressure signature matches the workshop mean
- Slight differences at engine outlet

Summary and Conclusions

- Euler and RANS simulations performed with the DLR TAU code for 38 workshop-provided and CENTAUR-generated grids

- Positions of shocks and expansions
  - Similar for grids with medium to fine resolution
  - Different for very coarse grids
- Pressure magnitudes at shocks and expansions
  - Higher for fine grids compared to coarse grids (less dissipative)
  - Higher for purely tetrahedral grids compared to mixed-element grids
- Fine grids needed to capture reflections of C25D nacelle LE shock

- Influence of viscosity larger than influence of grid setup

- TAU pressure signatures in good agreement to results of other codes

→ Best-practice for near-field prediction with the DLR TAU code improved

→ Robust and fast pressure signature prediction for simplified as well as complex cases

Outlook

- Improving best-practice for mesh generation for viscous simulations
- Ground propagation and ground loudness calculation
- Design and optimization of a supersonic configuration towards low boom – low drag

Acknowledgements

- Committee of the AIAA Sonic Boom Prediction Workshops for providing geometries, grids and statistical data

Backup Slides

Cases Analyzed and Grids Used

CENTAUR-generated Grids for JWB case

- Hybrid Euler grids
  - Unaligned tetrahedrons in cylindrical inner part
  - Mach cone aligned hexahedrons in farfield

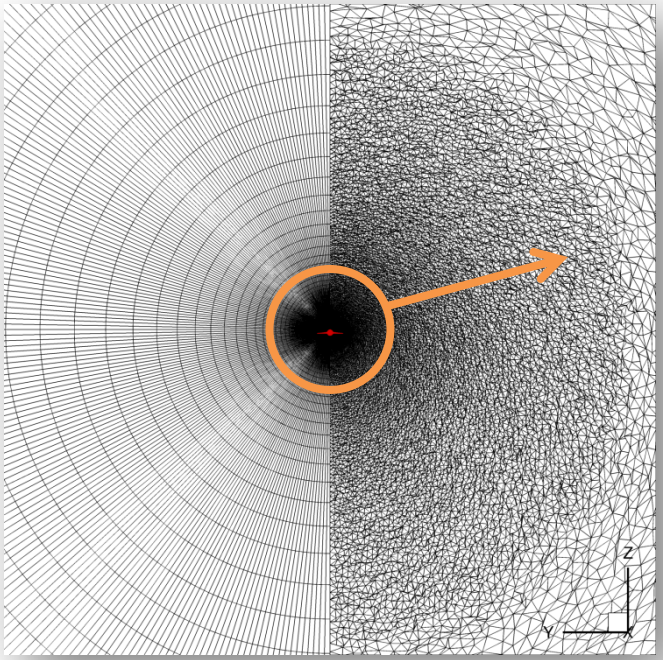

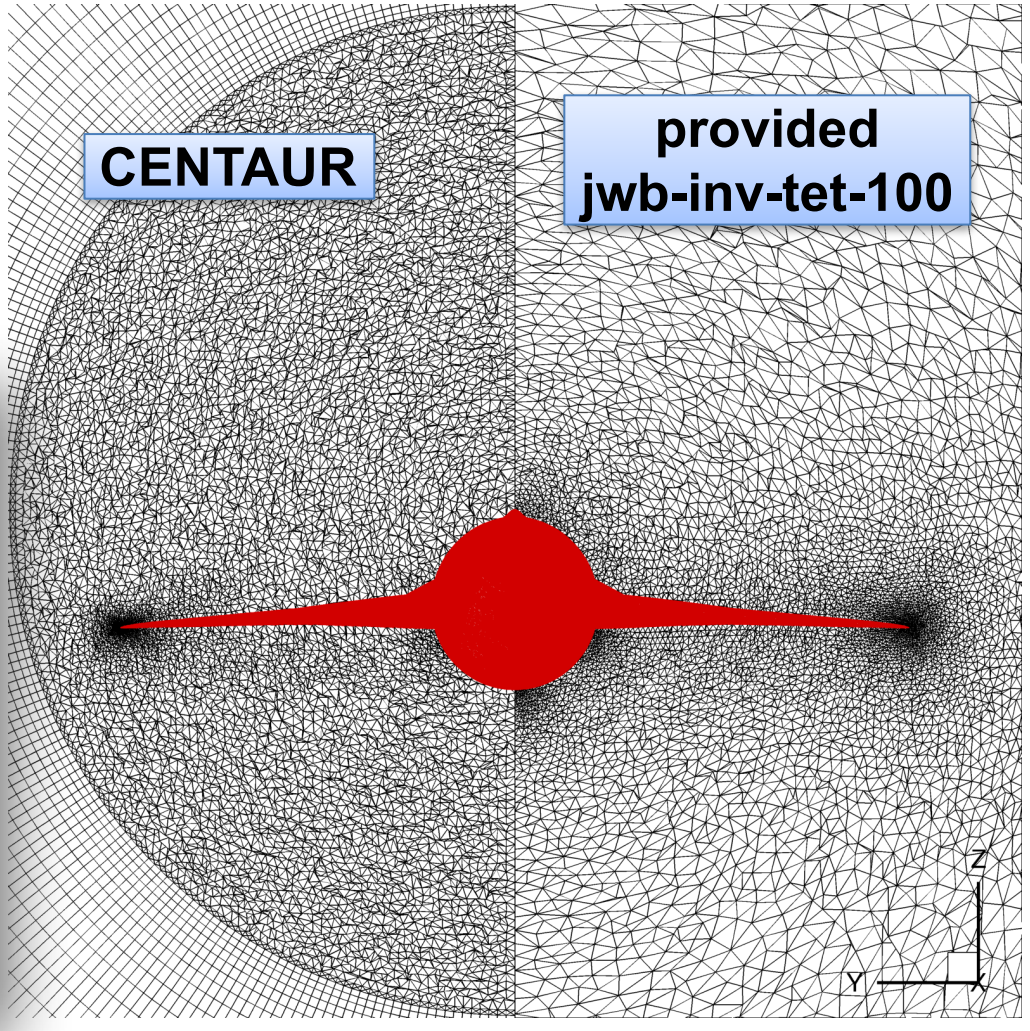

Cases Analyzed and Grids Used

CENTAUR-generated Grids for JWB case

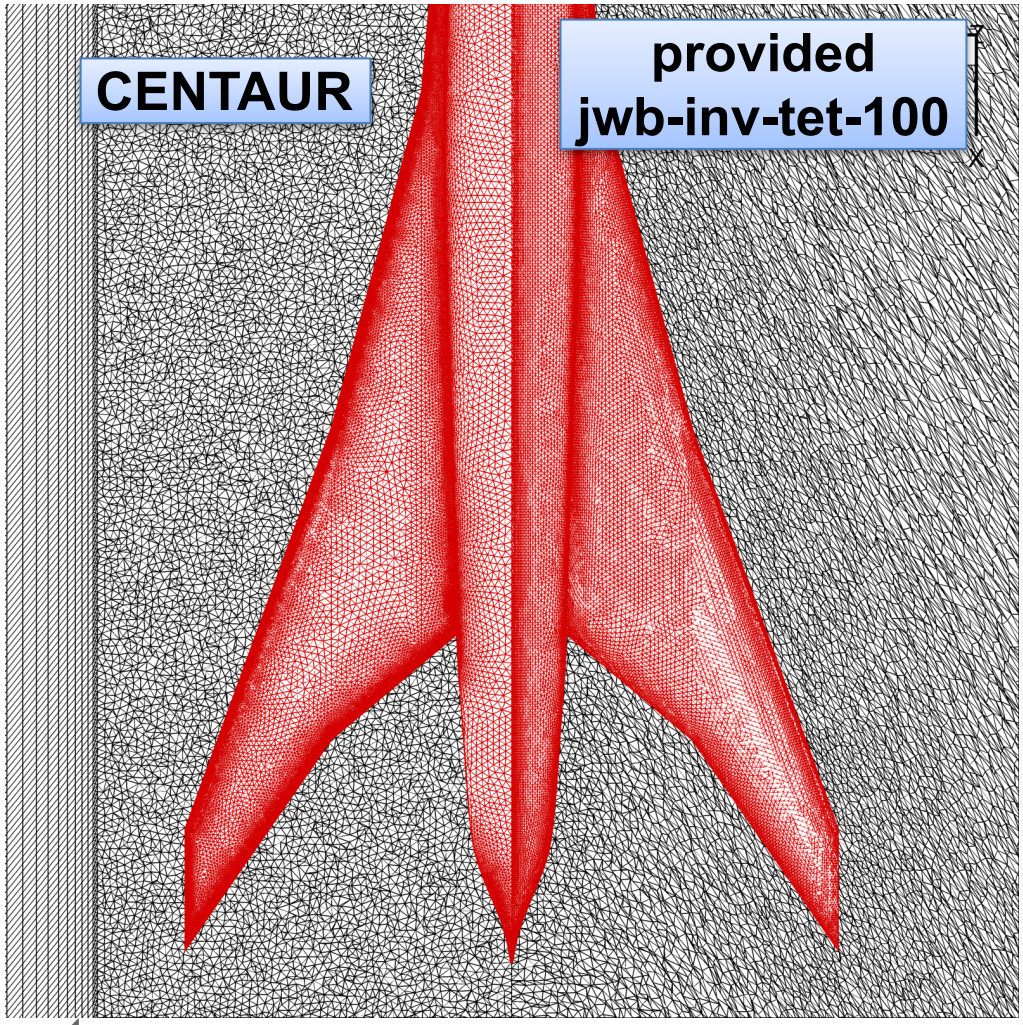

- Surface resolution (triangles) of coarse CENTAUR grid similar to coarse workshop-provided grid

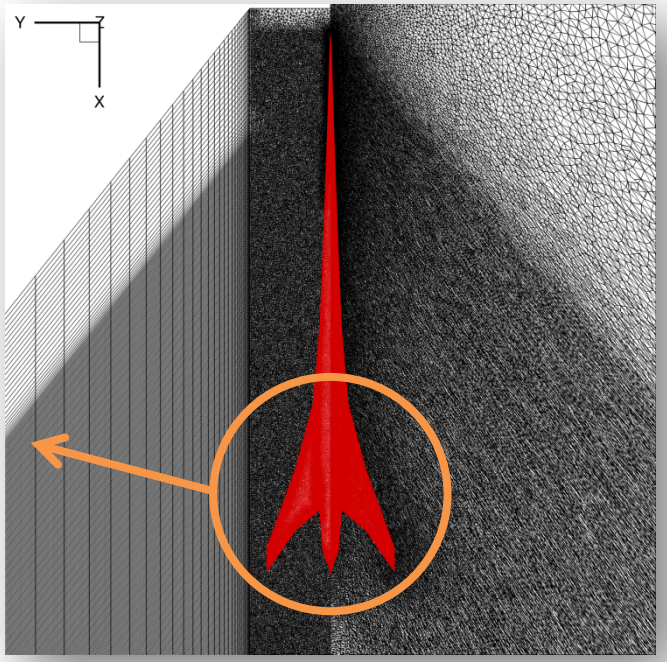

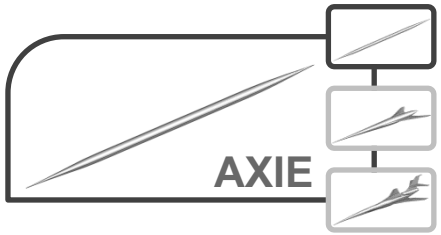

Grids

AXIE

CENTAUR-generated

- Core grid
  - ➢ Tetrahedra
- Collar grid
  - ➢ Hexahedra

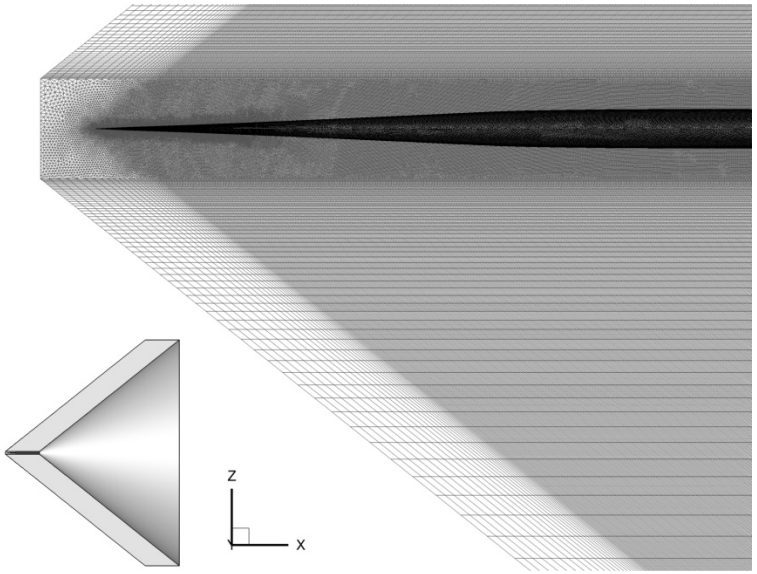

Workshop-provided

- Core grid
  - ➢ Tetrahedra
- Collar grid
  - ➢ Prisms/ Tetrahedra

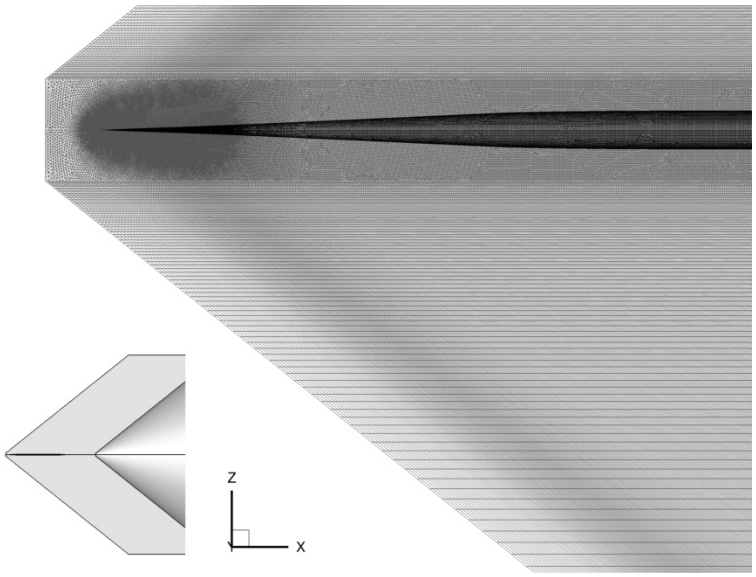

Results AXIE

Normalization and Pressure Signature Extraction

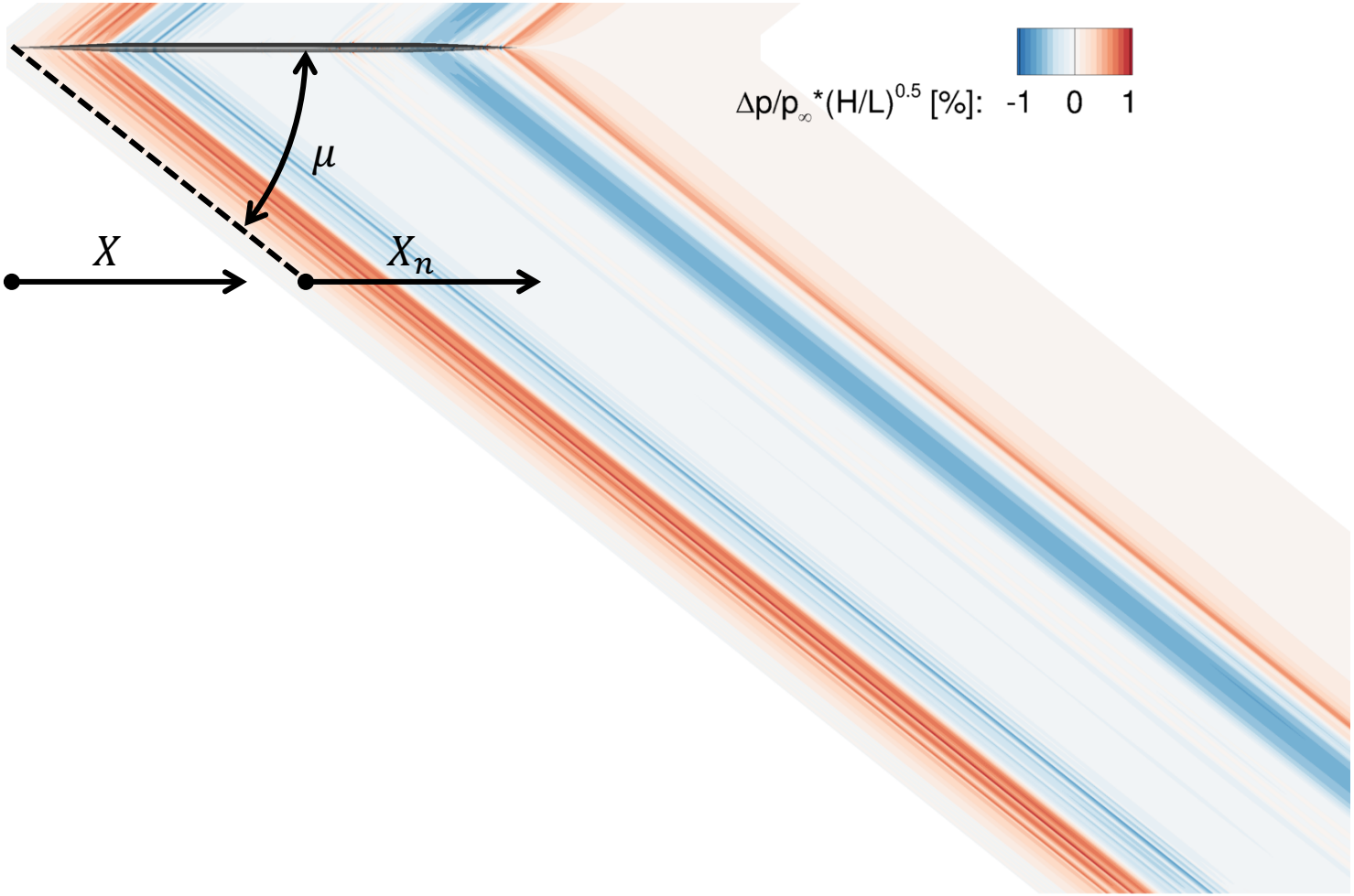

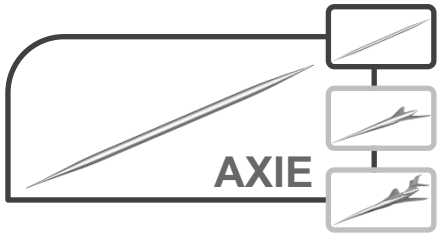

Results AXIE

Normalization and Pressure Signature Extraction

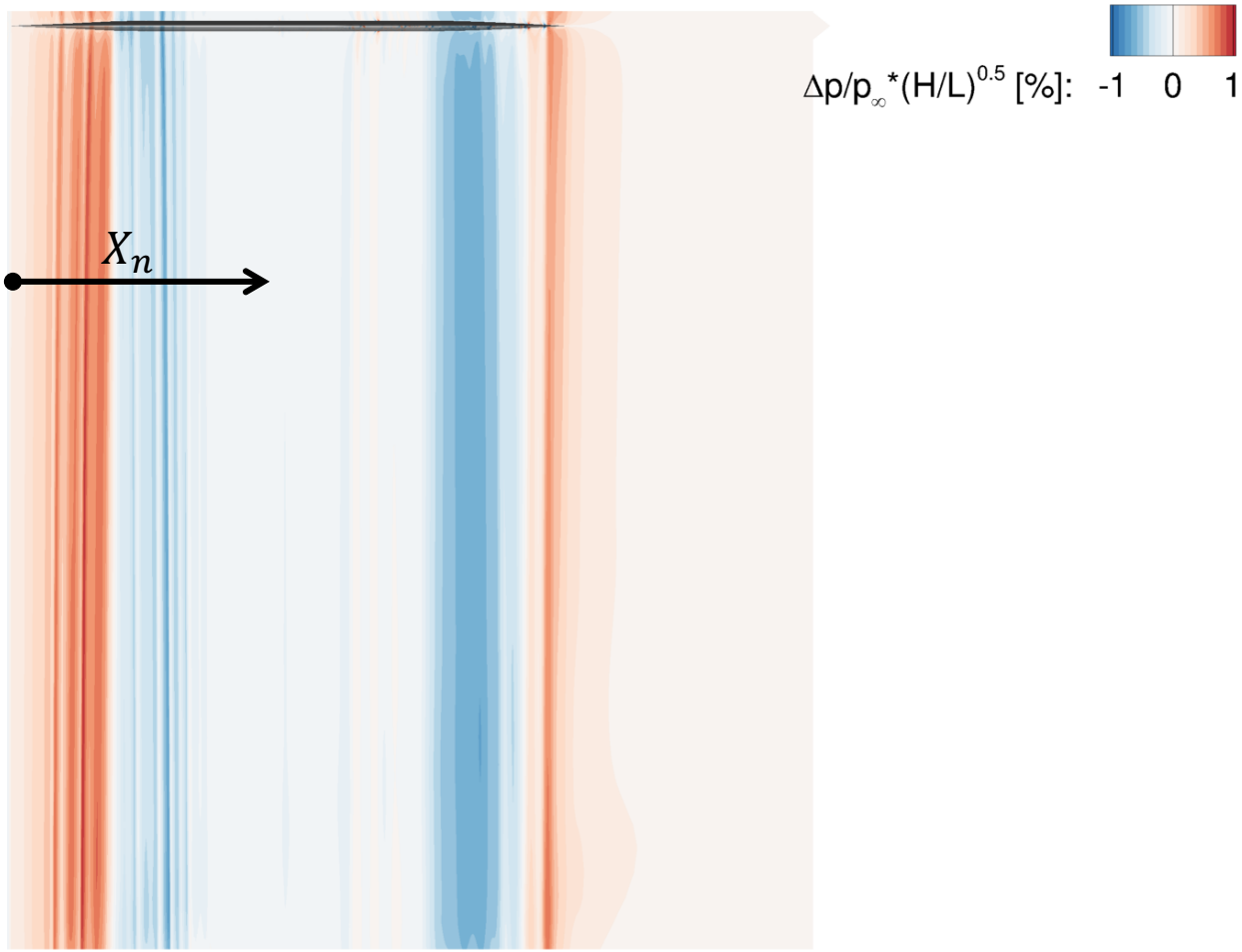

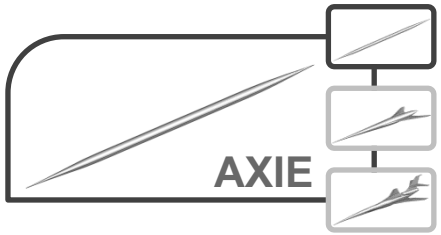

Results AXIE

Normalization and Pressure Signature Extraction

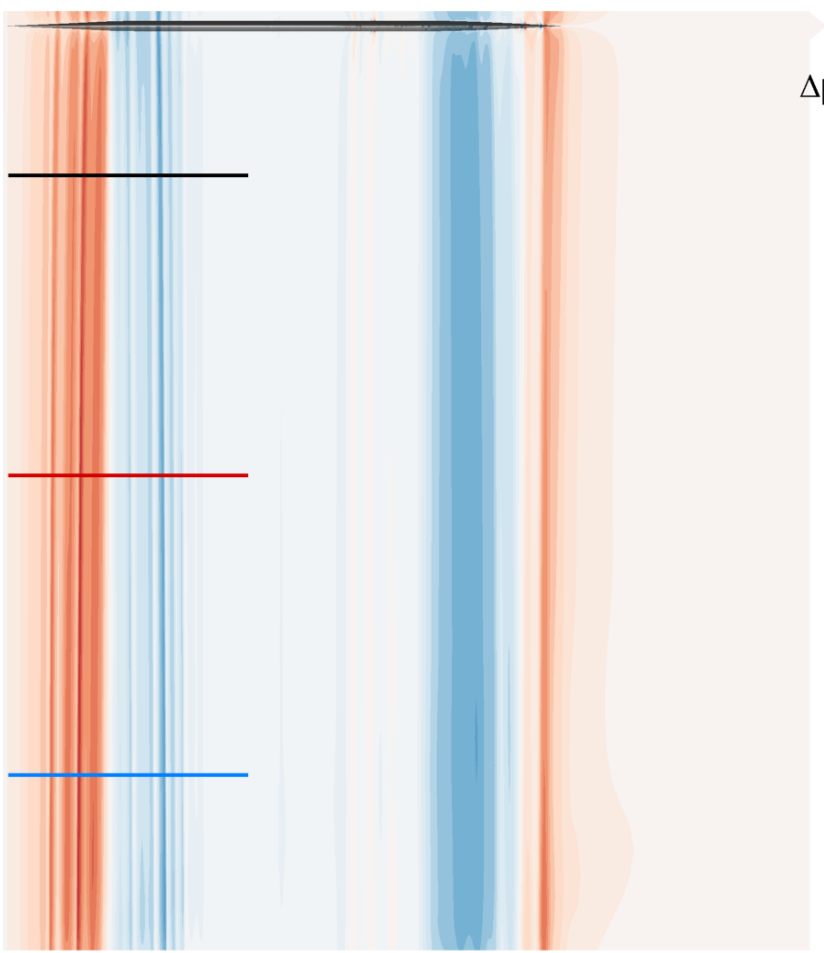

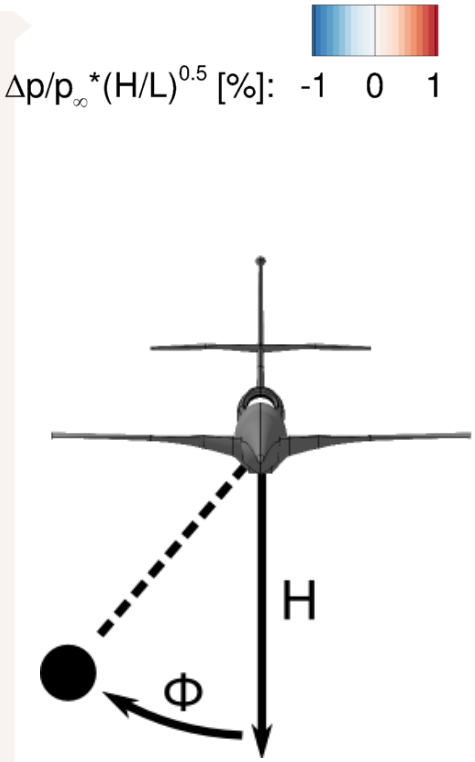

Results AXIE

Normalization and Pressure Signature Extraction

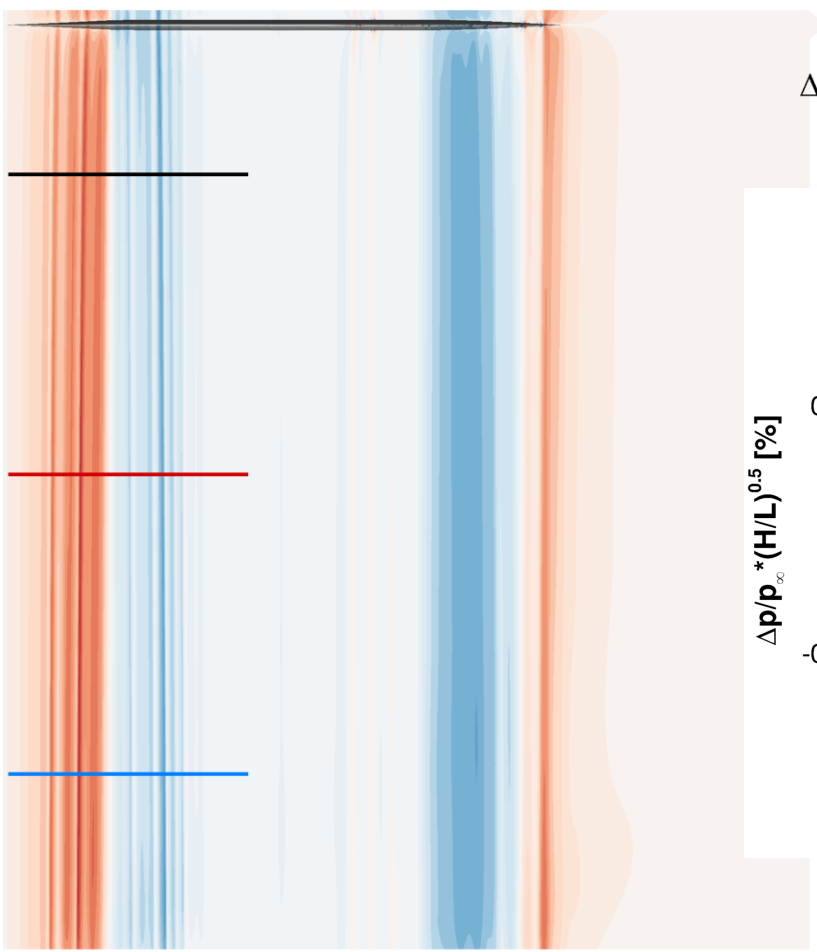

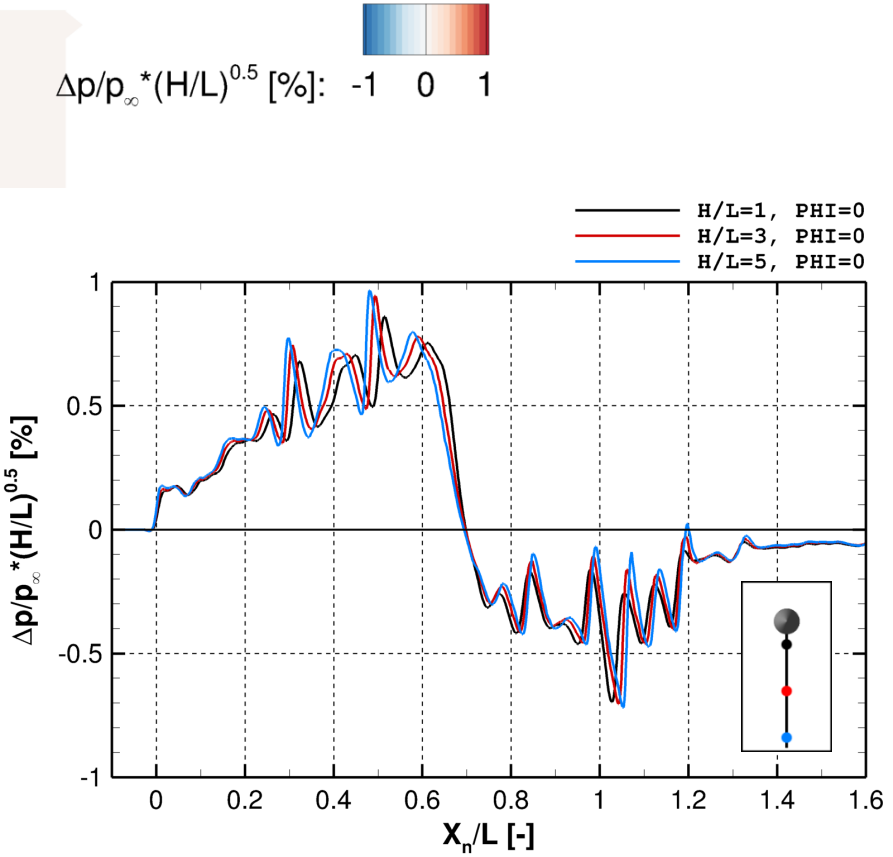

Results AXIE

Least Squares Reconstruction of Gradients

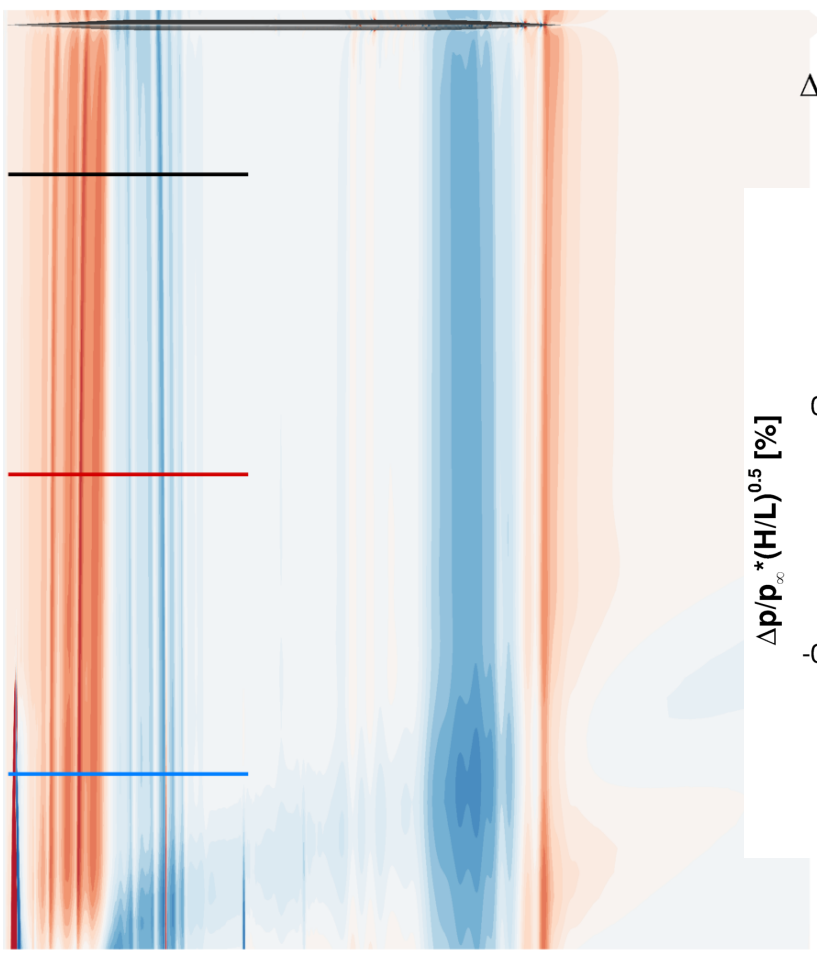

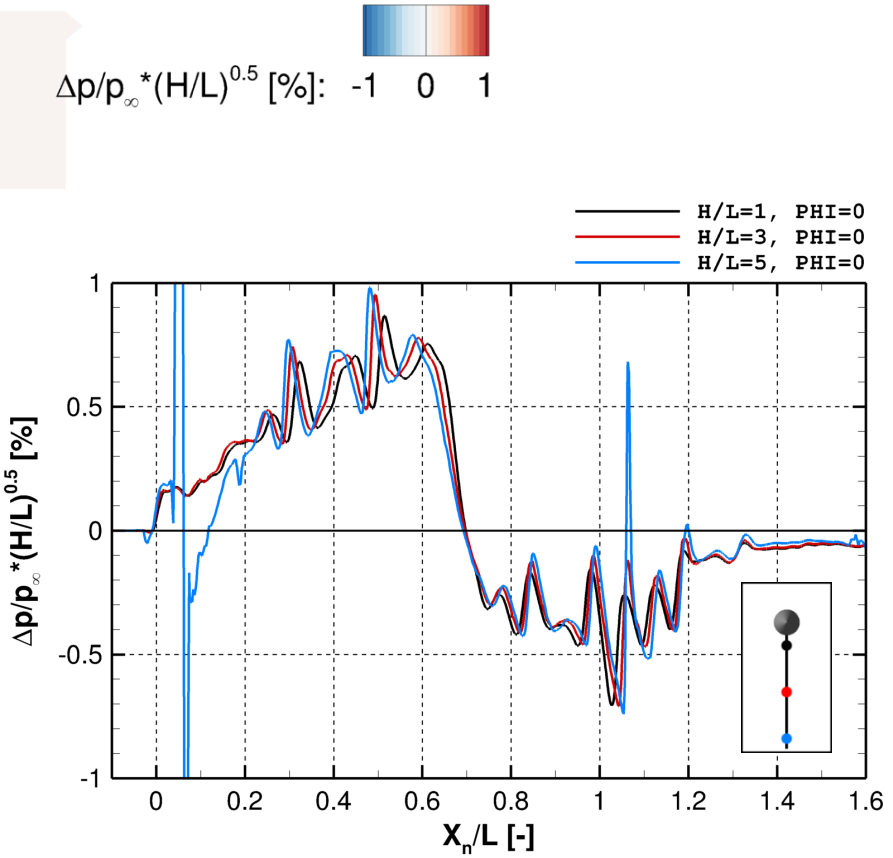

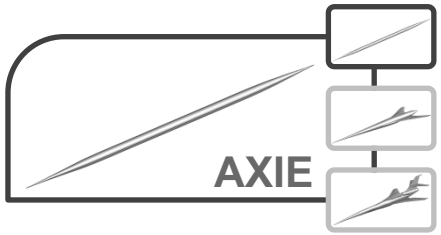

Results AXIE

Least Squares vs Green Gauss

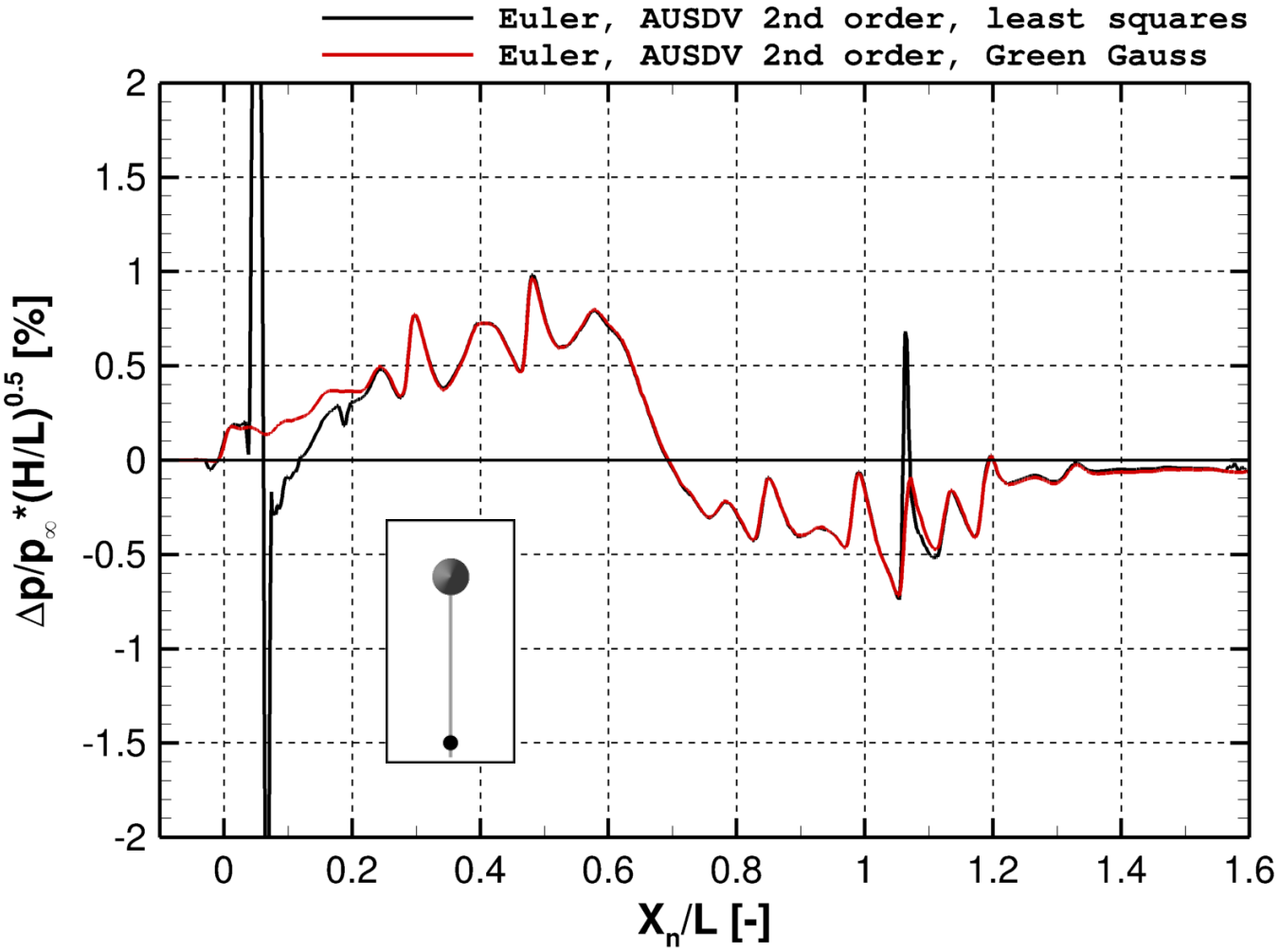

Highlights

Inflow and Farfield Boundary Condition Changes

- Supersonic inflow/outflow
  - Compute boundary fluxes with approximate Riemann solver instead of setting conservative variables at the boundary
  - The gradients of all variables are set to zero in the direction normal to the boundary

- Farfield
  - The farfield fluxes are evaluated via a characteristic method that is in line with the interior face-flux computation.
  - The corresponding flux parameters are inherited from the central, matrix-dissipative scheme

- Convergence improved as side effect (more robust start, significantly less iterations needed and residual lowered by 1-2 orders of magnitude)

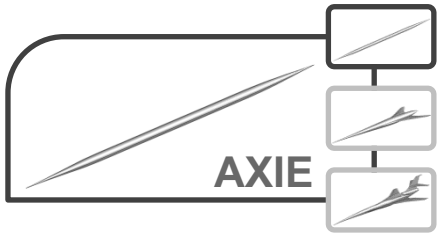

Results AXIE

Pressure Signature Convergence (H/L=5, PHI=0)

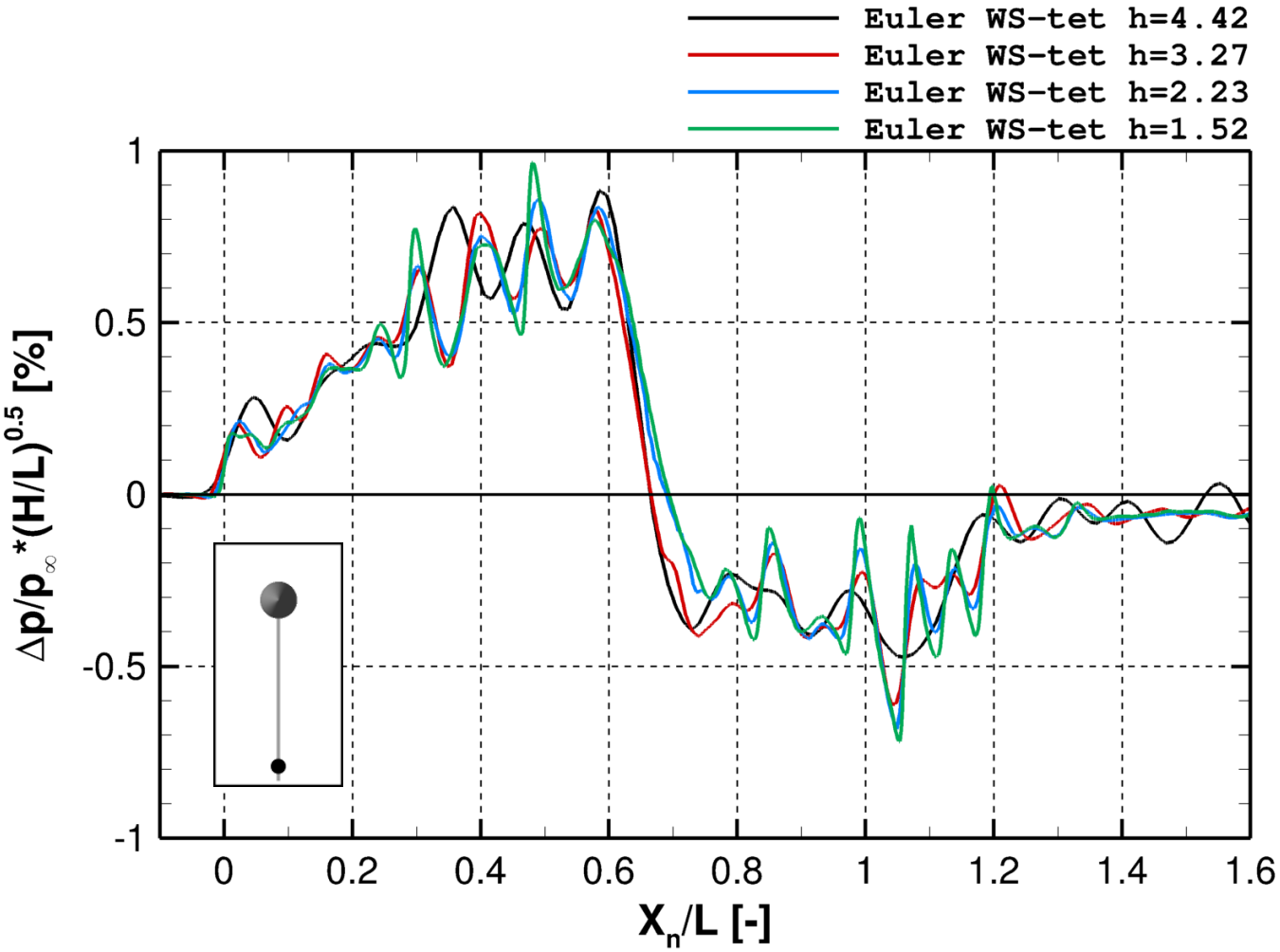

- Positions of shocks and expansions coincide for medium to fine grids
- Magnitudes are larger on fine grids (less dissipative)

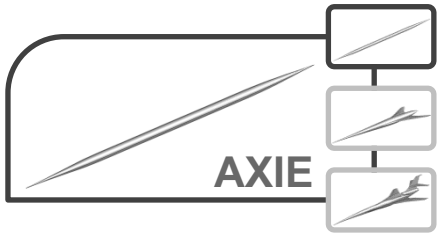

Results AXIE

TAU Signatures and SBPW2 Statistics (H/L=5, PHI=0)

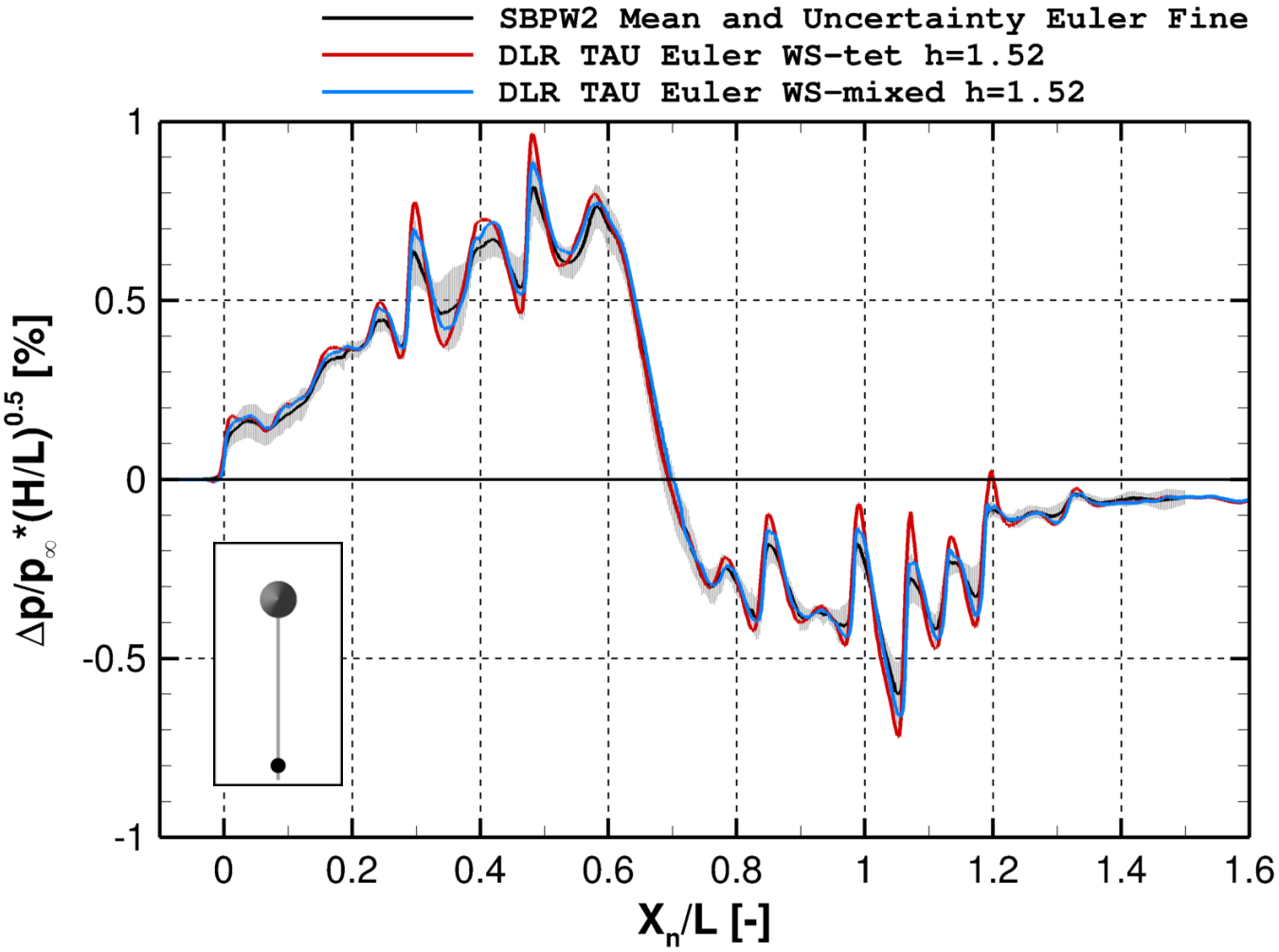

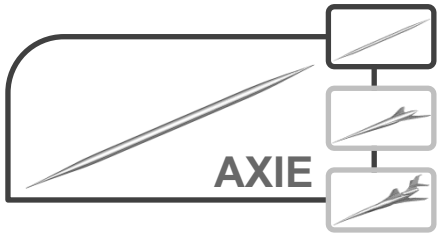

Results AXIE

Same grid

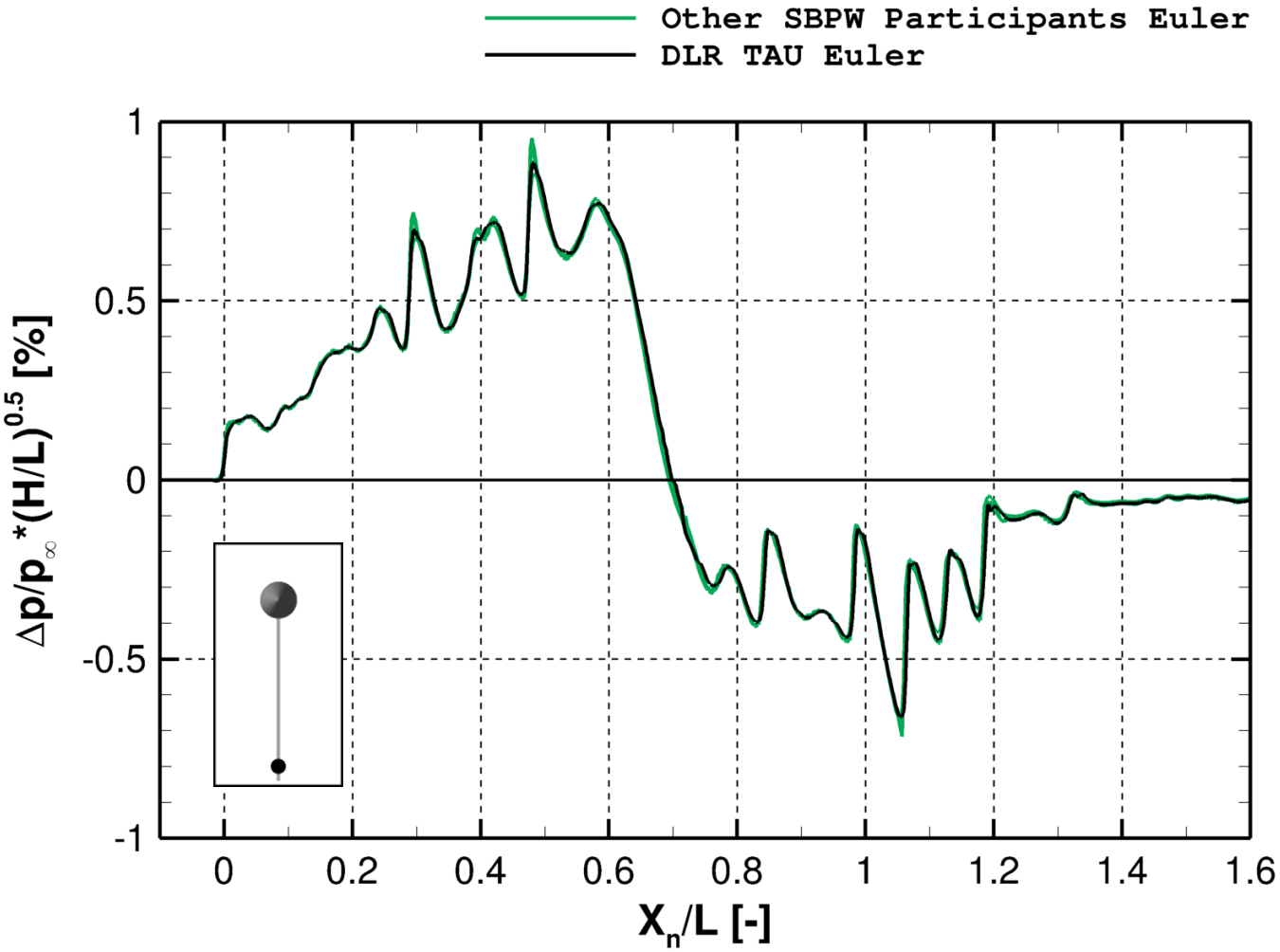

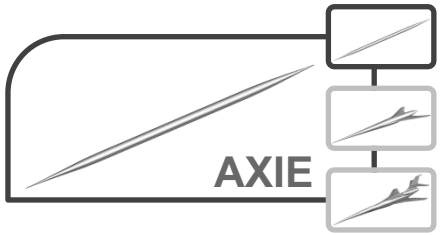

Results AXIE

Provided and CENTAUR-generated grid

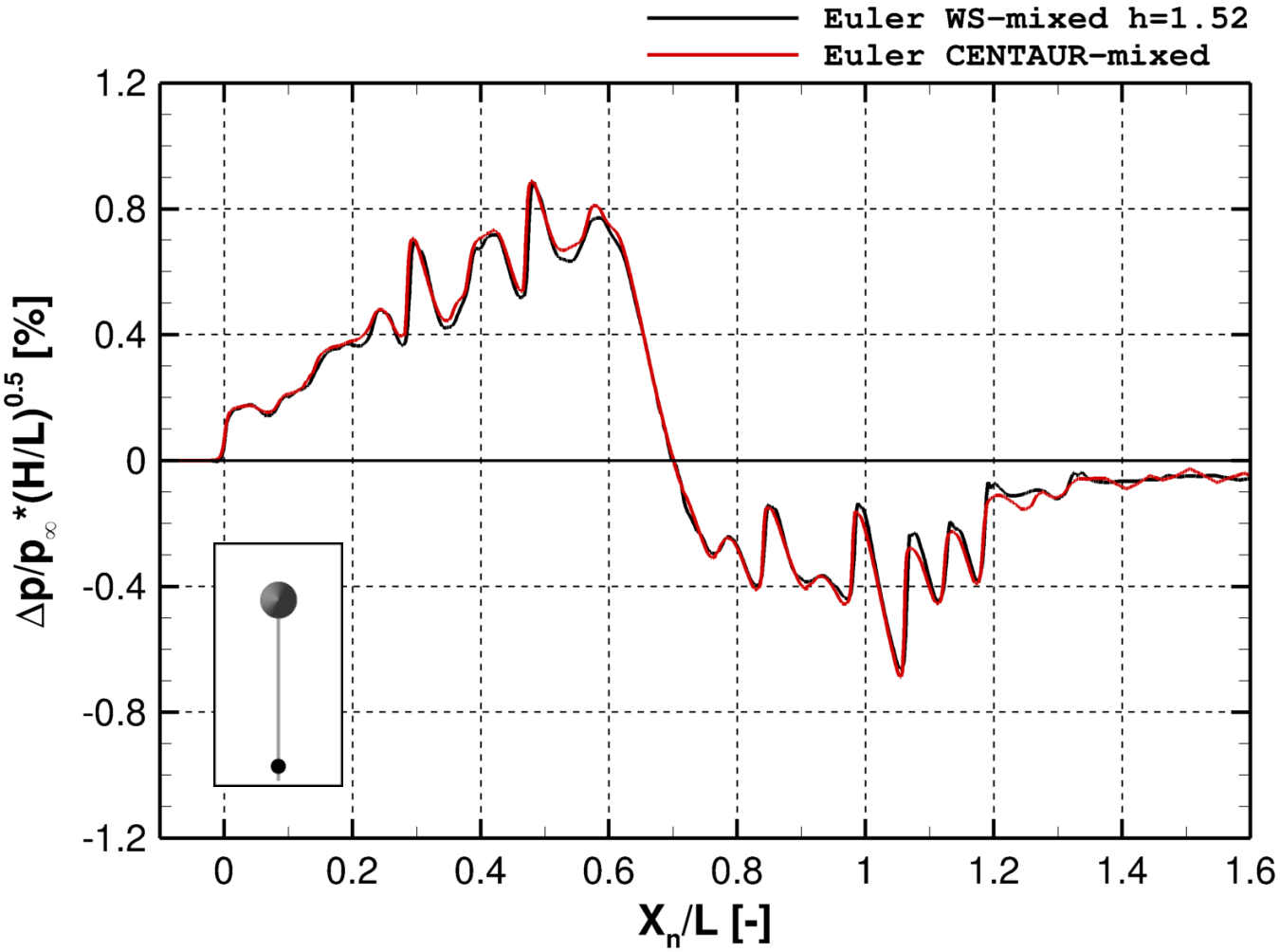

Results JWB

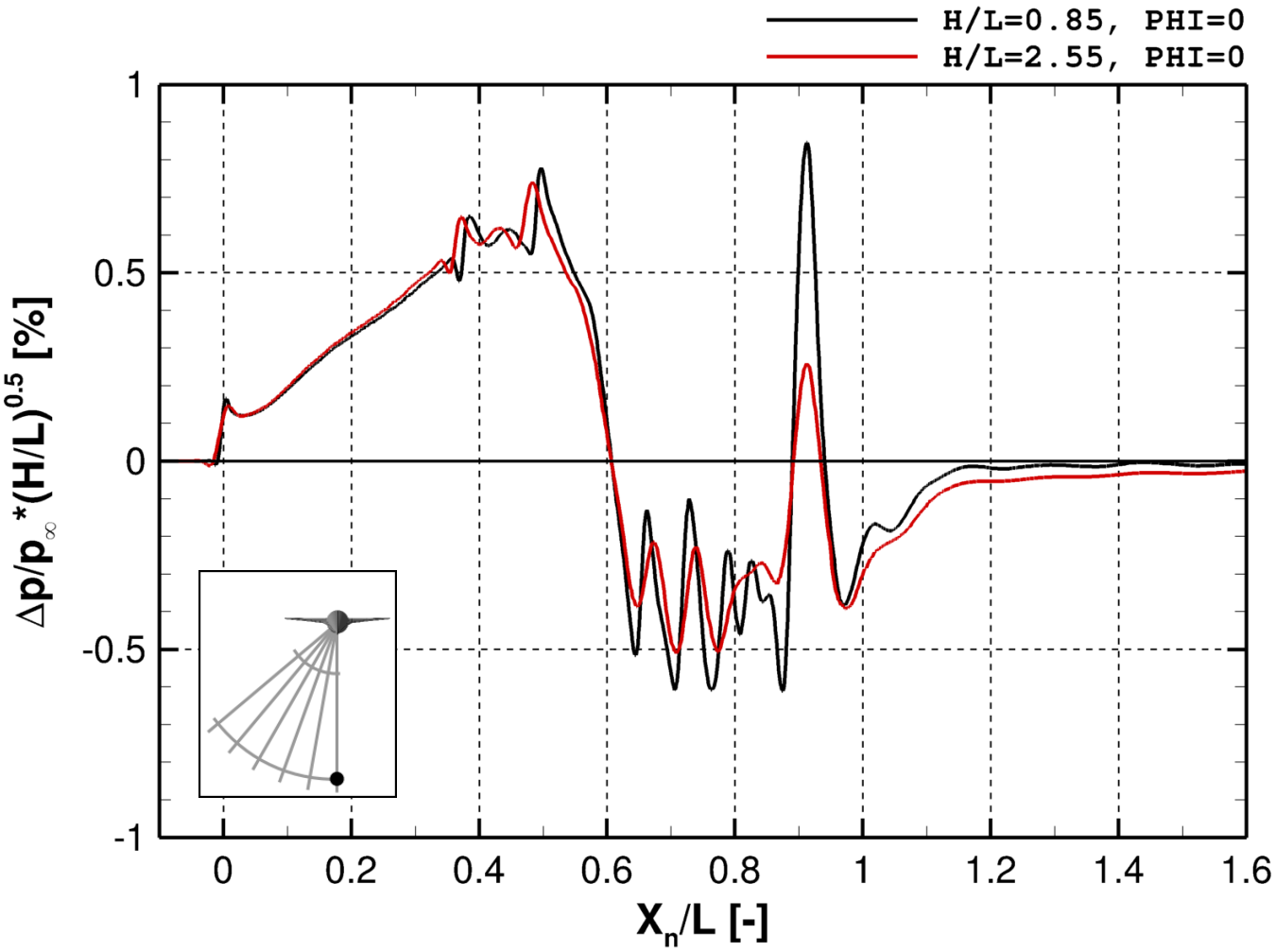
H/L=0.85, PHI=0
H/L=2.55, PHI=0
1
0.5
0
-0.5
-1
0
0.2
0.4
0.6
0.8
1
1.2
1.4
1.6
Δp/p∞*(H/L)^0.5 [%]
Xn/L [-]

Results JWB

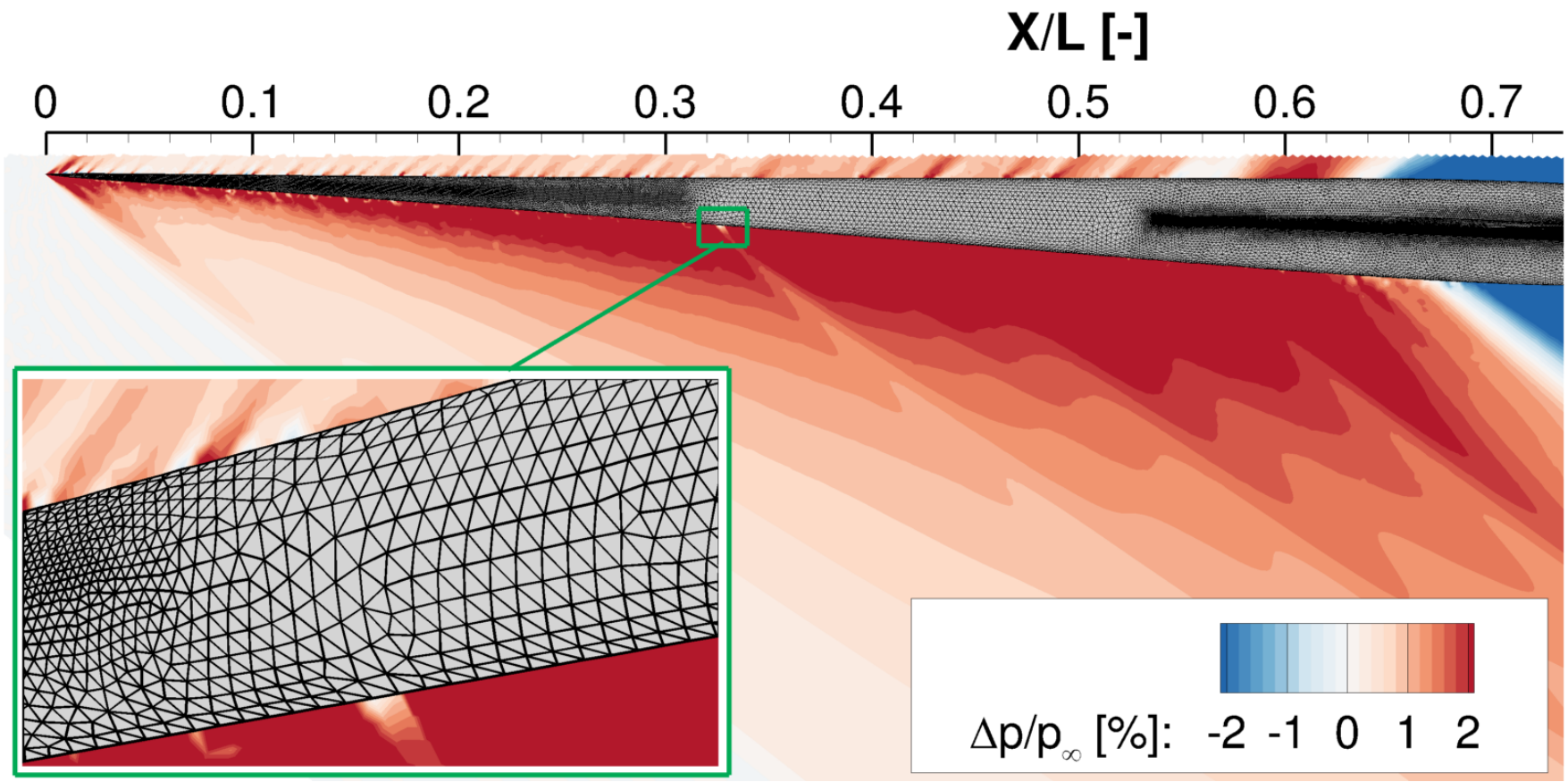

Results JWB

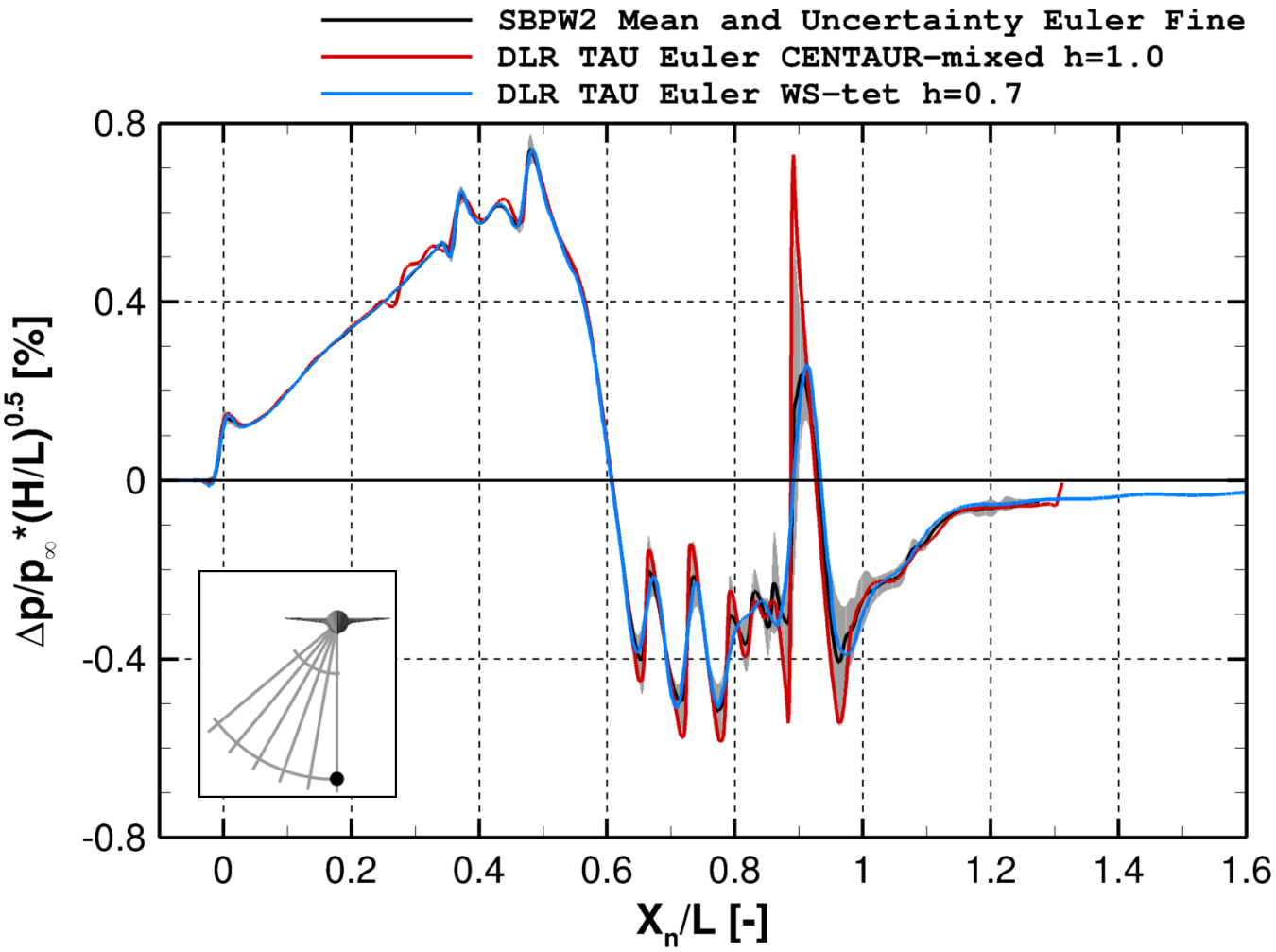
SBPW2 Mean and Uncertainty Euler Fine
DLR TAU Euler CENTAUR-mixed h=1.0
DLR TAU Euler WS-tet h=0.7
0.8
0.4
0
-0.4
-0.8
0
0.2
0.4
0.6
0.8
1
1.2
1.4
1.6
Δp/p∞*(H/L)^0.5 [%]
Xn/L [-]

Results JWB

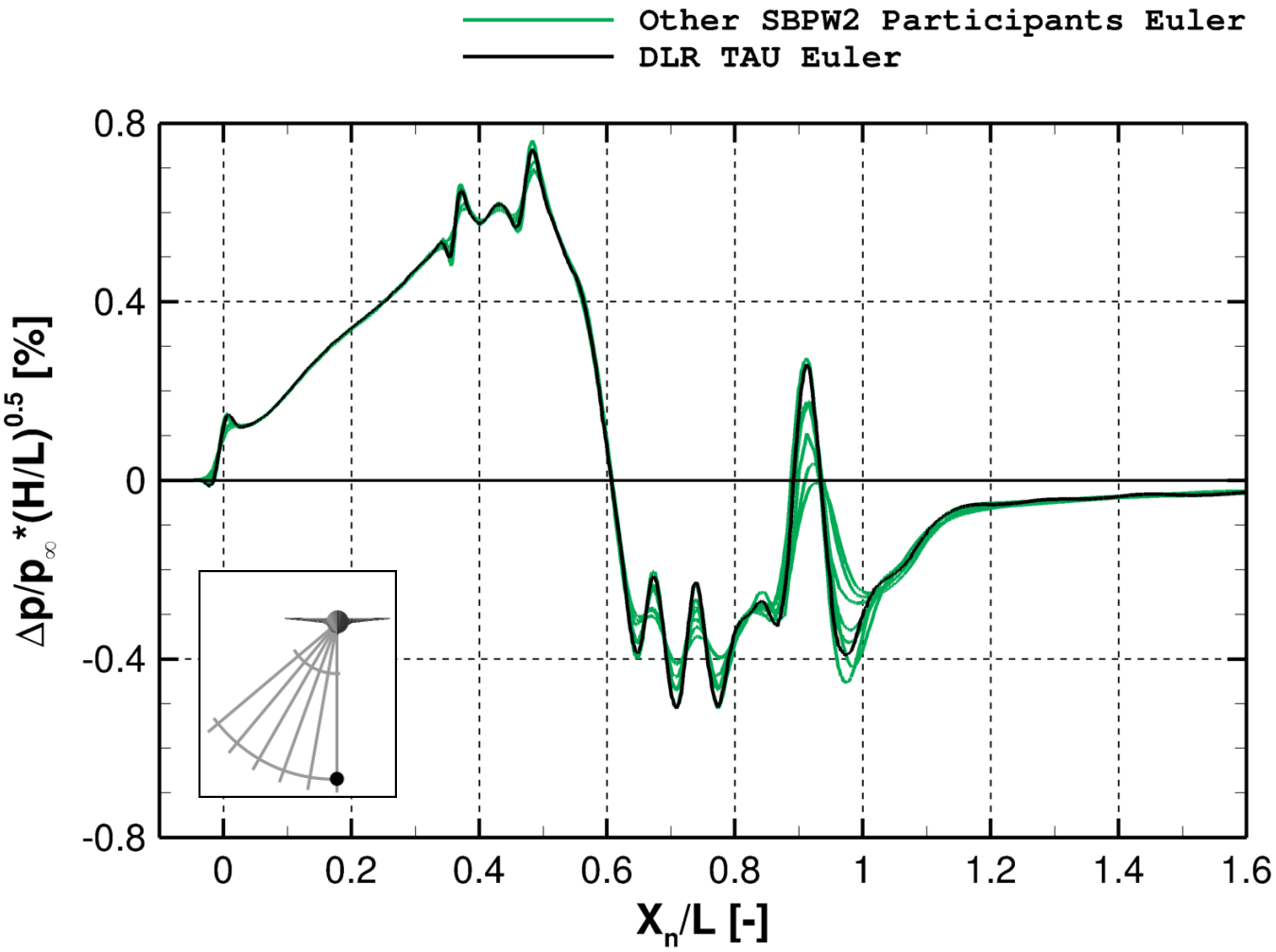
Other SBPW2 Participants Euler
DLR TAU Euler
0.8
0.4
0
-0.4
-0.8
0
0.2
0.4
0.6
0.8
1
1.2
1.4
1.6
Δp/p∞*(H/L)^0.5 [%]
Xn/L [-]

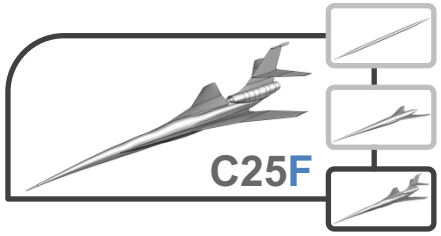

Results C25D flow-through

On-track Pressure Signatures (PHI=0)

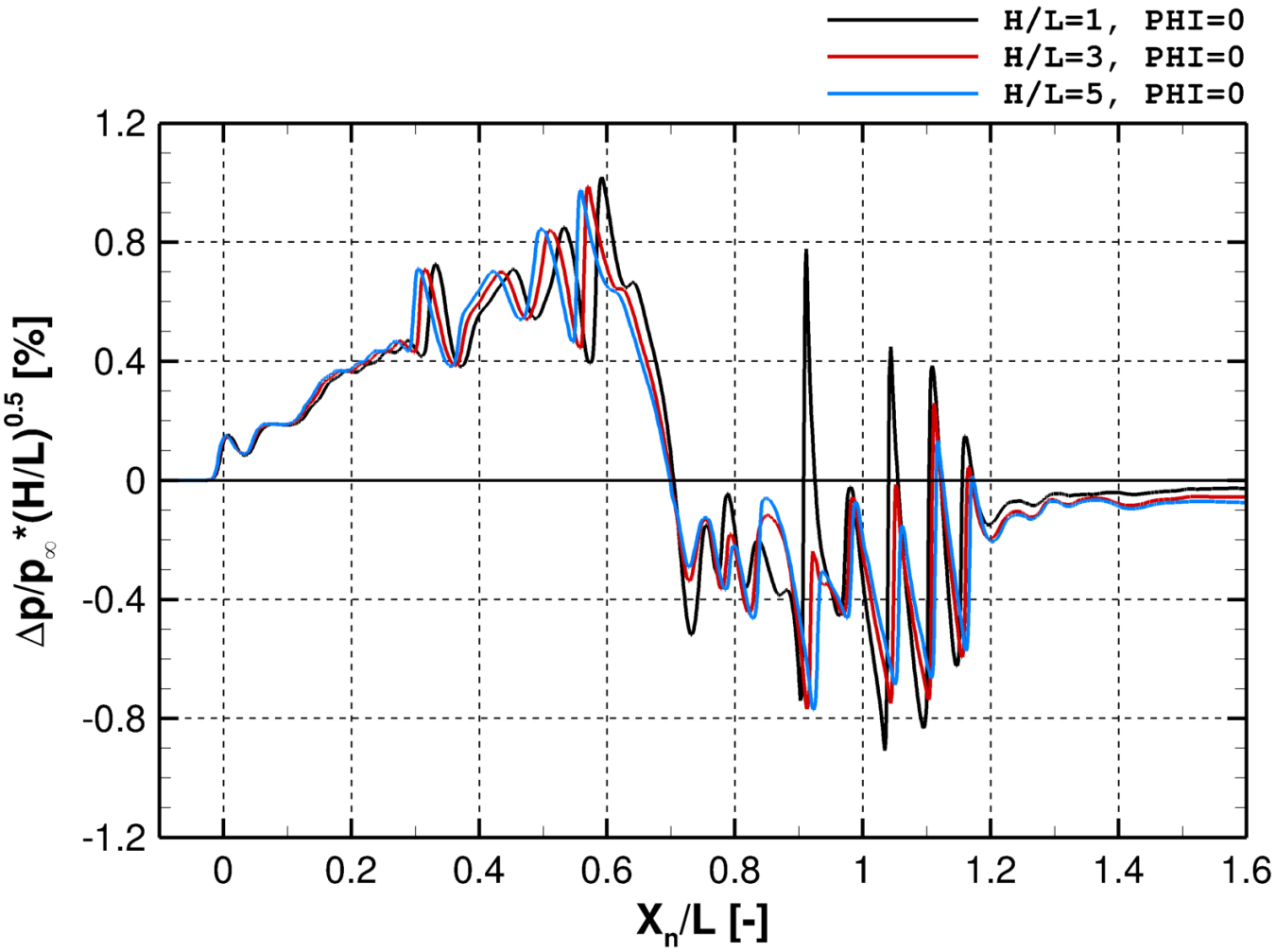

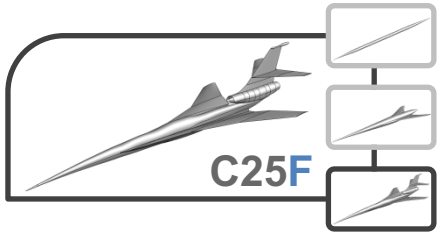

Results C25D flow-through

Off-track Pressure Signatures (H/L=5)

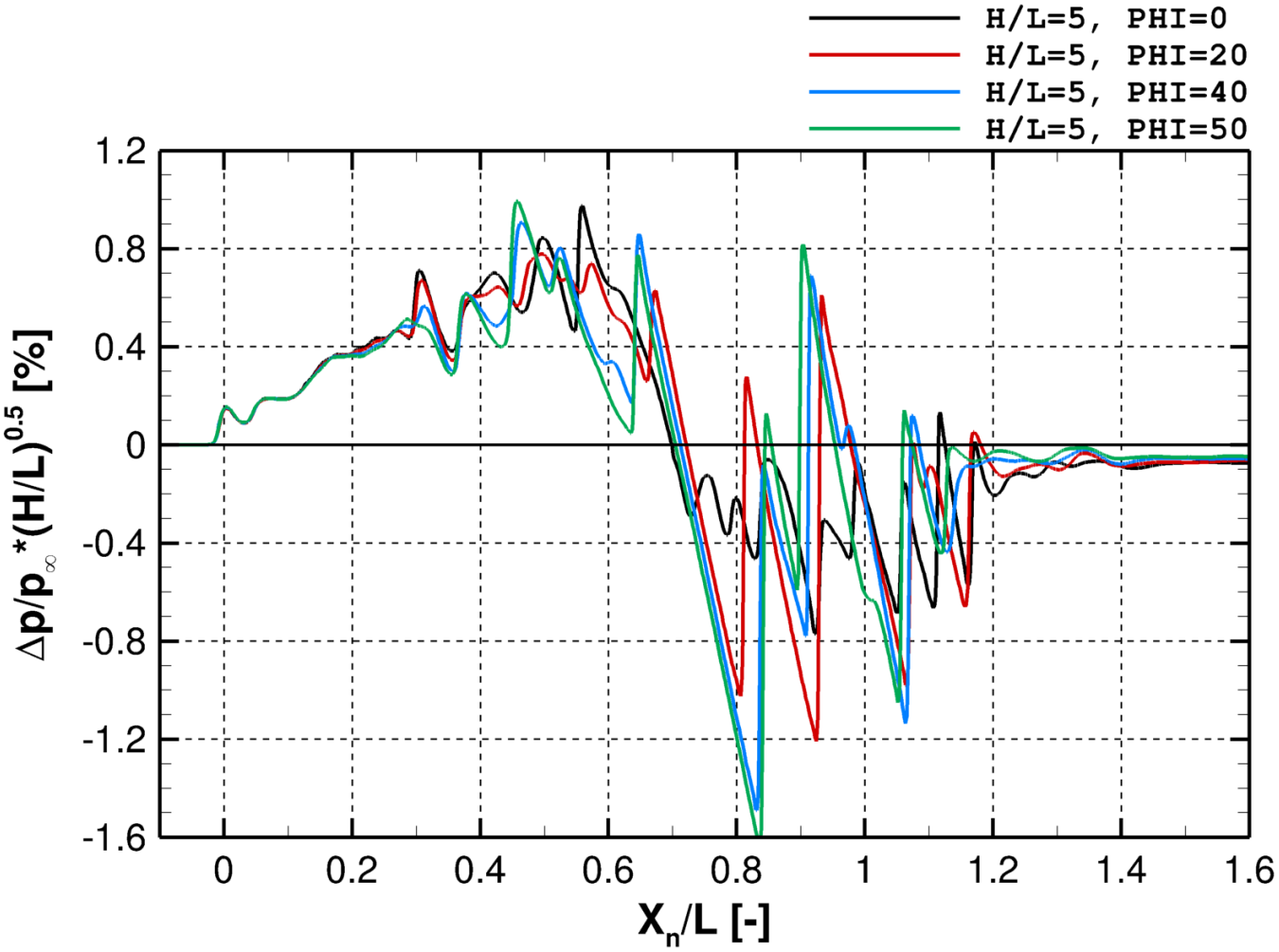

Results C25D flow-through

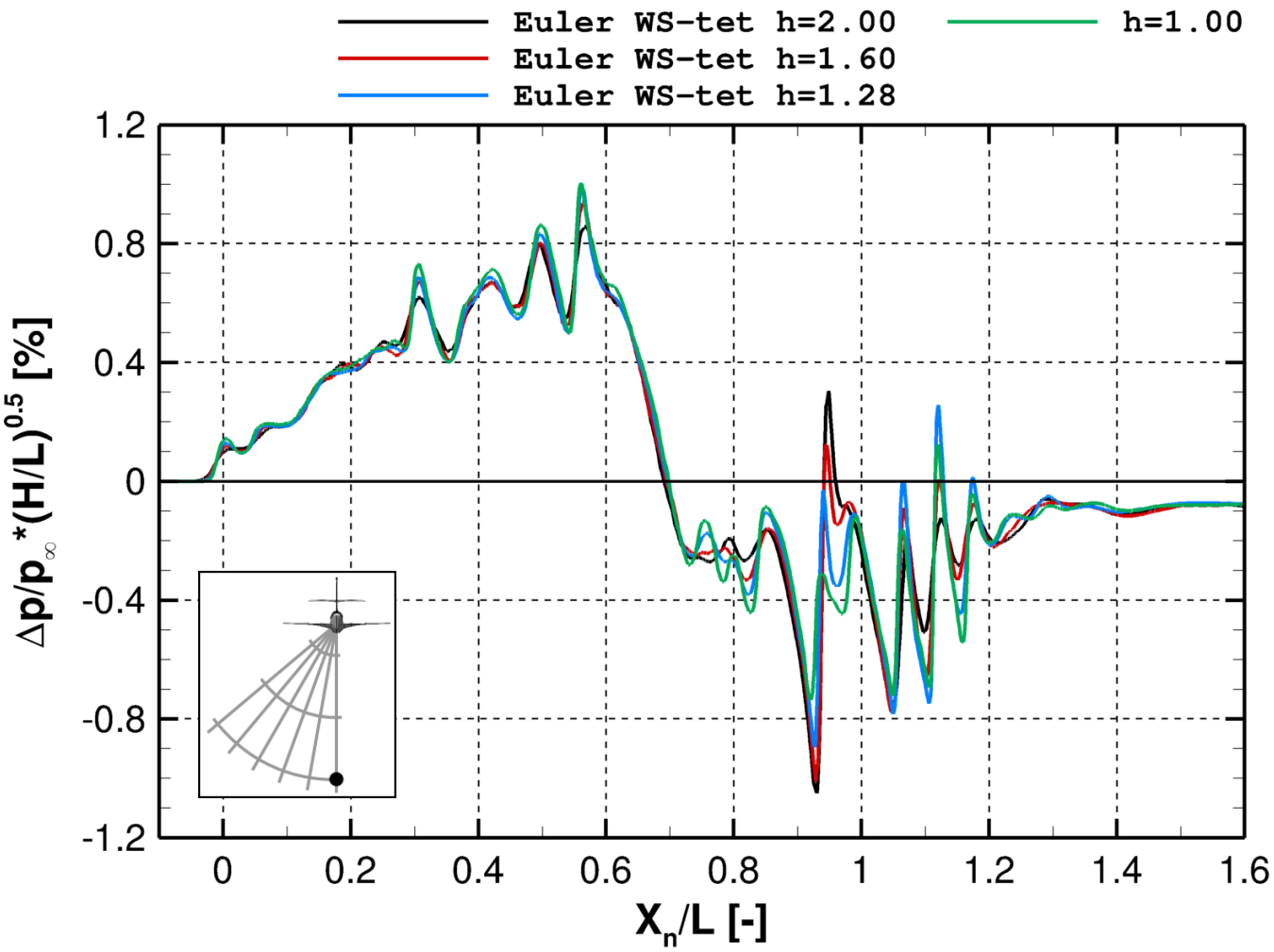

Results C25D flow-through

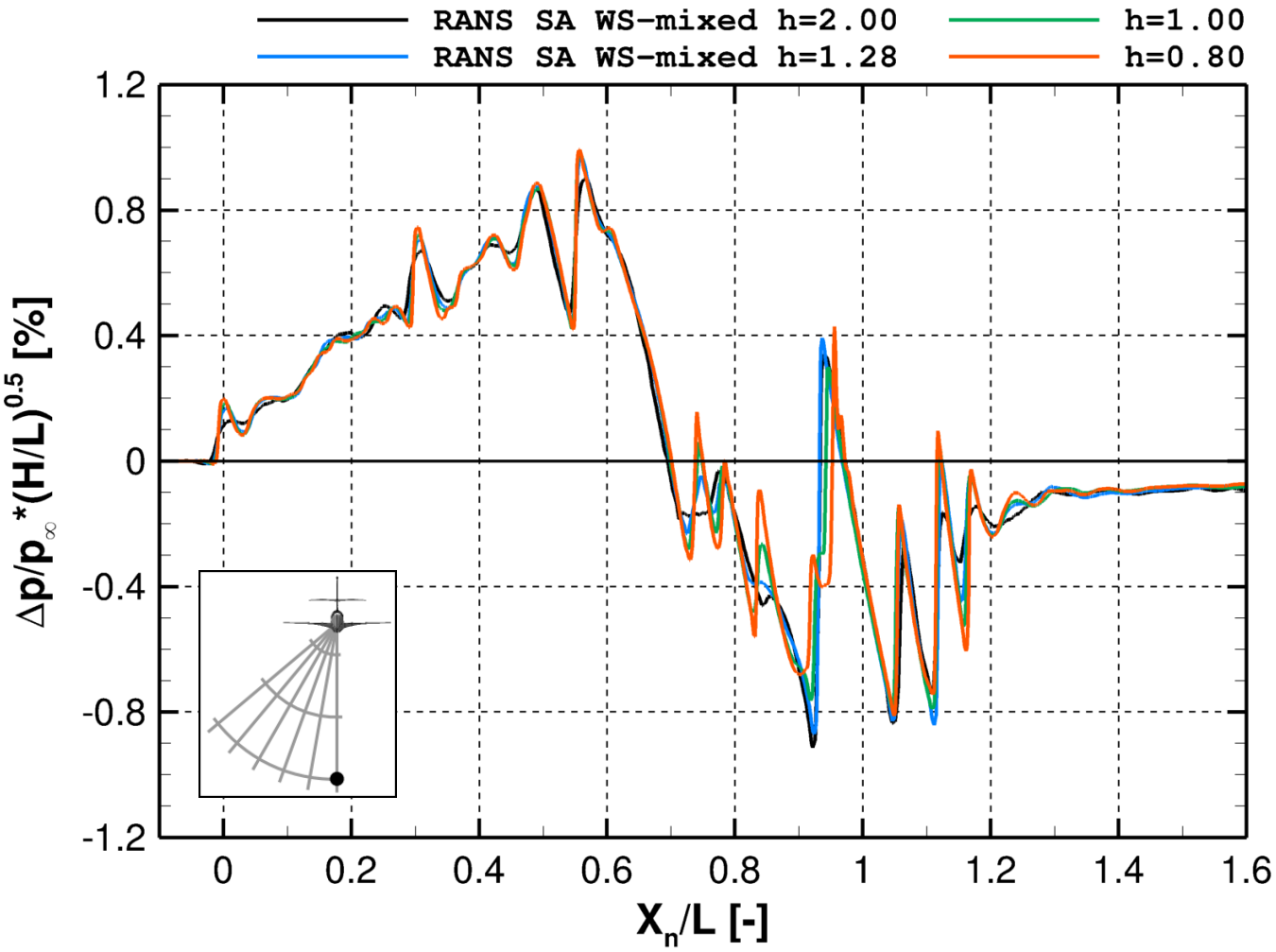

C25F

Results C25D flow-through

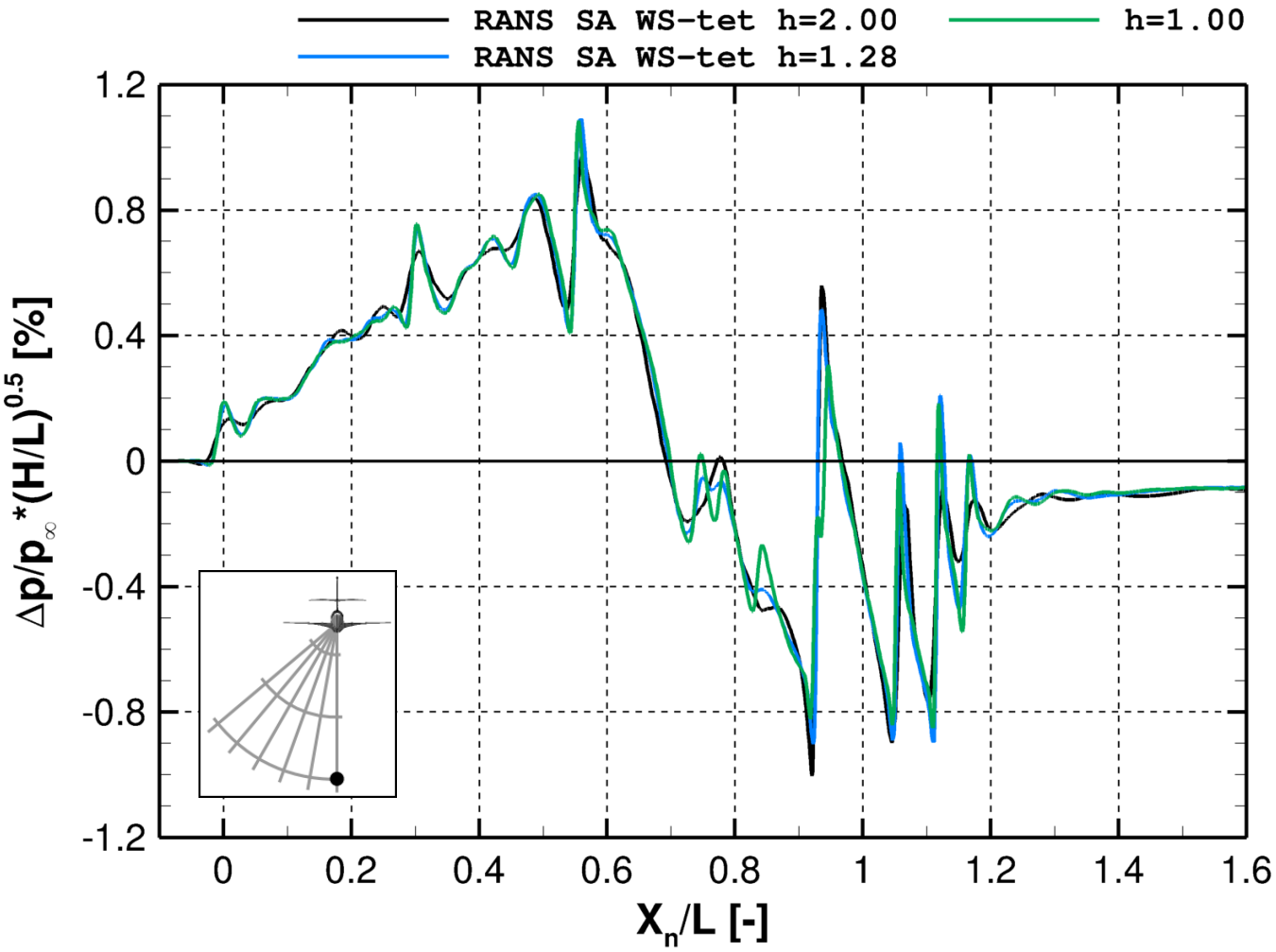

DLR

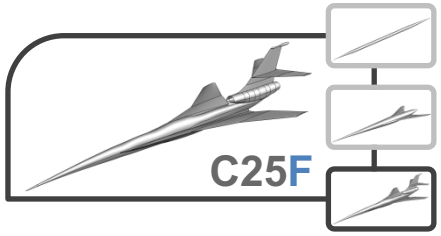

Results C25D flow-through

Same Grid Comparison (H/L=5, PHI=0)

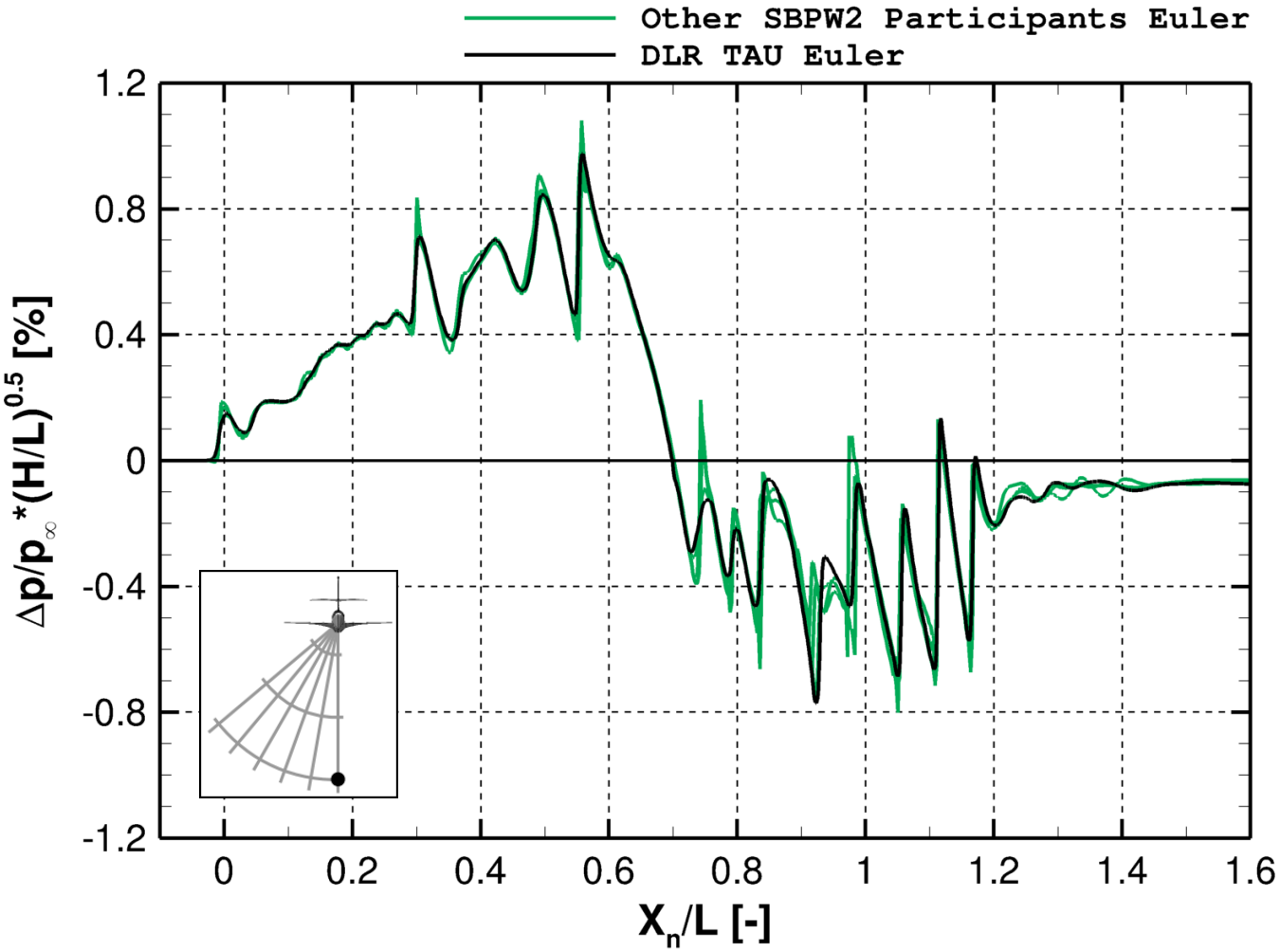

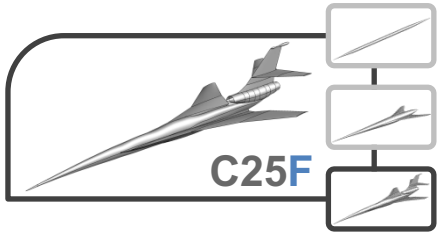

Results C25D flow-through

TAU Signatures and SBPW2 Statistics (H/L=5, PHI=0)

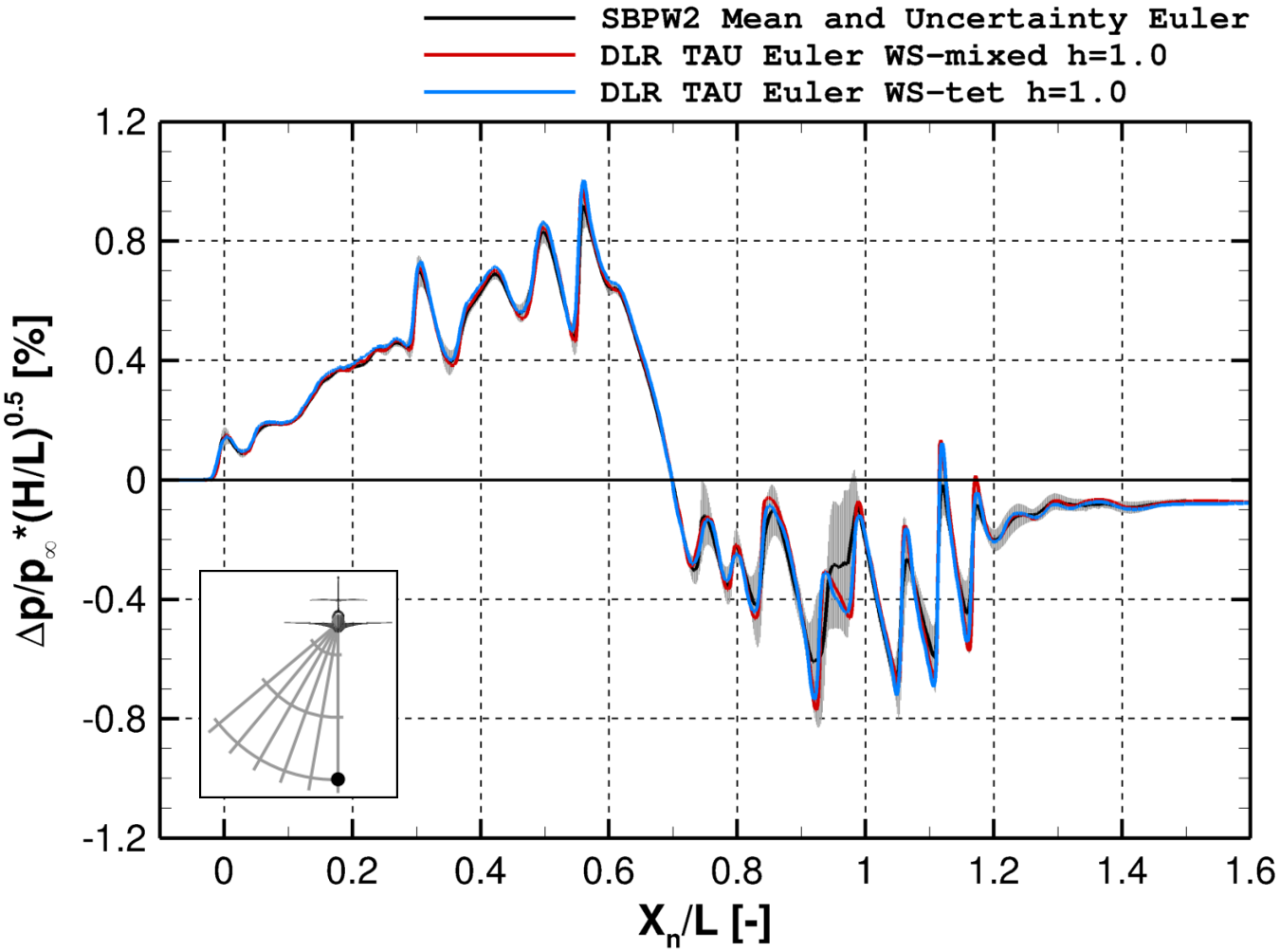

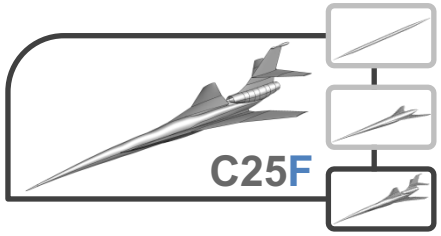

Results C25D flow-through

TAU Signatures and SBPW2 Statistics (H/L=5, PHI=0)

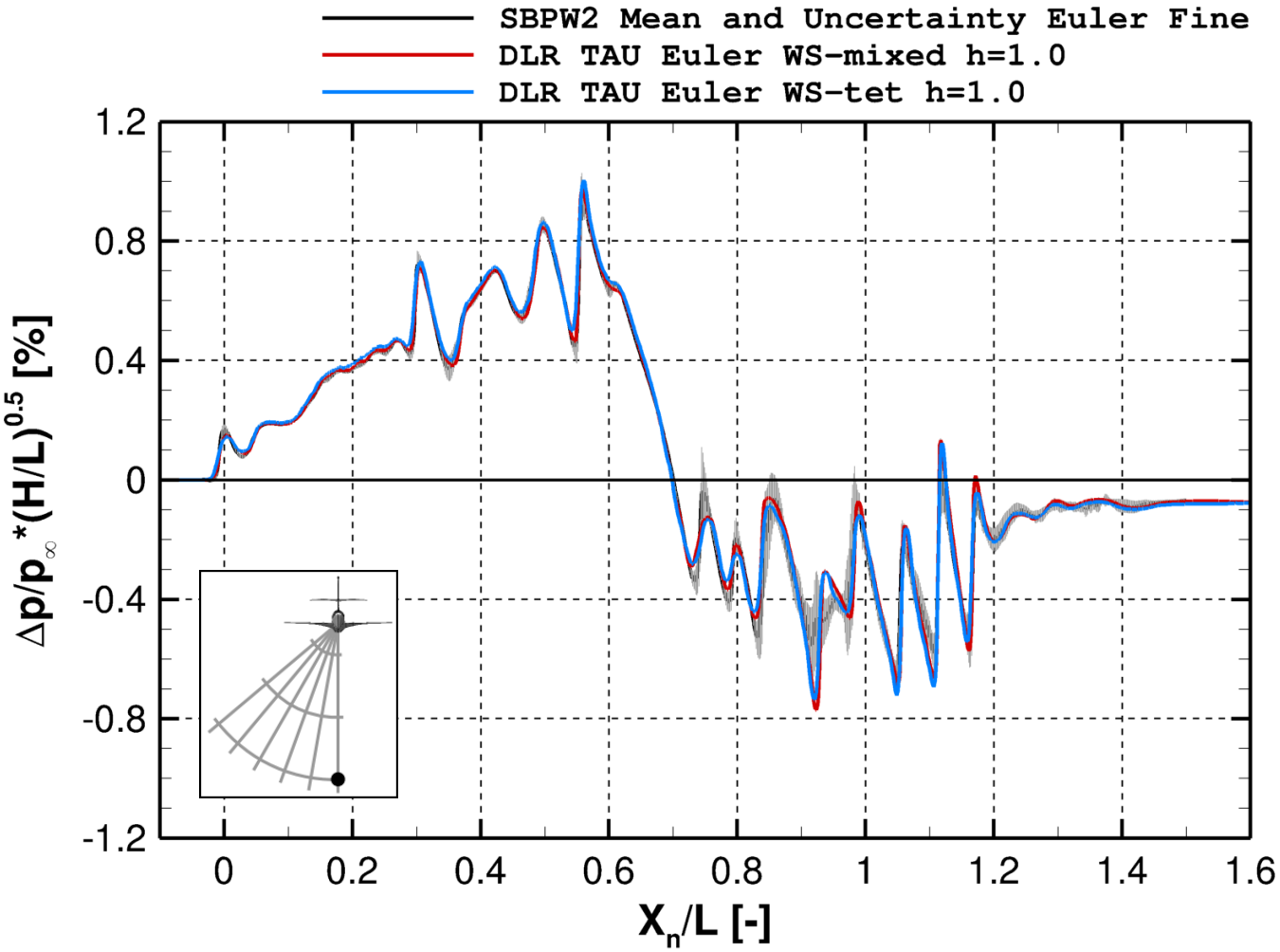

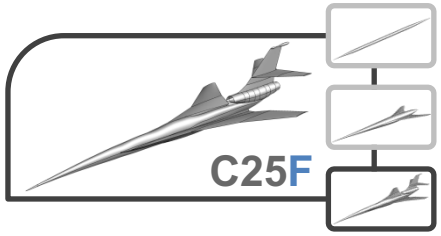

Results C25D flow-through

TAU Signatures and SBPW2 Statistics (H/L=5, PHI=0)

SBPW2 Mean and Uncertainty RANS
DLR TAU RANS SA WS-mixed h=1.0
DLR TAU RANS SA WS-tet h=1.0

$\Delta p/p_\infty * (H/L)^{0.5}$ [%]

1.2
0.8
0.4
0
-0.4
-0.8
-1.2

0 0.2 0.4 0.6 0.8 1 1.2 1.4 1.6

X_n/L [-]

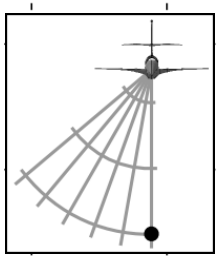

DLR

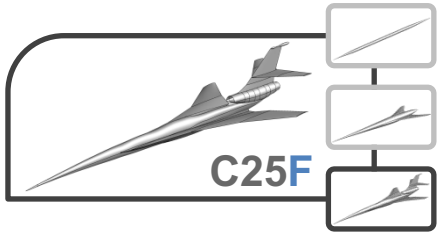

Results C25D flow-through

TAU Signatures and SBPW2 Statistics (H/L=5, PHI=0)

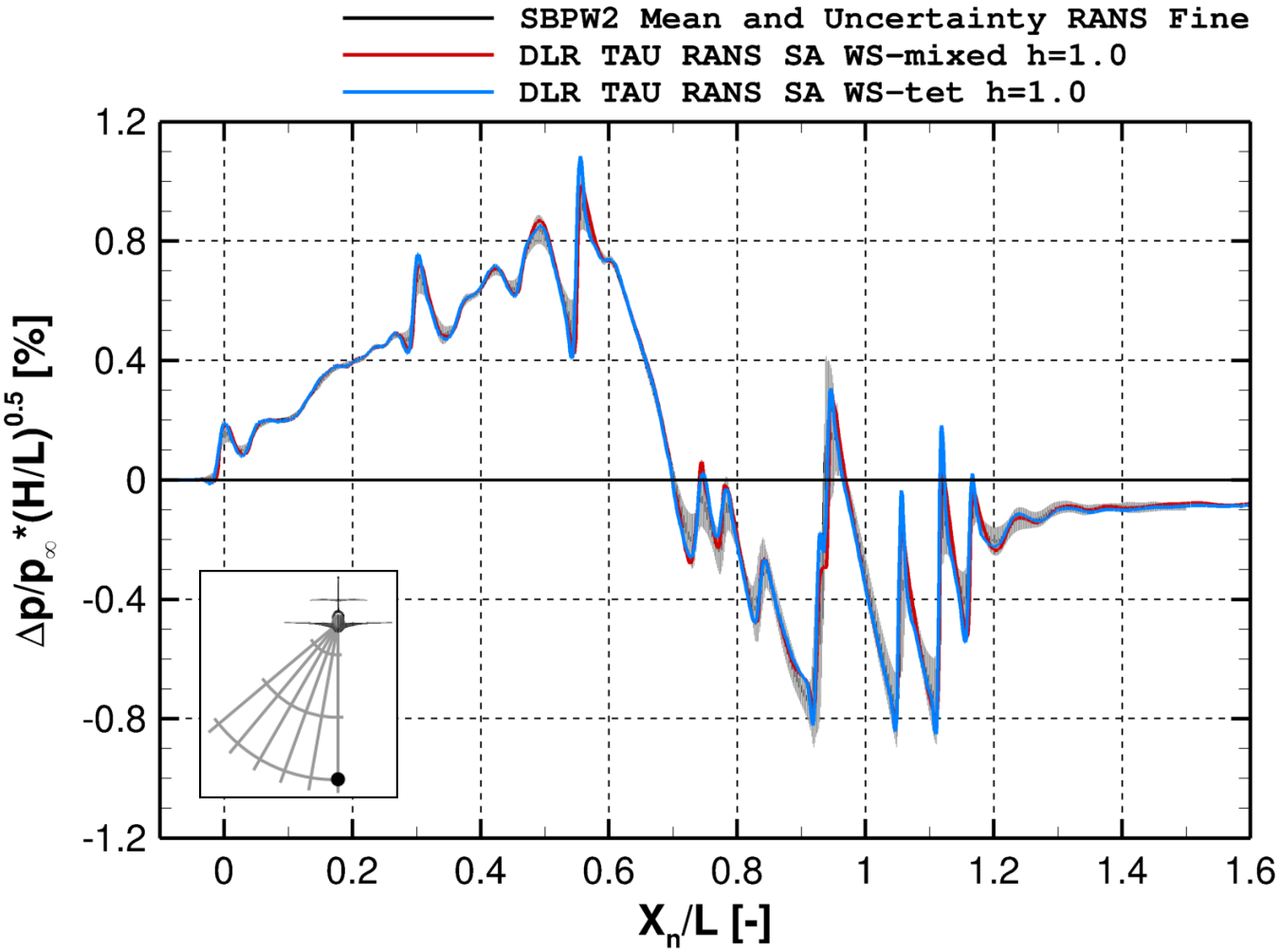

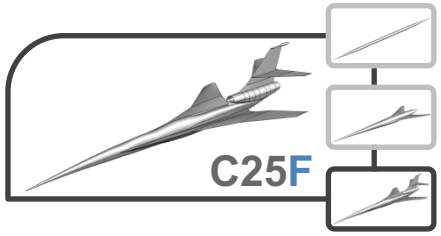

Results C25D flow-through

Same Grid Comparison (H/L=5, PHI=0)

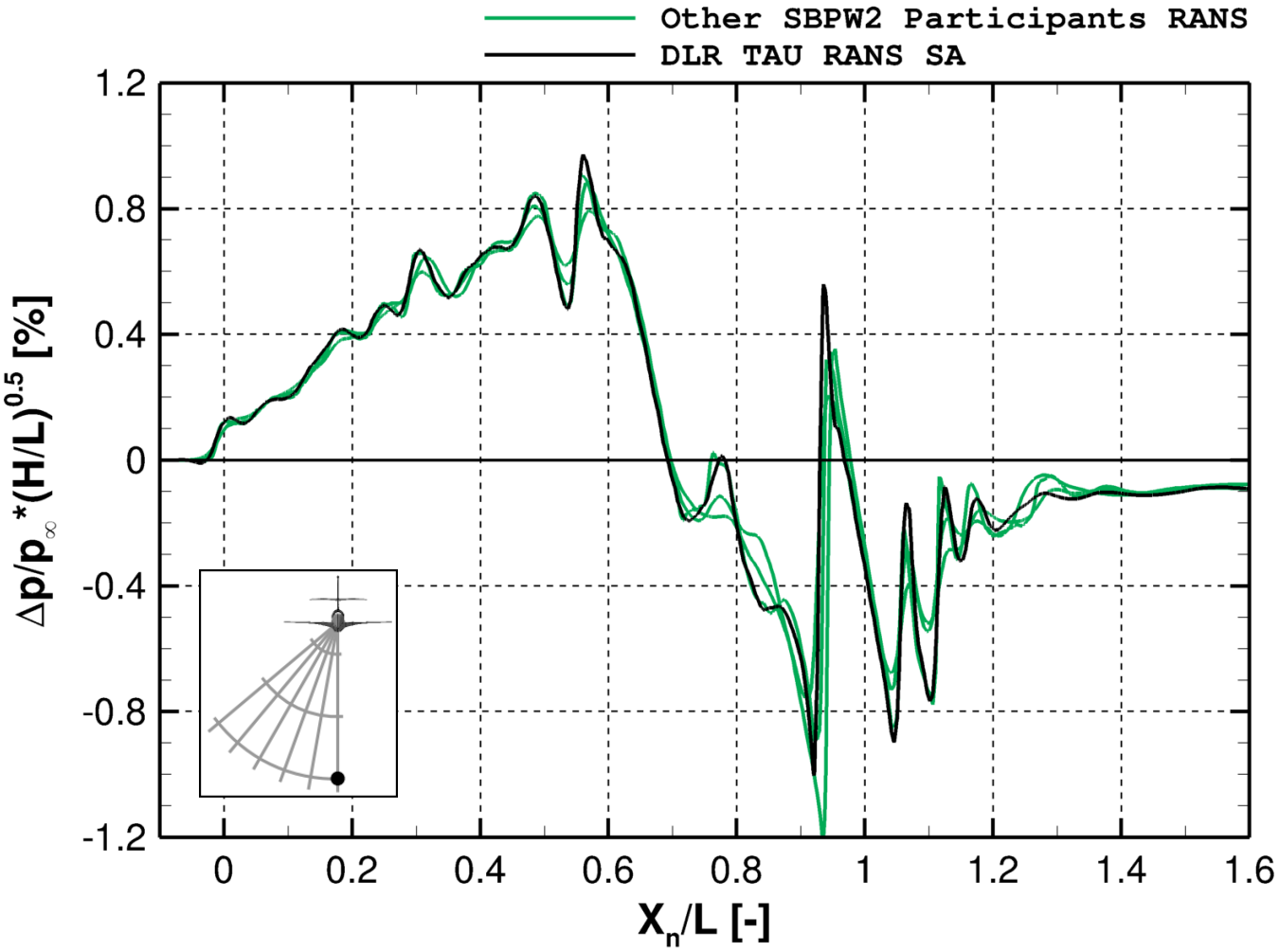

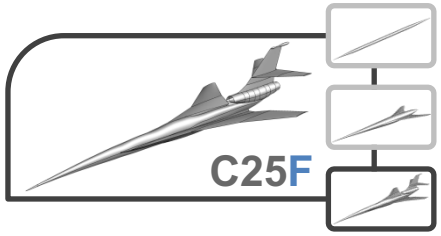

Results C25D flow-through

Same Grid Comparison (H/L=5, PHI=0)

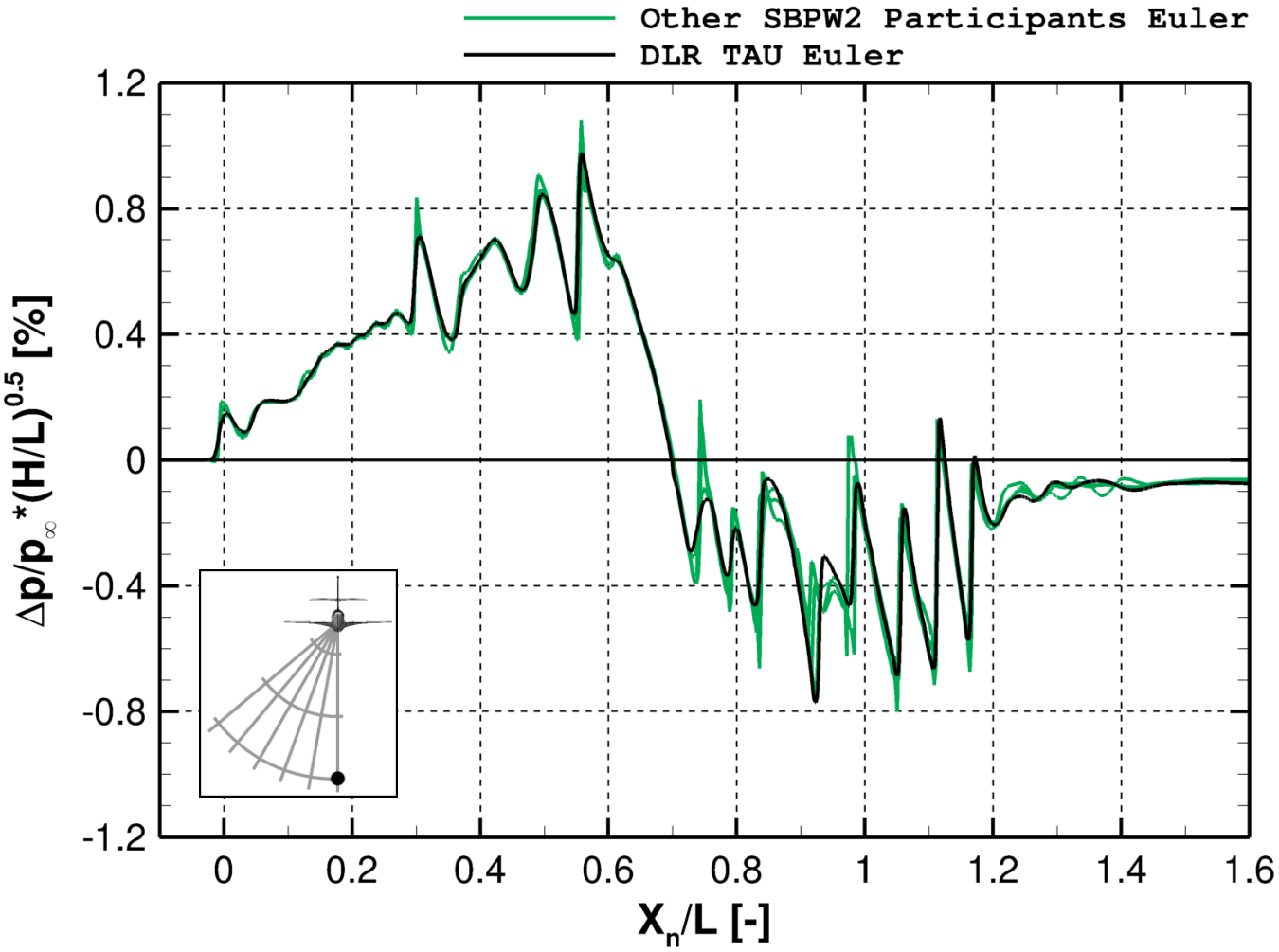

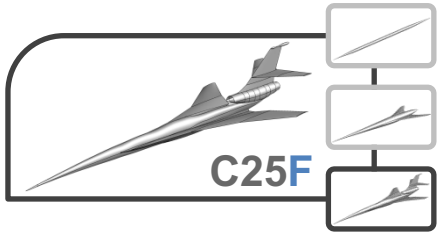

Results C25D flow-through

Same Grid Comparison (H/L=5, PHI=0)

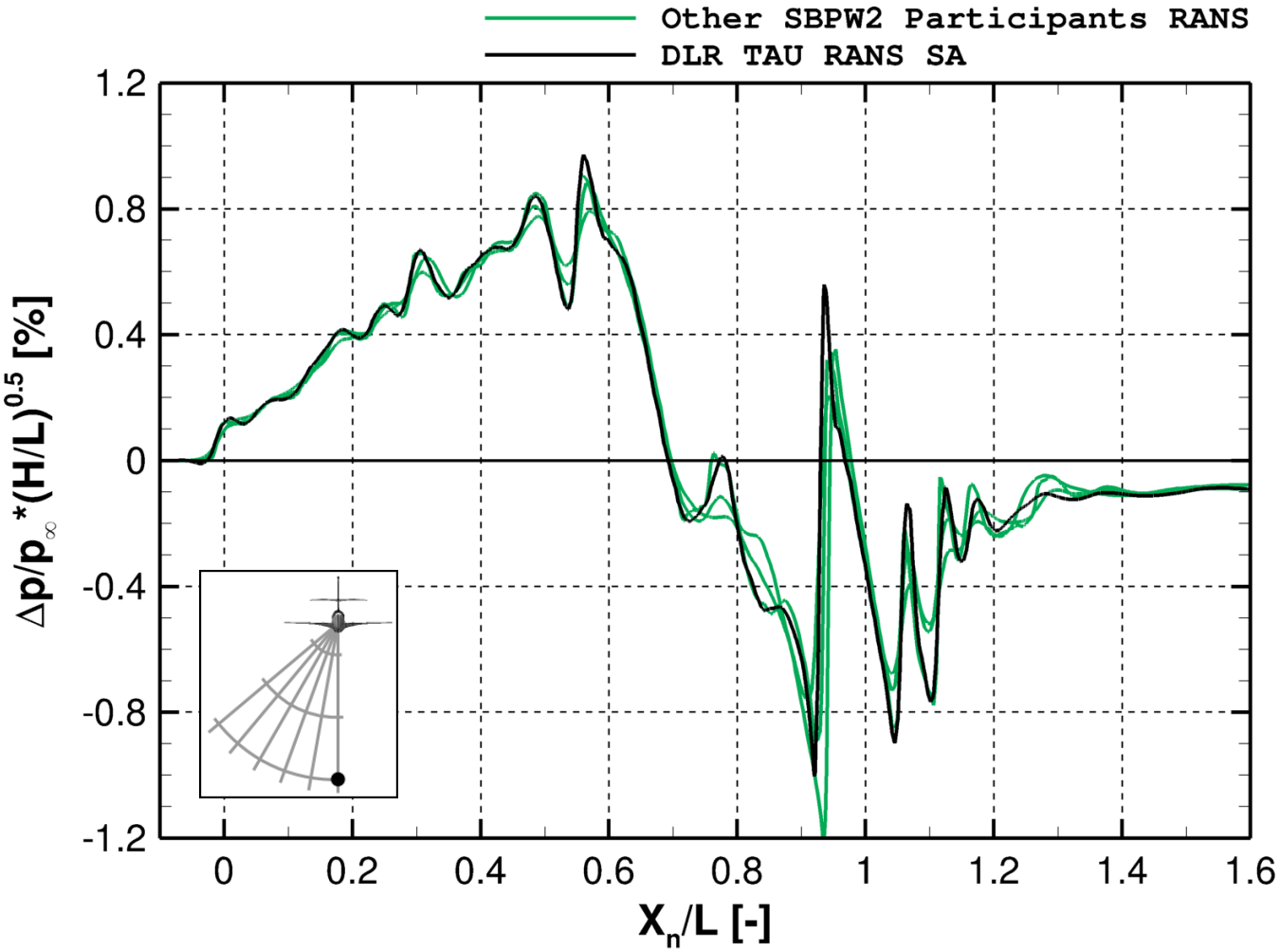

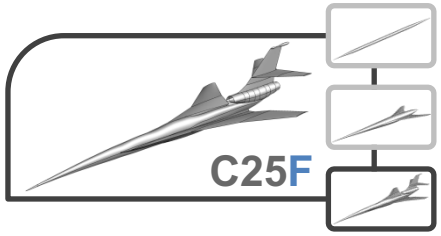

Results C25D flow-through

Provided and CENTAUR-generated grid

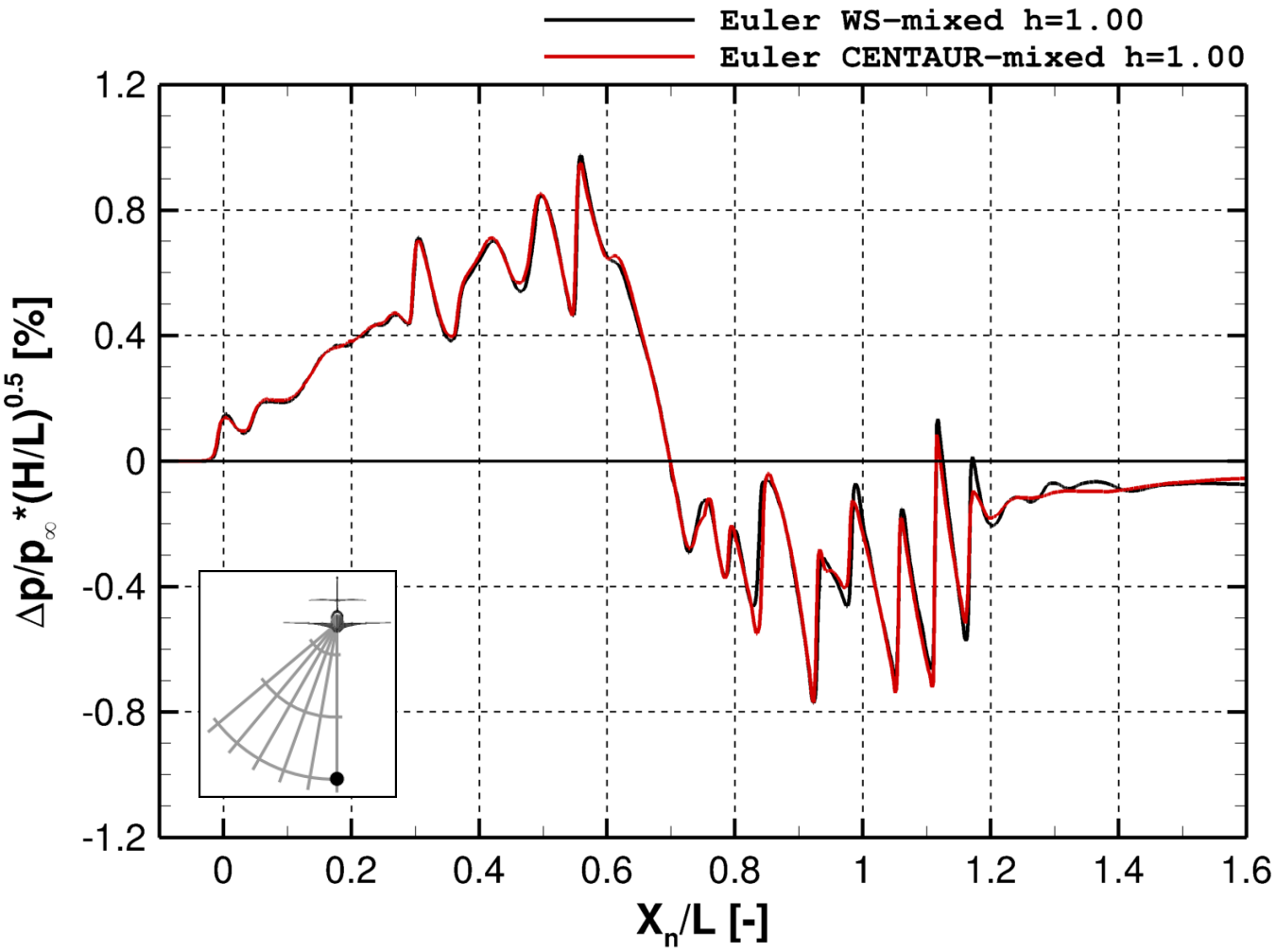

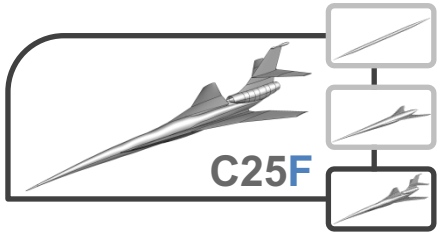

Results C25D flow-through

Forces

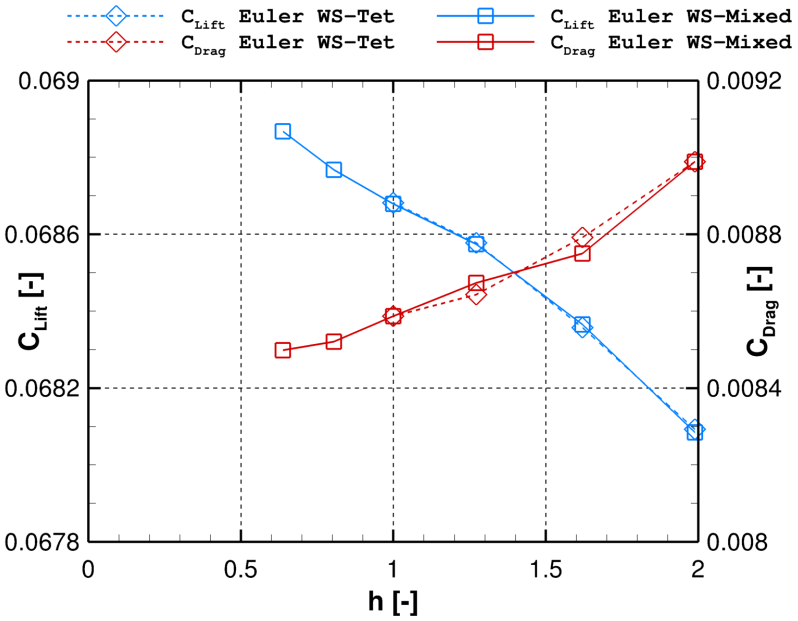

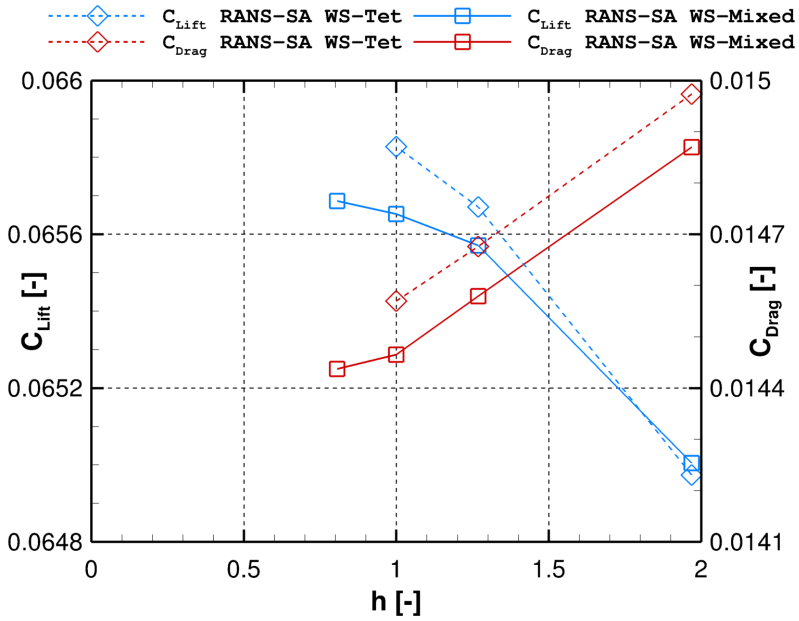

Results C25D powered